Characterization of the dysferlin protein and its binding partners reveals rational design for therapeutic strategies for the treatment of dysferlinopathies

Inauguraldissertation

zur
Erlangung der Würde eines Doktors der Philosophie
vorgelegt der
Philosophisch-Naturwissenschaftlichen Fakultät
der Universität Basel

von

Sabrina Di Fulvio
von Montreal (CAN)

Basel, 2013

Genehmigt von der Philosophisch-Naturwissenschaftlichen Fakultät
auf Antrag von

Prof. Dr. Michael Sinnreich
Prof. Dr. Martin Spiess
Prof. Dr. Markus Rüegg

Basel, den 17. September 2013

_____

Prof. Dr. Jörg Schibler
Dekan

Acknowledgements

I would like to express my gratitude to Professor Michael Sinnreich for giving me the opportunity to work on this exciting project in his lab, for his continuous support and guidance, for sharing his enthusiasm for science and for many stimulating conversations. Many thanks to Professors Martin Spiess and Markus Rüegg for their critical feedback, guidance and helpful discussions.

Special thanks go to Dr Bilal Azakir for his guidance and mentorship throughout this thesis, for providing his experience, advice and support. I would also like to express my gratitude towards past and present lab members for creating a stimulating and enjoyable work environment, for sharing their support, discussions, technical experiences and for many great laughs: Dr Jon Ashley, Dr Bilal Azakir, Marielle Brockhoff, Dr Perrine Castets, Beat Erne, Ruben Herrendorff, Frances Kern, Dr Jochen Kinter, Dr Maddalena Lino, Dr San Pun and Dr Tatiana Wiktorowitz. A special thank you to Dr Tatiana Wiktorowicz, Dr Perrine Castets, Katherine Starr and Professor Michael Sinnreich for their untiring help during the writing of this thesis.

Many thanks to all the professors, researchers, students and employees of the Pharmazentrum and Biozentrum, notably those of the seventh floor, and of the DBM for their willingness to impart their knowledge, ideas and technical expertise. Many thanks to Dr Patrick Matthias and Gabriele Matthias at the FMI for their assistance with the HDAC6 project, as well as to Dr Eric Shoubridge, Tim Johns, Steven Salomon and Christian Therrien at McGill University, Montreal for their generous technical assistance. Special thanks to Beat Erne and Michael Abanto for sharing their confocal microscopy expertise with me.

A huge thank you to my family and friends for their endless love, support and patience throughout my studies. I am especially grateful to my parents for their daily encouragement and unwavering confidence in me.

Summary

Dysferlinopathies are incurable recessively inherited muscular dystrophies caused by loss of the dysferlin protein. Dysferlin is essential for the plasma membrane repair of skeletal muscle cells and is required for myotube formation. To design treatment strategies for dysferlinopathies, we studied dysferlin's molecular biology and characterized the functionality of dysferlin's seven C2 domains, its degradation pathway and its interaction with a novel protein, histone deacetylase 6.

The results indicate that dysferlin and histone deacetylase 6 form a triad interaction with alpha-tubulin to modulate the acetylated alpha-tubulin levels of muscle cells, which may play a regulatory role during myotube formation. Furthermore, the characterization of dysferlin's C2 domains revealed that there is functional redundancy in their ability to localize dysferlin to, and effect repair of, the plasma membrane. Taking these results into consideration, we designed shorter, functional dysferlin molecules for usage in gene therapy.

To find a novel pharmacological therapy for patients with dysferlin deficiency, we investigated the inhibition of dysferlin's degradation pathway. We demonstrated that when salvaged from proteasomal degradation, missense mutated dysferlin retained its biological activities for plasmalemmal localization, plasmalemmal repair and myotube formation. Further studies using recombinant missense mutated dysferlin constructs showed that certain missense mutants are intrinsically biologically active; whereas others lack functionality even when their levels are increased by transient transfection or by inhibiting their proteasomal degradation. Proteasomal inhibition represents a novel potential pharmacological treatment strategy for patients with dysferlin deficiency.

Table of Contents

List of Abbreviations

AAV	Adeno-associated virus
AON	Antisense oligonucleotide
Arg (R)	Arginine
Asp (D)	Aspartic acid
Asp (N)	Asparagine
BMD	Becker muscular dystrophy
C2	Second-constant sequence
CBS	Cystathionine b-synthase
CK	Creatinine kinase
Cys (C)	Cysteine
DG	Dystroglycan
DGC	Dystrophin-glycoprotein complex
DMD	Duchenne muscular dystrophy
ECM	Extracellular matrix
ERAD	ER-associated degradation
FBS / FCS	Fetal bovine serum / Fetal calf serum
FDA	Federal Drug Administration
Fer-1	Fertility factor 1
FKRP	Fukutin-related protein
FKTN	Fukutin
GFP	Green fluorescent protein
HDAC6	Histone deacetylase 6
Hsp70	Heat shock protein 70
Leu (L)	Leucine
LGMD	Limb girdle muscular dystrophy
LGMD2B	Limb girdle muscular dystrophy type 2B
MG53	Mitsugumin 53
MM	Miyoshi Myopathy
PBS	Phosphate buffered saline
PEI	Polyethylenimine
PFA	Paraformaldehyde
Phe (F)	Phenylalanine
PM	Plasma membrane
Pro (P)	Proline
PVDF	Polyvinylidene difluoride
Ser (S)	Serine
SG	Sarcoglycan
snRNP	Small nuclear ribonucleic protein
Syt1	Synaptotagmin 1
TM	Transmembrane domain
Trp (W)	Tryptophan
Val (V)	Valine
WT	Wildtype

List of Figures

List of Tables

Preface

Dysferlinopathies are recessively inherited muscular dystrophies caused by the loss of the skeletal muscle protein, dysferlin. These diseases are severely debilitating; as patients become weaker they grow increasingly dependent on the aid and support of loved ones, and the deterioration in their health presents an increasing financial burden on the patient, their family and on the health system. Finding treatments or a cure for dysferlinopathies is imperative.

To understand how a gene leads to the disease, one must understand the biological mechanisms involved in order to gain insight as to how molecular alterations can lead to the pathology. This thesis investigated the molecular biology of dysferlin's C2 domains, plasmalemmal localization, membrane repair function, degradation pathway and involvement in myogenesis. Insights from these studies led to the rational design of minidysferlins suitable for AAV encapsidation, a novel pharmacological treatment strategy, and further validation for exon skipping in the treatment of dysferlinopathies.

This doctoral thesis has been developed at the Neuromuscular Research Center of Basel University Hospital within the research group of Professor Michael Sinnreich as part of the Neuroscience PhD program of Basel University. This thesis is written in manuscript-based format, and is divided into six chapters. It contains three published articles, incorporated into Chapters 2 through 4, and one manuscript in preparation, incorporated into Chapter 5.

Chapter 1 covers the introduction and provides a literature review of limb girdle muscular dystrophies and Duchenne Muscular Dystrophy, with special focus on dysferlinopathies. This chapter introduces muscular dystrophies caused by defective muscle membrane integrity and by defective muscle membrane repair. It reviews dysferlin's phylogeny, structure, function and treatment options that are currently under investigation. Finally, it defines the objectives and goals of this thesis.

Chapter 2 presents the identification of a novel dysferlin-binding protein, Histone deacetylase 6 (HDAC6), and characterizes the interaction between dysferlin, HDAC6 and

alpha-tubulin and their possible role in muscle cell differentiation.

Chapter 3 characterizes the modular dispensability of dysferlin's multiple C2 domains, with the goal of designing a small mini-dysferlin construct that could be packaged within an adeno-associated viral vector for gene therapy applications.

Chapter 4 investigates the degradation pathway of dysferlin and one of its missense-mutated variants. It demonstrates how this particular missense-mutated form of dysferlin retained its biological activity when salvaged from degradation, thus representing a novel pharmacological strategy for dysferlinopathies.

Chapter 5 characterizes the biological activity of additional missense-mutated dysferlin variants that were recombinantly engineered. The goal of this study was to expand the list of dysferlin patients harbouring missense-mutated dysferlin proteins that may be helped by the pharmacological treatment strategy presented in Chapter 4.

Chapter 6 presents a general discussion of the results of this thesis' work and discusses the rationale for the pursuit of several therapeutic strategies garnered from the studies presented in Chapters 2-5, with an outlook to the future.

Publications arising from this work:

1. "Dysferlin interacts with histone deacetylase 6 and increases alpha-tubulin acetylation."
Di Fulvio S, Azakir BA, Therrien C, Sinnreich M. PLoS One. 2011; 6(12):e28563.

2. "Proteasomal inhibition restores biological function of missense mutated dysferlin in patient-derived muscle cells."
Azakir BA, **Di Fulvio S**, Kinter J, Sinnreich M. J Biol Chem. 2012; 287(13):10344-54.

3. "Modular dispensability of dysferlin C2 domains reveals rational design for mini-dysferlin molecules."
Azakir BA, **Di Fulvio S**, Salomon S, Brockhoff M, Therrien C, Sinnreich M. J Biol Chem. 2012; 287(33):27629-36.

Contributions of Authors

1. B.A. Azakir, M. Sinnreich and I designed the experiments for this study. Experiments were performed by B.A. Azakir and I. B.A. Azakir performed the immunoprecipitation assays (Fig. 1A-C, 2 and 3.) and microtubule resistance assays (Fig. 5). I performed the immunofluorescence assays (Fig 1D,E) and myoblast differentiation assays (Fig. 6 and 7). Data from the experiments was analyzed by B.A. Azakir, M. Sinnreich and myself. C. Therrien constructed the plasmids used in the study. I wrote the paper with the help of B.A. Azakir and M. Sinnreich. This work was done under the supervision of Professor Dr M. Sinnreich.

2. B.A. Azakir and M. Sinnreich designed the experiments for this study. Experiments were performed by B.A. Azakir, with the help of myself and M. Brockhoff. J. Kinter performed the RNA analysis. B.A. Azakir wrote the paper with the help of M. Sinnreich and I. This work was done under the supervision of Professor Dr M. Sinnreich.

3. B.A. Azakir, M. Sinnreich and I designed the experiments for this study. I performed the experiments involving GFP-Dysferlin ΔExon32 (Fig. 1). Experiments involving GFP-

dysferlin C2 domain deletion constructs and midi- and mini-dysferlins were performed by B.A. Azakir and I (Fig. 2 and 4). Membrane injury repair assays were performed by B.A. Azakir (Fig. 3 and 5). Paper was written by B.A. Azakir and I, with the help of M. Sinnreich. This work was done under the supervision of Professor Dr M. Sinnreich.

Additional Publications:

1. "Dysferlin interacts with tubulin and microtubules in mouse skeletal muscle."
Azakir BA, **Di Fulvio S**, Therrien C, Sinnreich M. PLoS One. 2010 Apr 12;5(4):e10122.

2. "Sustained activation of mTORC1 in skeletal muscle inhibits constitutive and starvation-induced autophagy and causes a severe, late-onset myopathy."
Castets P, Lin S, Rion N, **Di Fulvio S,** Romanino K, Guridi M, Frank S, Tintignac LA, Sinnreich M and Rüegg MA. Cell Metabolism. 2013.

CHAPTER 1

1. Literature Review

Contraction of voluntary skeletal muscles generates the force needed for motility and strength. As such, skeletal muscle cells are submitted to significant contractile forces, which can cause disruptions of the muscle surface membrane (the sarcolemma). The dystrophin-glycoprotein complex (DGC) and associated peripheral components maintain muscle membrane integrity and structure, whereas the muscle membrane repair complex rapidly repairs sarcolemmal disruptions. Deficiencies in either of these protein complexes lead to muscular dystrophies, a heterogeneous group of debilitating muscle-wasting diseases for which treatment options are currently lacking.

1.1 The Dystrophin-Glycoprotein Complex (DGC)

The core of the DGC is formed by dystroglycan, dystrophin, sarcoglycans (alpha, beta, delta, epsilon and gamma subunits) and sarcospan. Delta-sarcoglycan binds to sarcospan. Gamma-sarcoglycan binds to the dystroglycan protein, which contains a membrane-spanning beta subunit and an extracellular alpha subunit. The extracellular faces of alpha-dystroglycan and of the sarcoglycans are heavily glycosylated (Holt et al., 1998). These modifying sugars allow the proteins to interact with extracellular matrix proteins, such as integrins, laminins, agrins and perlecans. Notably, alpha-dystroglycan binds to laminin-alpha2 (also called merosin), likely through interactions with its sugar chains.

On the intracellular side of the membrane, beta-dystroglycan binds to dystrophin's carboxy-terminus, a cytoplasmic protein. The amino-terminus of dystrophin binds to F-actin filaments of the intracellular cytoskeleton. The N-terminus of dystrophin also binds to the cytoplasmic syntrophin complex, composed of alpha, beta and gamma subunits. The syntrophin complex interacts with dystrobrevin, a cytoplasmic protein complex consisting of alpha and beta subunits.

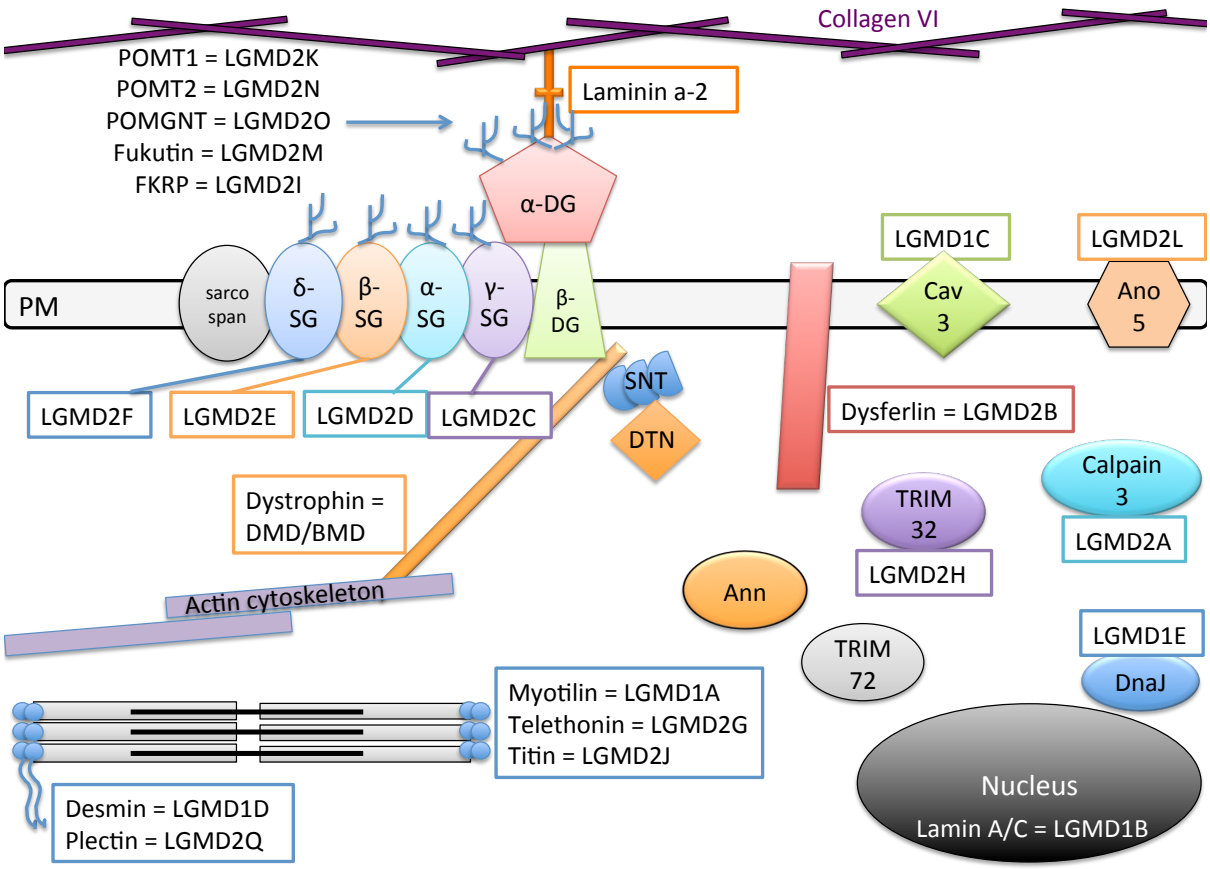

Figure 1.1: Proteins implicated in Limb Girdle Muscular Dystrophies

The membrane-embedded core of the dystroglycan complex (DGC) spans the plasma membrane (PM) and is composed of dystroglycan (DG) alpha and beta; the sarcoglycans (SG) alpha, beta, delta, epsilon and gamma; and sarcospan. The DGC links the extracellular matrix (ECM) (via dystroglycan's interaction with laminin a-2) to the actin cytoskeleton (via dystrophin). Alpha-dystroglycan is glycosylated by the enzymes POMT1, POMT2 and POMGNT, Fukutin (FKTN) and Fukutin-related protein (FKRP). Dystrophin also binds to the syntrophin (SNT) complex, which interacts with dystrobrevin (DTN).
Dysferlin, Caveolin 3 (Cav 3), TRIM72 (also called MG53), annexins (Ann) and calpain 3 are involved in membrane repair.
Anoctamin 5 (Ano5) is speculated to act as a chloride channel.
TRIM32 is an E3 ubiquitin ligase that mediates ubiquitin-directed protein degradation.
Myotilin, telethonin and titin are sarcomeric proteins involved in skeletal muscle contraction. Desmin assists in maintaining the structural integrity of the sarcomere. Plectin connects the sarcomere to the cytoskeleton.
In the nucleus, lamin A/C provides scaffolding for the nuclear envelop.
DnaJ is a co-chaperone in the endoplasmic reticulum that assists with protein folding.
Mutations in most of these protein components lead to their respective limb girdle muscular dystrophy (LGMD) or muscular dystrophy (MD).

The DGC is critical for linking the extracellular matrix (ECM) to the intracellular actin cytoskeleton, and maintaining the strength and structural integrity of the sarcolemma. Whether the DGC has additional functions in skeletal muscle (aside from the structural) is under active investigation. It is speculated that the DGC may act as docking sites for signaling proteins that are important for calcium homeostasis, nitric oxide signaling and nNOS regulation, as well as cell survival via laminin signaling (Grozdanovic et al., 1996; Kobayashi et al., 2008; Gumerson et al., 2011).

1.2 Muscular Dystrophies caused by defective muscle membrane integrity

Limb girdle muscular dystrophies (LGMDs) are a large and heterogeneous group of muscular diseases. Often, the first muscles to show weakness are those of the shoulders and pelvic regions. Patients will often first report difficulties climbing stairs, standing from a squatting position, or raising their arms above their head, which are all motions hampered by proximal muscle weakness.

LGMDs are autosomally inherited diseases, either through dominant inheritance (classified as type 1) or by recessive inheritance (classified as type 2). There exist few reports on the prevalence of LGMDs, although estimates range from one in 14500 to one in 123000 (van der Kooi et al., 1996; Urtasun et al., 1998). Mutations in various muscle proteins each produce their own distinctive LGMD (see Table 1.1), and they vary in the age of onset, severity and rate of progression.

Mutations in almost any component of the DGC result in structural instability of the muscle membrane, and lead to various forms of muscular dystrophy. Genetic alterations in any of the four sarcoglycans result in distinct LGMDs, named LGMD type 2C through 2F. Genetic aberrations in the enzymes responsible for glycosylating alpha-dystroglycan disrupt the link with the extracellular matrix. Mutations in *POMT1*, *POMT2* and *POMGNT* lead to LGMD2K, LGMD2N and LGMD2O, respectively. Fukutin (FKTN) and Fukutin-related protein (FKRP) are also believed to glycosylate alpha-dystroglycan, and mutations in these proteins lead to LGMD2M and LGMD2I, respectively. Mutations in alpha-dystroglycan's glycosylating enzymes are also the cause of secondary dystroglycanopathies, such as Fukuyama Congenital Muscular Dystrophy, Walker-

Table 1.1: Limb Girdle Muscular Dystrophies

Type	Inheritance	Gene symbol	Gene product	Locus	Onset (years)	Progression
1A	Dominant	*MYOT*	Myotilin	5q31.2	20-40	Slow
1B	Dominant	*LMNA*	Lamin A/C	1q22	< 10	Slow
1C	Dominant	*CAV3*	Caveolin 3	3p25.3	< 10	Variable
1D	Dominant	*DES*	desmin	2q35	15-50 y	Slow
1E	Dominant	*DNAJB6*	DnaJ homolog subfamily B member 6	7q36.3	30-50	Slow
1F	Dominant	unknown	unknown	7q32.1-q32.2	unknown	Unconfirmed
1G	Dominant	unknown	unknown	4q21	unknown	Unconfirmed
1H	Dominant	unknown	unknown	3p25.1-p23	unknown	Unconfirmed
2A	Recessive	*CAPN3*	Calpain 3	15q15.1	5-40	Depends on onset
2B	Recessive	*DYSF*	dysferlin	2p13.2	10-30	Slow, some rapid
2C	Recessive	*SGCG*	g-sarcoglycan	13q12.12	3-20	Variable
2D	Recessive	*SGCA*	a-sarcoglycan	17q21.33	3-20	Variable
2E	Recessive	*SGCB*	b-sarcoglycan	4q12	3-20	First decade, generally
2F	Recessive	*SGCD*	d-sarcoglycan	5q33.3	3-20	First decade, generally
2G	Recessive	*TCAP*	telethonin	17q12	2-15	Moderate
2H	Recessive	*TRIM32*	TRIM-32	9q33.1	15-30	Slow
2I	Recessive	*FKRP*	Fukutin-related protein	19q13.32	1-40	Unconfirmed
2J	Recessive	*TTN*	Titin	2q31.2	5-20	Unconfirmed
2K	Recessive	*POMT1*	Protein O-mannosyl-transferase 1	9q34.13	unknown	Unconfirmed
2L	Recessive	*ANO5*	Anoctamin 5	11p14.3	unknown	Unconfirmed
2M	Recessive	*FKTN*	fukutin	9q31.2	unknown	Unconfirmed
2N	Recessive	*POMT2*	Protein O-mannosyl-transferase 2	14q24.3	unknown	Unconfirmed
2O	Recessive	*POMGNT1*	POMGNT1	1p34.1	unknown	Unconfirmed
2Q	Recessive	*PLEC*	Plectin	8q24.3	unknown	Unconfirmed

Warburg Syndrome, Muscle-Eye-Brain disease, Congenital Muscular Dystrophy 1C and 1D.

Mutations in the dystroglycan protein itself have not been associated with human pathology, but were reported to lead to peri-implantation lethality in mice (Williamson et al., 1997). Although recently, a single case study of a Turkish patient with limb-girdle muscle dystrophy and cognitive impairment was shown to have a mutation in the dystroglycan gene (*DAG1*) (Hara et al., 2011).

Mutations in the dystrophin gene, *DMD*, give rise to Duchenne Muscular Dystrophy (DMD), or its less severe form Becker's Muscular Dystrophy (BMD), two X-linked (non-autosomal) muscle diseases. DMD has an incidence rate of 1:3500 and is an X-linked disease, affecting majorly boys. The onset is in early childhood, manifesting in a delay in walking, calf hypertrophy, proximal limb girdle weakness and the Gower's maneuver (whereby the kneeling patient climbs up his own legs to a standing position). The patients are nonambulatory by the age of 12, and typically do not survive into their second decade of life. Other problems arise in the respiratory system due to thoracic deformities, night blindness, intellectual problems and mild cardiomyopathy.

BMD has an incidence of 1:17000. The onset is later, the progression is slower and the patients live longer. But the same systems are affected, and the cardiomyopathy is more pronounced since the patients are more active.

The gene causing DMD and BMD was discovered in 1986 (Kunkel et al., 1986; Burghes et al., 1987). The molecular basis for the difference in DMD and BMD is the type of mutation involved: DMD typically results from nonsense mutations resulting in out-of-frame reading of the coding region, thus producing a non-functional protein. On the other hand, BMD is often caused by a deletion in the rod domain of the dystrophin protein resulting in a shorter but still functional protein.

DMD and BMD have been extensively studied. Many of the treatment techniques developed for these diseases can also be adapted for LGMDs.

1.3 Limb Girdle Muscular Dystrophies caused by defective muscle membrane repair

Despite having intact muscle membrane integrity and structure, impairments in skeletal muscle membrane repair can result in muscular dystrophy. When skeletal muscle contracts, microtears occur within the sarcolemma, which exposes the intracellular muscle compartment to the extremely high extracellular calcium concentrations. If not repaired rapidly, the influx of calcium would result in cytotoxicity and cell death.

Two membrane repair mechanisms are the tension reduction hypothesis and the membrane patch repair mechanism. If the tear is sufficiently small (<1 um), the line tension inherent to the lipid bilayer will cause automatic lipid flow over the tear site, thus resealing the injury in a calcium-independent manner (McNeil et al., 2003). If the tear is large enough that line tension is superseded by the membrane tension (an opposing force caused by the lipid membrane being attached to the underlying cytoskeleton), the calcium-dependent membrane patch repair process is activated (McNeil et al., 2003). The influx of calcium triggers the accumulation of subsarcolemmal vesicles to the site of injury. The vesicles are then fused to each other and to the plasma membrane, thus providing the additional lipid bilayer required to form a membrane patch across the injury site (Figure 1.2). The repair process is very rapid, occurring within seconds, while the membrane remodeling process continues for at least twenty minutes more (Marg et al., 2012). Important membrane repair proteins include the transmembrane protein dysferlin and the cytoplasmic proteins caveolin-3, calpains and mitsugumin 53 (MG53 or TRIM72). Mutations in most of these proteins lead to individual LGMDs.

1.4 Dysferlinopathies

Dysferlinopathies are LGMDs caused by mutations in the *DYSF* gene, which codes for the protein dysferlin. Dysferlinopathies encompass three clinical phenotypes: Limb girdle muscular dystrophy type 2B (LGMD2B), Miyoshi Myopathy (MM) and Distal anterior compartment myopathy (Illa et al., 2001). These myopathies are characterized by

progressive degeneration of the proximal or distal skeletal muscles. As the muscles deteriorate and atrophy, fatty and connective tissues replace them. Inflammatory infiltrates can also be observed on muscle biopsies.

There is no cure or treatments available for patients with dysferlinopathies. Instead, patients are typically treated according to their symptoms. Often, the inflammatory infiltration observed in the muscle is initially misdiagnosed as an inflammatory myopathy (such as polymyositis), and patients are treated with anti-inflammatory drugs (namely, corticosteroids), which are ineffective against the dysferlinopathy and can result in adverse side effects, such as muscle strength, reduced bone density, hypertension, cataracts and diabetes (Hoffman et al., 2002; Walter et al., 2013).

LGMD2B affects about 15-20% of individuals with autosomal recessive LGMDs (Pegoraro et al., 1993). The onset of this disease is in the late teens or early twenties and primarily affects the proximal shoulder girdle and pelvic girdle muscles. These patients are asymptomatic prior to onset, and often athletic. Patients typically lose ambulation by their fourth decade, but it can vary to as early as their second decade or much later than their fourth decade.

Miyoshi Myopathy (MM) has an onset in the second decade of life. However, the clinical manifestation of MM differs from LGMD2B: whereas the proximal muscles are affected in LGMD2B, MM initially affects the distal muscles, particularly the gastrocnemius muscle (Illa et al., 2001). Over time, the muscle weakness spreads to encompass proximal muscles as well. MM and LGMD2B occur with equal frequency among patients.

Distal anterior compartment myopathy shares many clinical similarities to Miyoshi Myopathy, except that the anterior tibialis muscles are initially affected, followed by rapid progression to upper and lower extremity proximal muscles (Illa et al., 2001).

Mutations in *DYSF* are located throughout the gene, and include duplications, insertions and deletions, but the majority are caused by single amino acid substitutions (71%). Nearly 40% of these substitutions are missense mutations, whereas 20% of the substitutions comprise nonsense mutations (Figure 1.3) (den Dunnen, 1998).

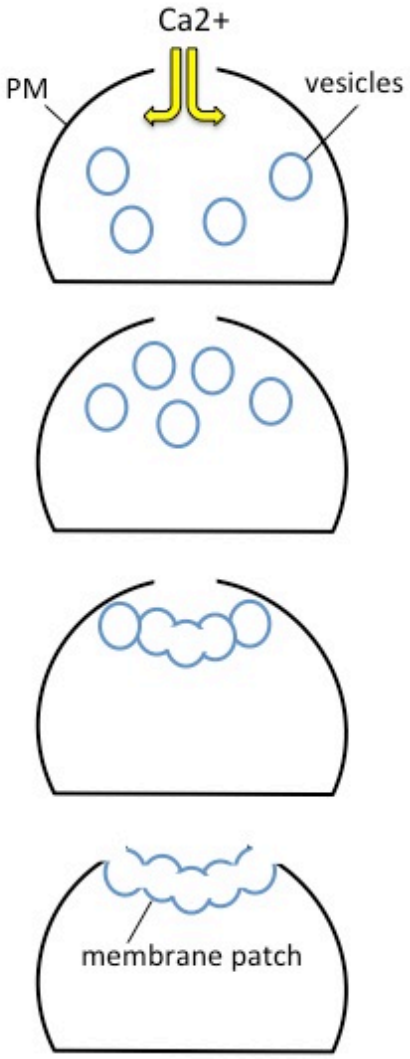

Figure 1.2: Plasma membrane repair process

Tears in the plasma membrane (PM) trigger the influx of extracellular calcium into the muscle cell or fiber. Calcium influx triggers the accumulation of subsarcolemmal vesicles to the site of injury. The vesicles fuse to each other and to the plasma membrane, thus forming a membrane patch across the injury site.

1.4.1 Dysferlin discovery and phylogeny

In 1998, two independent laboratories led by Drs Bushby and Brown discovered *DYSF* and connected it to LGMD2B and MM (Bashir et al., 1998; Liu et al., 1998). *DYSF* is located on chromosome 13 at position 2p13.3-p13.1. The more than 150 kilobases (kb) of genomic DNA encode 55 exons that consist of 6.9 kb of coding sequence.

Dysferlin is related to the *Fer-1* gene product of *Caenorhabditis elegans (C. elegans)* (Bashir et al., 1998). The fertility factor 1 (Fer-1) protein encoded by this gene is expressed in primary spermatocytes and is critical for the worm's spermatogenesis. The spermatid contains membranous organelles that are a rich source of stacked membrane material. During spermatogenesis, the membranous organelles fuse to the plasma membrane, providing the extra lipid bilayers needed for the pseudopod (Ward et al., 1981). The Fer-1 protein is critical for this calcium-dependent membrane fusion event, and mutations in *Fer-1* lead to impaired sperm motility and worm infertility (Achanzar et al., 1997; Washington et al., 2006). Fer-1 mRNA has also been detected in the muscle cells of *C. elegans* (Krajacic et al., 2009). Mutations in *Fer-1* were shown to alter the gene expression of muscle-enriched genes known to regulate muscle structure and function (Krajacic et al., 2009).

1.4.1 Mammalian Ferlin Proteins and Disease

To date, six human homologues of the ferlin family are known: dysferlin (Fer1L1), otoferlin (Fer1L2), myoferlin (Fer1L3), Fer1L4, Fer1L5 and Fer1L6. All six homologues are characterized by multiple C2 domains and a single C-terminal transmembrane domain (Figure 1.3). Most contain at least one DysF domain (Han et al., 2007). Only dysferlin and otoferlin have been associated with human pathology.

Dysferlin is a 236 kiloDalton (kDa) protein that contains seven C2 domains and two DysF domains. It is highly expressed in skeletal muscle and cardiac muscle, and is also found in the placenta. Dysferlin mRNA can also be weakly detected in brain, kidney and lung, and even more weakly in liver and pancreas. In muscle cells, dysferlin localizes to the plasma membrane and T-tubule network, as well as in cytoplasmic vesicles of as yet

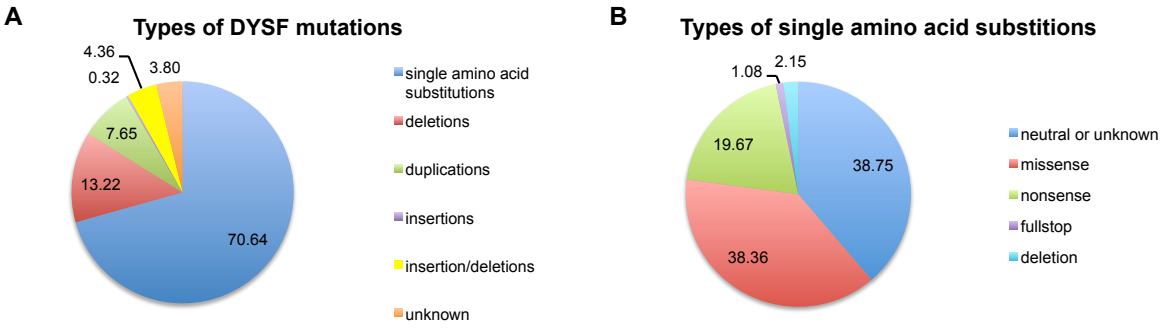

Figure 1.3: Types of DYSF mutations

Graphical representation of types of DYSF mutations (A) and further breakdown of single amino acid substitutions (B).

unknown origin (Bansal et al., 2003). Its levels are upregulated during muscle cell differentiation, when mature multinucleated myotubes are formed.

Otoferlin is a 226 kDa protein containing six C2 domains and lacking DysF domains (Han et al., 2007). Like Fer-1, otoferlin is essential for calcium-dependent membrane fusion events. Otoferlin is also found in skeletal muscle but is most highly expressed in vertebrate mechanosensory hair cells, specifically the ribbon synapse of auditory inner hair cell (Beurg et al., 2008). It acts as a calcium sensor and membrane fusion protein during auditory synaptic neurotransmission (Roux et al., 2006; Beurg et al., 2008; Ramakrishnan et al., 2009; Beurg et al., 2010; Johnson et al., 2010). Mutations in the *OTOF* gene lead to a recessively inherited form of human deafness called nonsyndromic prelingual deafness DFNB9 (Yasunaga et al., 1999; Varga et al., 2003).

Myoferlin shares the most structural similarity to dysferlin. It is a 230 kDa protein containing seven C2 domains and two DysF domains. Myoferlin is expressed in skeletal and cardiac muscles, and in low levels in the lung (Davis et al., 2000). Myoferlin is highly expressed in undifferentiated myoblasts and is necessary for calcium-dependent myoblast fusion events during myogenesis (Davis et al., 2000; Doherty et al., 2005). Its levels decrease post-fusion. Absence of myoferlin leads to impaired myoblast fusion (Doherty et al., 2005; Doherty et al., 2008). Although myoferlin has not been associated with human pathology, myoferlin-null mice have smaller body and muscle mass than wildtype littermates, which is believed to be due to defective myoblast fusion or reduced muscle diameter (Doherty et al., 2005). These studies also demonstrated that myoferlin null muscle exhibited slower, incomplete regeneration after injury, due to an impairment in forming large myofibers (Doherty et al., 2005). Recent additional roles attributed to myoferlin include endocytic recycling, epithelial cell adhesion and tumorigenesis (Bernatchez et al., 2007; Bernatchez et al., 2009; Leung et al., 2012; Leung et al., 2013).

Fer1L5 is a 241 kDa protein containing six C2 domains and two DysF domains, and is highly similar to myoferlin in sequence. It is expressed in small myotubes containing two to four nuclei (Posey et al., 2011). During myotube formation, direct binding between the endocytic recycling proteins, EHD1 and EHD2, and Fer1L5 is required to

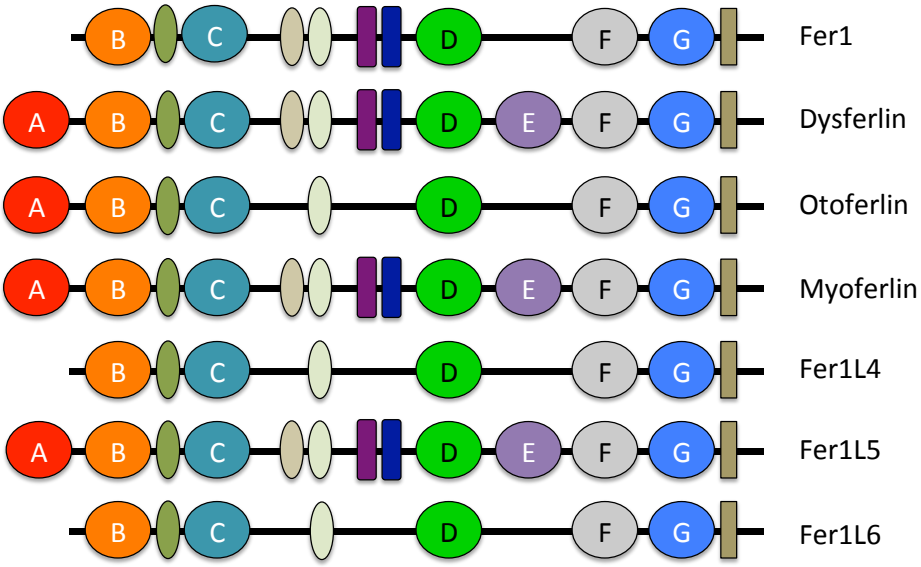

Figure 1.4: Ferlin proteins

To date, one *C. elegans* ortholog (Fer-1) and six human homologues of the ferlin family are known: dysferlin (Fer1L1), otoferlin (Fer1L2), myoferlin (Fer1L3), Fer1L4, Fer1L5 and Fer1L6. They are characterized by the presence of multiple C2 domains (coloured circles), two or three fer domains (coloured ovals) and a single C-terminal transmembrane domain (brown rectangle). They can further divided into two subgroups depending on the presence or absence of a DysF domain (purple rectangles).

translocate Fer1L5 to the plasma membrane (Posey et al., 2011).

Little is known about Fer1L4 and Fer1L6. They are 201 kDa and 209 kDa, respectively, and contain five C2 domains. Their sequence is similar to otoferlin. The roles of Fer1L4 and Fer1L6 are unknown at this time, although one patient with ovarian dysgenesis, which is characterized by the loss of follicles before puberty, was shown to have a deletion that encompassed the *Fer1L6* gene (Ledig et al., 2010).

1.4.2 Dysferlin structure

Dysferlin is a type II transmembrane protein with a large cytoplasmic region containing seven C2 domains (named C2A to C2G, from N-terminus to C-terminus), three fer domains and two DysF domains. Extracellular to the C-terminal transmembrane domain is a small 6-residue segment.

C2 domains were first described as the second-constant sequence (C2) in protein kinase C. They are independently folded domains of approximately 130 residues, which assemble into a beta-sandwich motif containing eight anti-parallel beta-sheets. C2 domains mediate lipid and protein-binding interactions. They are generally involved in membrane interactions or fusion events, or in the generation of secondary messenger lipids involved in signal transduction pathways (Shao et al., 1996). The best-characterized C2 domain-containing proteins are synaptotagmins, particularly synaptotagmin 1 (Syt1). Syt1 acts as a calcium-sensor for synaptic vesicles and interacts with the SNARE complex to mediate rapid fusion of synaptic vesicles to the plasma membrane during neurotransmitter release (Brose et al., 1992; Sudhof et al., 1996).

C2 domains containing five conserved glutamic acid or aspartic acid residues in the loops between their beta-sheets can coordinate multiple calcium ions (Sudhof et al., 1996), allowing them to interact with negatively-charged phospholipids or proteins. Many C2 domains lacking some or all of these residues are still able to interact with lipids and proteins, thus classifying them as calcium-independent C2 domains (Davletov et al., 1993). The C2A domain of dysferlin and myoferlin were shown to bind negatively-charged phospholipids, namely phosphatidylserine, phosphatidylinositol 4-phosphate

and phosphatidylinositol 4,5-bisphosphate, in a calcium-dependent manner (Davis et al., 2002; Therrien et al., 2009). The other C2 domains bound to phosphatidylserine with lower affinity in a calcium-independent manner, but showed no binding activity to either phosphatidylinositol 4-phosphate or phosphatidylinositol 4,5-bisphosphate (Therrien et al., 2009). The C2 domains of synaptotagmins and of dysferlin are reported to bind calcium ions and lipids cooperatively (Herrick et al., 2006; Marty et al., 2013). A Val67Asp mutation in dysferlin's C2A domain disrupts the cooperative calcium binding necessary for lipid interactions, as well as alters dysferlin's C2A binding to MG53 dimers (Davis et al., 2002; Matsuda et al., 2012).

Dysferlin contains two DysF domains, with one DysF nested within the other, as a consequence of an internal duplication. Dysferlin, myoferlin, Fer1L5 and Fer-1 all contain an internal duplication of the DysF domain. There is 57% sequence identity and 72% sequence similarity between the inner DysF domains of myoferlin and dysferlin (Patel et al., 2008), hinting at their structural similarity. A structural study of the inner DysF domain of myoferlin revealed it to be two long antiparallel beta-strands linked by a long loop consisting of short stretches of beta-strand, which form an antiparallel four-stranded sheet (Patel et al., 2008). The internal duplication can be structurally tolerated because it exists between secondary structure elements (Patel et al., 2008). Thus, the inner DysF domain would emerge from the loop of the outer DysF domain, and both domains would have the same fold.

Numerous mutations have been localized to the DysF domains; in 2008, 13% of missense mutations were mapped to the inner DysF domain (Patel et al., 2008). However, its function is still unknown. Given the presence of multiple arginine/aromatic stacks formed by conserved arginines and tryptophans within the inner DysF domain of myoferlin, it has been proposed that it may be involved in the structural integrity of the domain (Patel et al., 2008), such as has been noted for receptor proteins, such as gp130 and thrombospondin repeat-containing growth factors (Bravo et al., 1998; Tan et al., 2002).

1.4.3 Dysferlin function

Dysferlin is required for the membrane fusion events between the subsarcolemmal vesicles and the plasma membrane. Electron microscopy scans of muscle biopsies from dysferlin-deficient patients show a subsarcolemmal accumulation of unfused vesicles beneath the injury site and empty swollen cisternae in the Golgi apparatus (Piccolo et al., 2000; Selcen et al., 2001; Cenacchi et al., 2005). This observation is comparable to the fusion deficit seen in Fer-1 mutants in *C. elegans* (Achanzar et al., 1997; Washington et al., 2006). In 2003, Bansal et al provided the crucial study demonstrating the necessity of dysferlin in skeletal muscle membrane repair. Using a laser-induced injury assay on control and dysferlin-deficient mouse muscle fibers in the presence of a membrane impermeant fluorescent dye, the authors showed that the plasma membrane is repaired in a calcium-dependent manner, and that this process requires dysferlin expression (Bansal et al., 2003).

In the decade following dysferlin's discovery, it has been revealed that dysferlin is part of a membrane repair complex. A zebrafish model of dysferlinopathy showed that following sarcolemmal injury, dysferlin-enriched vesicles are mobilized from the plasma membrane, in addition to cytoplasmic annexin 6. They both arrive at the injury site and independently form a membrane patch (Roostalu et al., 2012). Subsequently, calcium-dependent phospholipid binding proteins, annexins A1 and A2, are recruited to the injury site and interact with dysferlin during the membrane patch formation (Lennon et al., 2003; Roostalu et al., 2012). During recruitment to the injury site, dysferlin complexes with caveolin-3 and mitsugumin 53 (MG53), a muscle-specific TRIM protein, for correct localization and proper membrane repair function (Matsuda et al., 2001; Cai et al., 2009; Waddell et al., 2011; Matsuda et al., 2012).

During and following membrane repair, the cytoskeleton requires rearrangement. AHNAK was shown to mediate cortical actin organization by binding to dysferlin's C2A domain, to actin and to annexin A2 (Hohaus et al., 2002; Benaud et al., 2004; Huang et al., 2007). This interaction is disrupted by calpain-3, a calcium-dependent cysteine protease, which cleaves AHNAK into smaller fragments and abolishes AHNAK binding to dysferlin (Huang et al., 2007; Huang et al., 2008).

In recent years, dysferlin has also been implicated in myogenesis (de Luna et al., 2006), calcium signaling (Covian-Nares et al., 2010), endothelial cell adhesion and angiogenesis (Sharma et al., 2010), endothelial trafficking of membrane bound proteins (Leung et al., 2011). At the start of this thesis, our research group had performed a liquid chromatography-tandem mass spectrometry analysis of a dysferlin affinity purification assay, which generated a list of potential dysferlin-interacting proteins. One of the proteins investigated was alpha-tubulin, and our research group determined that dysferlin could bind to alpha-tubulin in its monomeric form and its polymerized form (microtubules) via dysferlin's C2A and C2B domains (Azakir et al., 2010). This interaction was calcium-independent and it was suggested that dysferlin-containing vesicles may be transported along microtubules to the plasma membrane (Azakir et al., 2010).

1.5 Current treatments for dysferlinopathies

Currently, there are no cures or treatments available for LGMD2B. Patients are typically treated according to their symptoms. To improve quality of life and prolong survival, patients may be recommended to promote joint mobility (by physical therapy and stretching exercises) and ambulation (with mechanical aids) (Pegoraro et al., 1993).

1.5.1 Gene therapy strategies for dysferlinopathies

1.5.1.1 Full-length protein reconstitution

In the case of DMD, investigations into intramuscular injection of full-length dystrophin plasmid DNA performed in the early 1990s yielded low dystrophin expression (Acsadi et al., 1991). A decade later, electroporation of full-length dystrophin cDNA into the skeletal muscle of an adult *mdx* mouse (a well-characterized dystrophin-deficient mouse model for DMD) generated only 5.6% dystrophin-positive muscle fibers (Murakami et al., 2003). However, no functional assays were performed to see if the exogenously expressed dystrophin alleviated the dystrophic pathology. Presumably based on the poor success of this strategy in DMD, few full-length dysferlin cDNA transfer studies have been investigated.

1.5.1.2 Adeno-associated virus-mediated gene transfer

Adeno-associated virus (AAV) is the vector of choice for somatic gene therapy towards skeletal muscle diseases, given its ability to infect dividing and non-dividing cells, relatively low immunogenicity, lack of pathogenicity, low immunogenicity and ability to establish long-term transgene expression (Wu et al., 2006). In particular, AAV serotypes 1, 2, 5, 6, 8 and 9 are known to express well in muscle (Coura Rdos et al., 2007). Current developments in artificially-derived AAV vectors, which have the combined properties of two different natural AAVs, have shown improved skeletal muscle tropism, expression and titer (Koo et al., 2011; Lompre et al., 2013). AAV 2.5 showed no cellular immune response in a phase I clinical trial in Duchenne boys (Bowles et al., 2012).

It was observed that BMD patients harbouring deletions within the protein's rod domain produced truncated dystrophin proteins with minimal functional deficit (England et al., 1990; Matsumura et al., 1994). From this discovery, mini-dystrophins have been generated harbouring similar, and even larger, deletions such that the minimal functional dystrophin unit can be packaged within an AAV vector. Injection in *mdx* mice or in a dystrophin/utrophin double knockout mouse model of DMD resulted in pathophysiological rescue and extended lifespan (Wang et al., 2000; Sakamoto et al., 2002; Yuasa et al., 2002; Gregorevic et al., 2006). Long-term studies of AVV 2.8-encapsidated mini-dystrophin injected into a dog model of DMD (CXMDj) demonstrated stable and high levels of minidystrophin for at least 8 weeks without an immune reaction (Koo et al., 2011). Additionally, the minidystrophin injection conferred protection from dystrophic damage (Koo et al., 2011).

However, AAV's major limitation is its small cDNA insert capacity of 4.7kb. Dysferlin's cDNA consists of 6.9kb of coding DNA, thus severely restricting its applicability to AAV-mediated gene transfer therapy. Although it has been suggested that larger genomes can be packaged into AAV vectors (Grieger et al., 2005; Allocca et al., 2008), in-depth analysis showed that regardless of the size of the plasmid encoded vector or the capsid type, the packaged AAV vector genomes can not exceed 5.2 kb in length (Wu et al., 2010) and that large vector genomes observed in the aforementioned studies (Grieger

et al., 2005; Allocca et al., 2008) were probably generated through rare recombination events (Wu et al., 2010).

One alternative gene transfer strategy consists of packaging each half of dysferlin's cDNA into two AAV vectors and engineering them to concatemerize inside the muscle (Lostal et al., 2010). Dysferlin's cDNA was split at the exon 28/29 junction and cloned into two AAV2 vectors. Tail-vein injection of the virus into the dysferlin-deficient mouse led to expression of full-length dysferlin, albeit at very low levels, yet had a demonstrable improvement of the histological aspect of the muscle, a reduction in the number of necrotic fibers, restoration of membrane repair capacity and a global improvement in locomotor activity (Lostal et al., 2010).

1.5.1.3 Exon skipping strategies

In 2006, our research group discovered an atypical dysferlin-deficient family. The two daughters had a homozygous null mutations in their two *DYSF* alleles resulting in total loss of dysferlin protein, manifesting in the typical dysferlin-deficient pathology. On the other hand, their mother had one *DYSF* allele with the null mutation, and the other *DYSF* allele had a lariat branch point mutation resulting in natural in-frame skipping of exon 32. This allele produced a *DYSF* mRNA lacking its 32nd exon, which translated into a protein with an internal truncation of dysferlin's C2D domain. Remarkably, this patient only had a mild form of the disease, leaving her ambulatory well into her seventies (Sinnreich et al., 2006).

This natural example of exon-skipping in a dysferlin-deficient patient suggested the feasibility of a novel therapeutic strategy for dysferlinopathies. In 2010, exon skipping of dysferlin's exon 32 successfully demonstrated the splicing of dysferlin mRNA lacking its 32nd exon in control and dysferlin-deficient patient-derived muscle cells using either antisense oligonucleotides (AON) or a modified U7 small nuclear RNP (snRNP) containing the target antisense sequence (Wein et al., 2010). Another natural example of dysferlin skipping of exon 49 was recently described in a small group of Portuguese dysferlinopathy patients (Santos et al., 2010). A recent study investigated which *DYSF*

exons may be amenable to skipping and identified four *DYSF* exons that were efficiently skipped and producing in-frame mRNAs using AONs (Aartsma-Rus et al., 2010).

Exon skipping is currently the most promising therapeutic strategy for treating DMD. Since a significant number of DMD mutations reside within the same few exons, one can remove the exon containing the mutation. This typically results in the conversion of the severe DMD phenotype into the milder BMD phenotype. This strategy is the most advanced and promising treatment for DMD and is currently in phase I/II clinical trials (van Deutekom et al., 2007; Kinali et al., 2009; Cirak et al., 2011).

1.6 Objectives

The main objectives of this thesis are as follows:

Objective I - To determine the significance of dysferlin's interaction with alpha-tubulin, as was previously described by our research group following a liquid-chromatography-mass spectrometry analysis of the dysferlin interactome.

- This thesis objective will be addressed in Chapter 2.

Objective II – To determine if there is functional redundancy between dysferlin's seven C2 domains in their ability to localize to and repair the muscle plasma membrane.

- This thesis objective will be addressed in Chapter 3.

Objective III – To determine if a small mini-dysferlin can be generated that retains the functionality of full-length dysferlin, which would be small enough to encapsidate within an adeno-associated viral vector.

- This thesis objective will be addressed in Chapter 3.

Objective IV – To determine the degradation pathway(s) of wildtype dysferlin and missense-mutated dysferlin.

- This thesis objective will be addressed in Chapter 4.

Objective V – To determine whether missense-mutated dysferlin retains its biological activity, despite being flagged for degradation by the cell's quality control system.

- This thesis objective will be addressed in Chapters 4 and 5.

CHAPTER 2

2 Dysferlin interacts with histone deacetylase 6 and increases alpha-tubulin acetylation

2.1 Preface

At the time of this work, dysferlin's role in membrane repair was being expanded to include additional roles in myogenesis, cellular adhesion and intracellular calcium signaling. We had previously identified alpha-tubulin as a novel dysferlin-binding partner. However the significance of this interaction was not understood. This work describes a novel binding protein for dysferlin, histone deacetylase 6 (HDAC6), and its triad interaction with dysferlin and polymerized alpha-tubulin, as well as possible implications in skeletal muscle myogenesis.

2.2 Abstract

Dysferlin is a multi-C2 domain transmembrane protein involved in a plethora of cellular functions, most notably in skeletal muscle membrane repair, but also in myogenesis, cellular adhesion and intercellular calcium signaling. We previously showed that dysferlin interacts with alpha-tubulin and microtubules in muscle cells. Microtubules are heavily reorganized during myogenesis to sustain growth and elongation of the nascent muscle fiber. Microtubule function is regulated by post-translational modifications, such as acetylation of its alpha-tubulin subunit, which is modulated by the histone deacetylase 6 (HDAC6) enzyme. In this study, we identified HDAC6 as a novel dysferlin-binding partner. Dysferlin prevents HDAC6 from deacetylating alpha-tubulin by physically binding to both the enzyme, via its C2D domain, and to the substrate, alpha-tubulin, via its C2A and C2B domains. We further show that dysferlin expression promotes alpha-tubulin acetylation, as well as increased microtubule resistance to, and recovery from, Nocodazole- and cold-induced depolymerization. By selectively inhibiting HDAC6 using Tubastatin A, we demonstrate that myotube formation was impaired when alpha-tubulin was hyperacetylated early in the myogenic process; however, myotube elongation occurred when alpha-tubulin was hyperacetylated in myotubes. This study suggests a novel role for dysferlin in myogenesis and identifies HDAC6 as a novel dysferlin-interacting protein.

2.3 Introduction

Recessive mutations in the *DYSF* gene cause Limb girdle muscular dystrophy type 2B (LGMD2B) (Liu et al., 1998), Miyoshi Myopathy (Liu et al., 1998) and Distal anterior compartment myopathy (Illa et al., 2001). Dysferlin is a large type II transmembrane protein composed of two DysF domains and seven C2 domains that mediate lipid (Davis et al., 2002; Therrien et al., 2009) and protein binding interactions (Matsuda et al., 2001; Lennon et al., 2003; Huang et al., 2007; Cai et al., 2009; Azakir et al., 2010). Dysferlin is predominantly expressed in skeletal and cardiac muscle (Bashir et al., 1998), and its expression is upregulated during myogenesis (Bansal et al., 2004; Doherty et al., 2005). The subcellular localization of dysferlin is at the sarcolemma, T-tubule membranes and in intracellular vesicular compartments of as yet unknown origin (Bansal et al., 2003; Klinge et al., 2010). Dysferlin is a critical component of the calcium-dependent sarcolemmal repair complex, but recent studies have proposed additional roles for dysferlin in myogenesis (de Luna et al., 2006; Belanto et al., 2010; Demonbreun et al., 2011), intercellular calcium signaling (Covian-Nares et al., 2010) and cellular adhesion (Sharma et al., 2010). Our recent work identified alpha-tubulin and microtubules as novel binding partners of dysferlin (Azakir et al., 2010), suggesting a possible role for dysferlin in microtubule dynamics or stability.

The upregulation of microtubule acetylation is essential for myogenesis (Gundersen et al., 1989). Microtubule acetylation is regulated by alpha-tubulin acetyltransferases and deacetylases, the most notable one being histone deacetylase 6 (HDAC6) (Hubbert et al., 2002). Unlike most classical HDACs, which are located in the nucleus and deacetylate nuclear substrates such as histones, HDAC6 contains a nuclear exclusion signal and a cytoplasmic retention signal making it a cytoplasmic enzyme (Hubbert et al., 2002; Bertos et al., 2004). HDAC6 has two catalytic hdac domains used to deacetylate alpha-tubulin (Hubbert et al., 2002; Zhang et al., 2003; Rey et al., 2011), cortactin (Zhang et al., 2007; Rivieccio et al., 2009; Rey et al., 2011) and Hsp90 (Kovacs et al., 2005). HDAC6-mediated microtubule deacetylation plays important regulatory roles in microtubule dynamics (Tran et al., 2007; Zilberman et al., 2009), cellular motility (Zhang et al., 2007; Bazzaro et al., 2008; Wu et al., 2010; Rey et al., 2011) and motor protein motility (Reed et al., 2006).

In this study, we identified HDAC6 as a novel dysferlin interacting protein. Our results revealed that dysferlin binds to HDAC6 and alpha-tubulin, and prevents HDAC6 from deacetylating its substrate, alpha-tubulin. We also demonstrated that inhibition of HDAC6 activity in the early stages of myoblast differentiation results in impaired myogenesis, whereas increased microtubule acetylation in myotubes results in myotube elongation. We suggest that the increasing dysferlin expression observed during myogenesis could be required to decrease HDAC6-mediated microtubule deacetylation.

2.4 Results

Dysferlin interacts with HDAC6 and prevents alpha-tubulin deacetylation

We had previously performed a mass spectrometric analysis of the dysferlin protein complex (Azakir et al., 2010) and identified HDAC6 as a potential dysferlin interactor. This protein was also identified in another study (de Morree et al., 2010). To confirm this interaction, we performed binding assays using recombinant and native dysferlin and HDAC6 proteins. Recombinant dysferlin was able to bind either to recombinant FLAG-HDAC6 expressed in HEK293T cells (Figure 2.1A) or to native HDAC6 from homogenized murine testes (Figure 2.1B), which are a rich source of the enzyme. Co-immunoprecipitation assays performed in mouse skeletal muscle extracts showed that native dysferlin co-immunoprecipitated with native HDAC6 (Figure 2.1C).

To determine if dysferlin and HDAC6 co-localized in the same subcellular compartment, GFP-myc-dysferlin and FLAG-HDAC6 were transfected into Cos7 cells. Immunostaining showed partial co-localization between the two proteins in the cytoplasm and in the vicinity of the plasma membrane (Figure 2.1D). To determine if the proteins co-localized in muscle cells, FLAG-HDAC6 was transfected into a human myoblast cell line (134/04), which harbours two wildtype DYSF alleles, and cells were differentiated into myotubes. Immunostaining with anti-dysferlin and anti-FLAG antibodies demonstrated that the proteins partially co-localized in the cytoplasm and in the vicinity of the plasma membrane (Figure 2.1E).

To identify which of dysferlin's seven C2 domains could be involved in the interaction with HDAC6, we constructed a series of single C2 domain deletion mutants from full-length wildtype (WT) dysferlin, which harbours an N-terminal GFP tag and C-terminal myc-His tags (Figure 2.2A). Each mutant (ΔC2A to ΔC2G), or WT dysferlin or a GFP vector was expressed in HEK293T cells, immobilized on nickel affinity beads, and incubated either with recombinant FLAG-HDAC6 (Figure 2.2B) or with native HDAC6 from homogenized murine testes (Figure 2.2C). In both assays, dysferlin's C2D domain was required for the interaction with HDAC6.

Given that HDAC6 is a major alpha-tubulin deacetylase, we assayed for dysferlin's effect on alpha-tubulin acetylation. Alpha-tubulin acetylation levels increased in HEK293T cells expressing wildtype dysferlin (WT) or the following C2 domain deletion mutants: ΔC2B, ΔC2C, ΔC2E, ΔC2F and ΔC2G (Figure 2.2D). Cells expressing ΔC2A or ΔC2D showed no change in alpha-tubulin acetylation levels compared to GFP vector-expressing cells, indicating that dysferlin requires its C2A and C2D domains to prevent HDAC6 from deacetylating alpha-tubulin.

Dysferlin requires alpha-tubulin binding to prevent HDAC6 from deacetylating alpha-tubulin

We recently showed that dysferlin interacts with alpha-tubulin through its C2A and C2B domains, although this interaction is weaker with the C2B domain than with the C2A domain (Azakir et al., 2010). Figures 2.2B and 2.2C show that the ΔC2A deletion mutant interacted less strongly with alpha-tubulin when compared to wildtype dysferlin or the other six deletion mutants, which is in agreement with our previously published results. Notably, the interaction was not fully abolished since the ΔC2A deletion mutant retains its C2B domain, which also interacts with alpha-tubulin, albeit weakly. Theorizing that dysferlin requires both of its alpha-tubulin binding domains to interact with HDAC6, we used a truncated dysferlin mutant lacking its three N-terminal C2 domains, but retaining its DysF domains (DD) and the transmembrane domain (TM) (DD-DEFG-TM) (Figure 2.3A). As expected, this N-terminally truncated mutant did not pull down alpha-tubulin, and also showed weaker binding to HDAC6 (Figure 2.3B). This suggests that

dysferlin also requires both of its alpha-tubulin binding domains (C2A and C2B) to fully interact with HDAC6.

We assessed whether the truncated mutant DD-DEFG-TM could affect alpha-tubulin acetylation levels in HEK293T cells. As shown in Figure 2.3C, DD-DEFG-TM did not alter the amount of acetylated alpha-tubulin, similarly to ΔC2A and ΔC2D deletion mutants. In agreement with Figure 2.2D, these results highlight the importance of dysferlin's C2A domain in preventing alpha-tubulin deacetylation.

Having shown that dysferlin's alpha-tubulin binding domains are important for impairing HDAC6-mediated deacetylation of alpha-tubulin, we theorized that dysferlin may be having this effect by affecting HDAC6's ability to interact with its substrate. To assess how dysferlin may affect HDAC6's interaction with alpha-tubulin, we performed an alpha-tubulin immunoprecipitation assay in HEK293T cells expressing FLAG-HDAC6 along with either wildtype dysferlin (WT), the ΔC2A or ΔC2D deletion mutants, or with the truncated mutant (DD-DEFG-TM). As shown in Figure 3D, in the absence of dysferlin, HDAC6 is able to bind to alpha-tubulin. However, in the presence of full-length dysferlin, alpha-tubulin no longer pulled down HDAC6, but only dysferlin. This effect was only observed if dysferlin retained its C2D domain as well as its alpha-tubulin binding C2A and C2B domains; if these domains were deleted, dysferlin did not prevent HDAC6 from interacting with alpha-tubulin. This is demonstrated by the ΔC2D and DD-DEFG-TM constructs, which showed an unimpaired HDAC6 interaction with alpha-tubulin (Figure 2.3D). Because the ΔC2A construct still had partial alpha-tubulin binding capabilities and an intact C2D domain, it was able to decrease HDAC6's interaction with alpha-tubulin, but not abolish it completely as did wildtype dysferlin. These results suggest that dysferlin prevents HDAC6 from interacting with its substrate, thus hindering alpha-tubulin deacetylation.

Dysferlin expression increases alpha-tubulin acetylation and resistance to microtubule depolymerization

Having demonstrated that recombinant dysferlin affects alpha-tubulin acetylation levels in HEK293T cells, we assessed whether native dysferlin expression also affected alpha-

tubulin acetylation in muscle cells. We used three human myoblast cell lines: 134/04 cells harbouring two wildtype DYSF alleles, ULM1/01 cells harbouring two nonsense DYSF alleles, and 180/06 cells harbouring one missense DYSF allele and one nonsense DYSF allele. The cells were cultured, lysed and immunoblotted for acetylated-alpha-tubulin and alpha-tubulin levels. As shown in Figure 2.4A, wildtype cells (134/04) had higher levels of acetylated alpha-tubulin than dysferlin-deficient cells (180/06 and ULM1/01). To confirm that the effect was specific to dysferlin expression, wildtype dysferlin (WT) or the ΔC2A deletion mutant was overexpressed in 134/04 cells. In agreement with Figures 2.2D and 2.3C, dysferlin overexpression in muscle cells resulted in increased alpha-tubulin acetylation levels, whereas expression of the ΔC2A deletion mutant did not affect alpha-tubulin acetylation (Figure 2.4B).

Microtubule post-translational modifications occur subsequent to microtubule stabilization; therefore alpha-tubulin acetylation can be considered as a marker of stabilized microtubules (Westermann et al., 2003). Stabilized microtubules are more resistant to microtubule depolymerization. We theorized that the increased alpha-tubulin acetylation levels observed in dysferlin-expressing cells were indicative of a pool of microtubules with increased resistance to depolymerization. To test this theory, we employed cold-induced and Nocodazole-induced microtubule depolymerization assays. In the cold-induced depolymerization assay, 134/04, 180/06 and ULM1/01 cells were incubated at 4^{o}C for increasing lengths of time, and microtubule resistance was assessed by the amount of acetylated alpha-tubulin remaining post-treatment. As shown in Figures 2.5A and 2.5E, 134/04 cells retained significantly higher acetylated alpha-tubulin levels following cold treatments (30, 45 and 60 min) than dysferlin-deficient 180/06 and ULM1/01 cells. In the Nocodazole-induced depolymerization assay, 134/04, 180/06 and ULM1/01 cells were treated with increasing concentrations of Nocodazole, and microtubule resistance to depolymerization was assessed by the amount of acetylated alpha-tubulin remaining post-treatment. As shown in Figures 2.5B and 2.5F, 134/04 cells retained significantly higher acetylated alpha-tubulin levels following Nocodazole treatment (3μg/ml and 9μg/ml) than dysferlin-deficient 180/06 and ULM1/01 cells. To demonstrate that the effect was specific to dysferlin expression, wildtype dysferlin (WT) or ΔC2A were expressed in HEK293T cells, which were similarly treated with Nocodazole. As shown in Figures 2.5C and 2.5G, cells transfected

with WT dysferlin showed significantly more acetylated alpha-tubulin levels post-Nocodazole treatment when compared to untransfected (CTL) cells. In agreement with our previous results, this effect required dysferlin's C2A domain, as cells transfected with ΔC2A showed acetylated alpha-tubulin levels that were comparable to untransfected (CTL) cells. These results suggest that dysferlin expression correlates with increased microtubule resistance to Nocodazole treatment, indicative of the presence of a larger pool of stable microtubules.

Once the microtubule depolymerising agent is removed, microtubules will repolymerize during a recovery phase (Musa et al., 2003). To study the effect of dysferlin expression on microtubule recovery from Nocodazole treatment, cells were treated with Nocodazole for 45min and then the drug-containing media was removed and replaced with fresh media, thus allowing repolymerization of microtubules. After defined lengths of time, the alpha-tubulin acetylation levels were measured as a marker of microtubule repolymerization and stabilization. Figures 2.5D and 2.5H show that dysferlin expression (134/04 cells) resulted in faster recovery from Nocodazole treatment than was observed in dysferlin-deficient cells (180/06 or ULM1/01 cells). Taken together, these results show that dysferlin expression increases cellular alpha-tubulin acetylation levels, as well as promotes microtubule resistance to, and recovery from, induced depolymerization.

Hyperacetylation of alpha-tubulin impairs myogenesis

Microtubule acetylation and dysferlin expression are both upregulated during myogenesis (Gundersen et al., 1989; Doherty et al., 2005). To demonstrate this in our cultured human myoblasts, 134/04 cells were cultured in differentiation media for up to four days to induce myotube formation. Lysates from these cells and from homogenized mouse skeletal muscle were immunoblotted for dysferlin and acetylated-alpha-tubulin levels. Results showed that both dysferlin and acetylated alpha-tubulin levels increased during myogenic differentiation (Figure 2.6A). Immunofluorescent staining for acetylated alpha-tubulin levels in 134/04 cells show significantly higher levels in differentiated myotubes than in undifferentiated myoblasts (Figure 2.6B). On the other hand, dysferlin-deficient myoblasts (180/06) do not differentiate into

myotubes and the acetylated alpha-tubulin were unchanged even after four days in differentiation media (Figure 2.6B).

Our data suggests that upregulated dysferlin expression would increase microtubule acetylation via its interaction with HDAC6. Given that microtubule acetylation is a late-stage event in myogenesis, we theorized that early upregulation of dysferlin would result in prematurely increased acetylation levels, which could have detrimental effects on myotube formation. However, dysferlin has previously been shown to play a role in myogenesis (de Luna et al., 2006; Demonbreun et al., 2011), for instance by affecting myogenin expression (de Luna et al., 2006). Therefore, it would not be possible to attribute any potential myogenic effect from overexpressing dysferlin in dysferlin-deficient myoblasts specifically to dysferlin's role on alpha-tubulin acetylation. Therefore, we used instead an HDAC6-specific inhibitor that causes alpha-tubulin hyperacetylation, to mimic the effect of dysferlin overexpression on alpha-tubulin acetylation specifically. Tubastatin A is a more selective derivative of the HDAC6 specific inhibitor Tubacin, which specifically inhibits alpha-tubulin deacetylation without affecting HDAC6's other substrates (Haggarty et al., 2003; Zhang et al., 2003; Tran et al., 2007; Bazzaro et al., 2008; Butler et al., 2010).

Myoblast differentiation assays were performed by treating 134/04 human myoblasts and C2C12 murine myoblasts continuously with Tubastatin A beginning at different stages of myoblast differentiation: at the stage when myoblasts were undifferentiated (Day 0), at the stage when myoblasts were beginning to form myotubes (Day 2) or at the stage when myotubes were terminally differentiated (Day 4) (Figure 2.7A). Acetylated alpha-tubulin levels in the cell lysates were assessed to confirm Tubastatin A efficacy (Figure 2.7B). The cells were immunostained for desmin and DAPI (Figure 2.7C). Desmin-stained myotubes were counted and categorized according to length (Figure 2.7D). The number of nuclei per myotube was also counted and the average number of nuclei in each category of myotube length was determined (Figure 2.7E).

When treated early (Day 0, Day 2), myotube formation was significantly impaired (Figure 2.7C), resulting in fewer myotubes being formed (Figure 2.7F). The myotubes that did form were significantly shorter than mock-treated myotubes; additionally no

long myotubes (>500μm) were produced (Figure 2.7D). Conversely, when myotubes were hyperacetylated after terminal differentiation (Day 4), a significantly larger proportion of myotubes were longer than 600μm when compared to mock-treated cells (Figure 2.7D), indicating that myotube length was increased. The average number of nuclei in this category of myotubes (>600μm) was not significantly different from mock-treated cells (Figure 2.7E), indicating that the increased length was not due to increased myoblast fusion. These results suggest that microtubule hyperacetylation in the early-stages of myoblast differentiation is detrimental to myogenesis, whereas late-stage hyperacetylation can promote myotube elongation.

2.5 Discussion

Dysferlin is a multi-C2 domain transmembrane protein involved in skeletal muscle membrane repair, and has also been implicated in myogenesis, cellular adhesion and intercellular calcium signaling. In light of the growing evidence supporting dysferlin's multifunctionality, understanding dysferlin's biology will depend on identifying its interacting proteins. To this end, we previously undertook a proteomic search through the analysis of immunoprecipitated proteins from mouse skeletal muscle using liquid chromatography-tandem mass spectrometry (Azakir et al., 2010). In this study, we identified HDAC6 as a novel dysferlin binding partner, and present a new function for dysferlin in the modulation of alpha-tubulin acetylation via an interaction with this microtubule deacetylase.

We show that dysferlin prevents HDAC6 from deacetylating alpha-tubulin by physically binding both to the enzyme via its C2D domain and to the substrate, alpha-tubulin, via its alpha-tubulin binding C2A and C2B domains. Consequently, dysferlin expression increased the alpha-tubulin acetylation levels in muscle cells. The increased alpha-tubulin acetylation levels in dysferlin-expressing cells reflect a larger pool of stable microtubules, which we showed are more resistant to Nocodazole-induced depolymerization and cold-induced depolymerization. Dysferlin expression also promoted faster microtubule recovery from depolymerization, resulting in more microtubules being repolymerized, stabilized and consequently post-translationally modified by acetylation.

A question that emerges from this study is how dysferlin prevents HDAC6 from interacting with its substrate. One possibility is that dysferlin targets HDAC6 via its C2D domain and then reinforces the interaction by binding to alpha-tubulin. Dysferlin may then directly or indirectly block HDAC6 from interacting with alpha-tubulin, thus inhibiting its ability to deacetylate microtubules. This is demonstrated by the observation that (i) loss of dysferlin's C2A domain resulted in a decreased interaction between HDAC6 and alpha-tubulin (Figure 2.3D) and (ii) loss of both of dysferlin's C2A and C2B domains resulted in decreased binding between dysferlin and HDAC6 (Figure 2.3B). Another possibility is that dysferlin binds to alpha-tubulin via its C2A and C2B domains, and uses its HDAC6-binding C2D domain to block or dislodge the enzyme from alpha-tubulin. This is suggested by the alpha-tubulin co-immunoprecipitation experiment (Figure 2.3D), in which full-length dysferlin was pulled down by alpha-tubulin but HDAC6 was not. It is further possible that dysferlin may sequester HDAC6 away from its substrate, as Figure 2.2 demonstrated a strong interaction between full-length dysferlin and HDAC6 that may be indicative of a cytoplasmic subpopulation of the two proteins, which would not be observed in the alpha-tubulin co-immunoprecipitation experiment. Further studies would be required to elucidate the mechanism involved in dysferlin's interaction with HDAC6.

To study the effect of alpha-tubulin hyperacetylation on myogenesis, we used Tubastatin A, a selective HDAC6 inhibitor. When HDAC6 was inhibited early during differentiation, myotube formation was impaired, whereas HDAC6 inhibition in differentiated myotubes promoted myotube elongation.

Impaired myogenesis arising from early microtubule hyperacetylation could be caused by disrupted microtubule dynamics and protein targeting. Dynamic microtubules are required to target the cell periphery and HDAC6 inhibition has been shown to decrease microtubule dynamics (Tran et al., 2007; Zilberman et al., 2009). Premature HDAC6 inhibition could promote a more stabilized microtubule pool, thus impairing the microtubule reorganization from a radial configuration in undifferentiated myoblasts to the organized longitudinal array observed in differentiated myotubes. Alpha-tubulin hyperacetylation would also compromise the microtubule tracks used for protein,

vesicle and organelle delivery. Proteins, such as CLASPs, depend on spatial cues along microtubules to locally regulate microtubule dynamics, which are provided by discrete regions of microtubule acetylation (Akhmanova et al., 2001). Such signals would be disrupted by microtubule hyperacetylation.

In myotubes, on the contrary, increased microtubule acetylation could promote myotube elongation by affecting microtubule polarization and motor protein movement. It has been proposed that the linear microtubule array in differentiated myotubes directly promotes myotube elongation by providing polarization, which restricts myotube elongation to a single axis (Saitoh et al., 1988; Guerin et al., 2009). Furthermore, microtubule acetylation enhances kinesin-1 recruitment to microtubules and anterograde movement along microtubules (Reed et al., 2006; Geeraert et al., 2010), thus permitting the delivery of cytoskeletal remodelling factors, target site recognition molecules or adhesion molecules (Kaverina et al., 1999; Krylyshkina et al., 2002). Additionally, microtubule acetylation has been proposed to designate stabilized microtubules extending all the way to a destination (Reed et al., 2006), thus promoting the delivery of proteins necessary for myotube formation and elongation.

Dysferlin expression is upregulated during myogenesis, with higher levels being observed in differentiated myotubes (Bansal et al., 2004; Doherty et al., 2005). We showed that Tubastatin A treatment of undifferentiated myoblasts resulted in impaired myotube formation, such as is observed in dysferlin-deficient myoblasts (de Luna et al., 2006; Demonbreun et al., 2011). Thus, our study suggests that early expression of dysferlin would promote premature microtubule hyperacetylation by way of inhibiting HDAC6, which would impair myotube formation. On the other hand, later expression of dysferlin would promote myotube formation and elongation through increased microtubule acetylation. This could explain the temporal expression pattern of dysferlin during myogenesis. The observed reduction in the number of long myotubes, and concomitant increase in short myotubes, in dysferlin-deficient cell cultures (Belanto et al., 2010; Demonbreun et al., 2011) is in keeping with our explanation for the temporally-regulated dysferlin expression during myogenesis. We theorize that the impaired myotube elongation in these cells might in part be explained by active HDAC6, which would maintain low levels of acetylated microtubules.

For the design of dysferlin gene therapies, our study would caution against the use of ubiquitous promoters or promoters expressed early in muscle development, such as CMV and CAG (Evans et al., 2008). Instead our data would support the use of promoters that are expressed at later stages of muscle differentiation, such as C5-12 (Spangenburg et al., 2004) and the human α-skeletal actin promoter (Evans et al., 2008).

In summary, we have identified HDAC6 as a novel dysferlin-interacting protein, and demonstrated that the interaction between these two proteins is mediated by dysferlin's C2D domain and that dysferlin prevents HDAC6 from deacetylating alpha-tubulin by physically binding to both the enzyme and to the substrate, alpha-tubulin. Finally, we demonstrated the importance of late alpha-tubulin hyperacetylation during the myogenic process, and propose that dysferlin may act as an inhibitor of HDAC6-mediated microtubule deacetylation during myogenesis.

2.6 Experimental Procedures

Ethics Statement

All animals were handled in strict accordance with good animal practice as defined by the relevant national and/or local animal welfare bodies, and all animal work was approved by the appropriate committee: Cantonal Veterinary Office of Basel, Switzerland (Approval IDs: 2391 and 51). Primary human myoblasts (134/04, 180/06 and ULM1/01) were obtained from EuroBioBank (www.eurobiobank.org) along with the required regulatory permissions (Approval ID: LMU 107/01).

Cell Cultures

C2C12 murine myoblasts and Human embryonic kidney derived cells (HEK293T) were purchased from ATCC (Burlington, Ontario) (ATCC number CRL-1573 and CRL-1772 respectively) (Azakir et al., 2010). 134/04 cells contain two wildtype DYSF alleles; 180/06 cells harbour one DYSF allele containing the missense mutation C1663T (Arg555Trp) and an additional null allele 3708delA (D1237TfsX24). Myoblast culture ULM1/01 harbours two null alleles: a C4819T (R1607X) substitution and a 5085delT (F1695LfsX48) deletion. Myoblast cultures were immortalized with a retrovirus

carrying the E6E7 early region from human papillomavirus type 16, as previously described (Lochmuller et al., 1999). Cells were maintained in growth media (10% FBS (Gibco) in DMEM (Sigma)).

Plasmids, Constructs, Antibodies

FLAG-tagged HDAC6 was purchased from AddGene (Plasmid number 13823). The GFP-myc-His-Dysferlin was a kind gift from Dr. K. Bushby, Newcastle (Klinge et al., 2007; Azakir et al., 2010). GFP-tagged dysferlin C2-domain deletion mutants were cloned from the full-length dysferlin construct, each having a single C2 domain deleted. Deletion of the C2 domains coding region was performed by PCR mutagenesis using domain spanning oligonucleotides and the QuikChange Site-Directed Mutagenesis Kit (Stratagene), using either the single (Makarova et al., 2000) or double mutagenic primers approach (Supplementary Table S1). The procedure was performed according to the manufacturer's protocols. Dysferlin truncation construct (DD-DEFG-TM), retaining its DysF domains (DD) and C2D-E-F-G domains (DEFG) and transmembrane domain (TM), was cloned from the full-length dysferlin construct. The C-terminal DD-DEFG-TM portion was first cloned into the pcDNA/TO/myc-His vector (Invitrogen), and then eGFP was added N-terminally in a second cloning step (Supplementary Table S1). All clones were sequenced in both DNA strands to confirm the deletions and the conservation of the reading frame.

Mouse monoclonal antibodies against dysferlin, FLAG and acetylated alpha-tubulin were purchased from Vector Laboratories, Sigma and Santa Cruz, respectively. Rabbit polyclonal antibodies against HDAC6 and alpha-tubulin were purchased from Abcam. Rabbit polyclonal GFP antibody was purchased from Invitrogen. Secondary antibodies, Alexa Fluor 680 goat anti-mouse IgG and InfraRed Dye 800 goat anti-rabbit IgG, were purchased from Invitrogen and Rockland, respectively.

Co-immunoprecipitation assays, pulldown assays and Western blot

Cells were transfected using Lipofectamine 2000 (Invitrogen) in OptiMEM (Gibco) for 48hours. Cells were lysed and immunoprecipitated (IP) as previously described (Azakir et al., 2010). For pulldown assays, dysferlin-transfected cells were similarly lysed, and supernatants were incubated with His-Select Nickel Affinity (Ni-NTA) Gel (Sigma) in the

presence of 20mM Imidazole (Sigma) overnight at 4°C, washed with 50mM Imidazole, and incubated with FLAG-HDAC6-expressing cell extracts (similarly prepared), or with wildtype murine testes homogenates (prepared as described (Azakir et al., 2010)), overnight at 4°C in IP buffer. Beads were washed with 50mM Imidazole and separated by SDS-PAGE. Proteins were transferred onto PVDF membranes, blocked in Blocking buffer (3% Top-Block (LubioScience) with 0.05% sodium azide (Sigma)), incubated overnight with the indicated antibodies in Blocking buffer plus 0.05% Tween-20 (Merck) and detected by Fluorimetric analysis (Odyssey version 2.1.12). All experiments were performed in triplicates. Densiometric analysis was performed using ImageJ 1.43u (NIH, USA). Statistical analysis was performed using the Student's T-test with a significance level of at least 0.05.

Microtubule depolymerization and recovery assays

For microtubule depolymerization assays, cells were grown to confluency and treated for 45min with the indicated concentration of Nocodazole (Sigma) in growth media, or alternatively incubated at 4°C for the indicated lengths of time. Cells were washed, lysed and western blotted as described above. For recovery experiments, cells were treated similarly, then Nocodazole was replaced with fresh media and cells were incubated at 37°C, 5% CO_2 for the indicated lengths of time. Cells were washed, lysed and western blotted as described above. All experiments were performed in triplicates. Densiometric analysis was performed using ImageJ 1.43u (NIH, USA). Statistical analysis was performed using the Student's T-test with a significance level of at least 0.05.

Immunofluorescence assays

Cells were grown on matrigel-coated coverslips in growth media or in differentiation media for four days to induce myotube formation. Cells were fixed with 4% paraformadehyde (PFA) for 20min, blocked 15min in 2% fish skin gelatin, 1% normal goat serum, 0.15% Triton X-100 in PBS and incubated for 1hour at room temperature with the indicated antibodies. Incubation with anti-FLAG antibodies was performed at 37°C for 2 hours. Cells were captured on a LSM 710 inverted confocal microscope (Zeiss) and analyzed using Zen 2009 LE software (Zeiss). All experiments were performed in triplicates.

Myoblast differentiation assays

Cells were grown to 80% confluency then switched to differentiation media (2% horse serum (Sigma) in DMEM). Cells were treated with 7.5uM Tubastatin A (BioVision, LubioScience) either at the same time at media switch (Day 0 or D0), after 48hours in differentiation media (Day 2 or D2) or after 72hours (Day 4 or D4). 24 hours later (Day 5), cells were lysed and western blotted as described above, or fixed with 4% PFA for 20min, blocked 15min in 2% fish skin gelatin, 1% normal goat serum, 0.15% Triton X-100 in PBS, then stained for desmin and DAPI. Myotubes were imaged with a Leica DMI6000B fluorescence microscope with the Volocity 5.2.0 software (Improvision Ltd) and analyzed with AnalySIS^{D} 5.0 (Soft-imaging). All experiments were performed in triplicates. Statistical analysis was performed using the Student's T-test with a significance level of at least 0.05.

2.7 Acknowledgements

We thank Muscle Tissue Culture Collection (MTCC) and Dr. Schneiderat from EuroBioBank for providing the human myoblast cultures used in this work. The Muscle Tissue Culture Collection is part of the German network on muscular dystrophies (MD-NET, service structure S1, 01GM0601) funded by the German ministry of education and research (BMBF, Bonn, Germany). The Muscle Tissue Culture Collection is a partner of Eurobiobank (www.eurobiobank.org) and TREAT-NMD (www.treat-nmd.eu). We thank Dr. Bushby (Newcastle, UK) for the GFP-myc-His-dysferlin cDNA. We thank Dr. Matthias and Gabriele Matthias (Basel, Switzerland) for the HDAC6-knockout mouse testes. We thank Dr. Spiess for helpful discussions. We thank Beat Erne (Basel, Switzerland) and Steven Salomon (Montreal, Canada) for technical assistance.

2.8 Figures and Figure Legends

Figure 2.1: Dysferlin co-immunoprecipitates with HDAC6

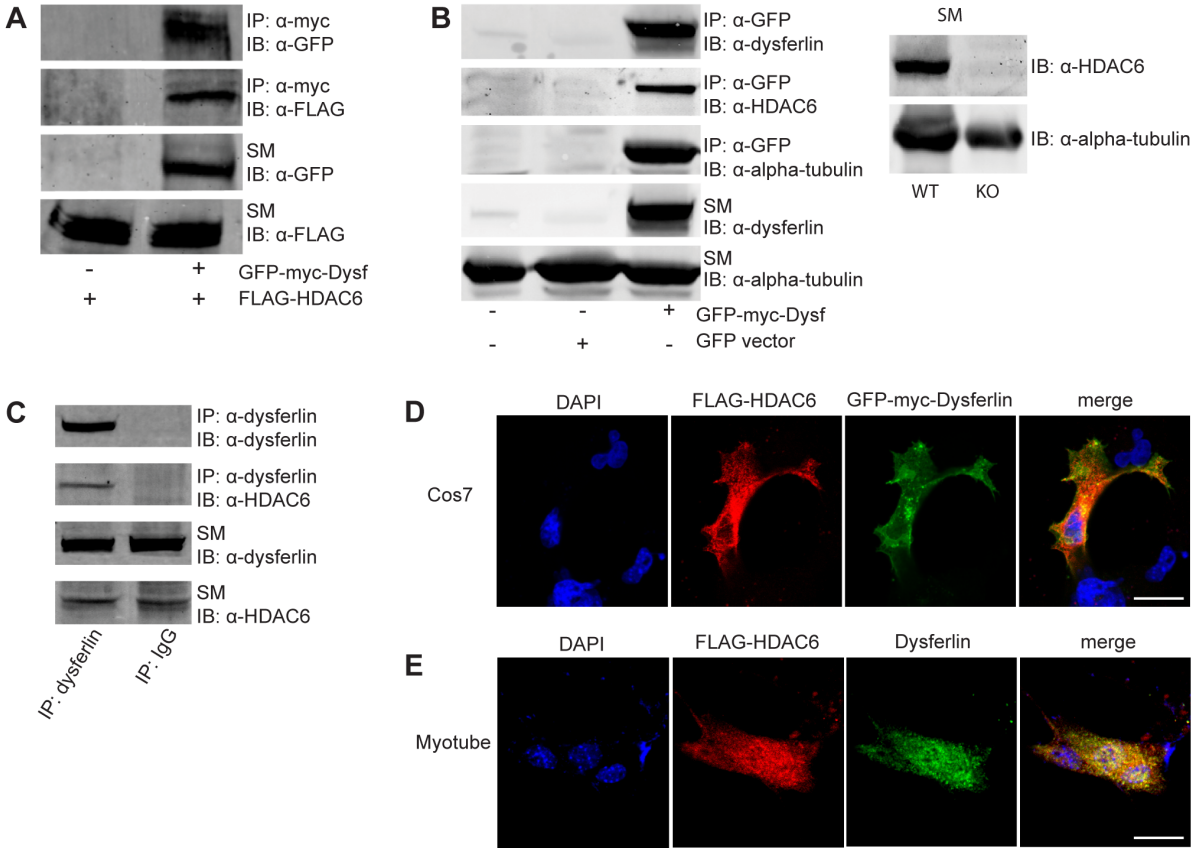

Figure 2.1: Dysferlin co-immunoprecipitates with HDAC6.

(A) HEK293T cells were transfected with GFP-myc-dysferlin (GFP-myc-Dysf) and FLAG-HDAC6, and recombinant dysferlin was immunoprecipitated (IP) with anti-myc antibodies. Immunoprecipitates were separated by SDS-PAGE and immunoblotted (IB) with the indicated antibodies. SM = starting material, 5% of total protein loaded. (B) GFP-myc-dysferlin (GFP-myc-Dysf) or GFP vector were transfected in HEK293T cells, immunoprecipitated with anti-GFP antibodies and incubated with testes homogenate from wildtype C57Bl/6 mice, which is a rich source of HDAC6. Immunoprecipitates were immunoblotted with the indicated antibodies. Alpha-tubulin was used as a loading control. (Right panel) HDAC6 protein levels in testes of wildtype C57Bl/6 mice (WT) versus HDAC6 knockout mice (KO), which were immunoblotted with anti-HDAC6 antibodies to demonstrate the specificity of the detected band. (C) Native dysferlin was immunoprecipitated with anti-dysferlin antibodies in mouse skeletal muscle extracts. Immunoprecipitates were separated by SDS-PAGE and immunoblotted with anti-dysferlin and anti-HDAC6 antibodies. (D) GFP-myc-dysferlin and FLAG-HDAC6 were overexpressed in Cos7 cells. Cells were fixed and immunostained with anti-GFP and anti-FLAG antibodies. (E) 134/04 cells were transfected with FLAG-HDAC6 and differentiated into myotubes. Cells were fixed and immunostained with anti-dysferlin and anti-FLAG antibodies. Scale bar: 20μm.

Figure 2.2: Dysferlin binds HDAC6 through its C2D domain and prevents alpha-tubulin deacetylation

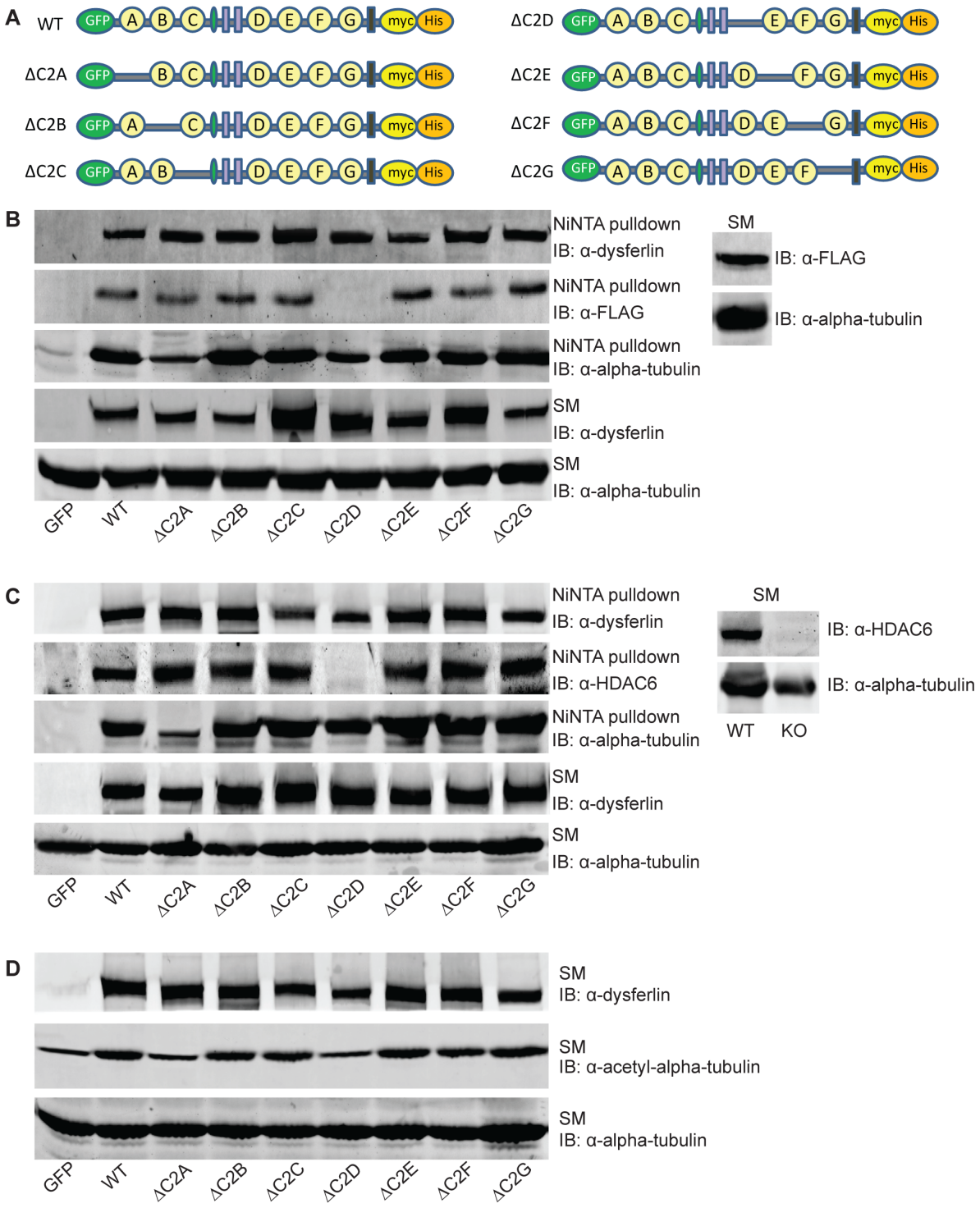

Figure 2.2: Dysferlin binds HDAC6 through its C2D domain and prevents alpha-tubulin deacetylation.

(A) Schematic of dysferlin C2 domain deletion constructs. (B) Wildtype dysferlin (WT), dysferlin deletion mutants (ΔC2A through ΔC2G) or GFP vector were transfected in HEK293T cells, pulled-down on Ni-NTA beads, and incubated with FLAG-HDAC6-transfected HEK293T cell lysates. Immunoprecipitates were immunoblotted with the indicated antibodies. (Right panel) FLAG-HDAC6 expression levels in transfected HEK293T cell lysates, immunoblotted with anti-FLAG antibody. (C) Wildtype dysferlin (WT), dysferlin deletion mutants (ΔC2A through ΔC2G) or GFP vector were transfected in HEK293T cells, pulled-down on Ni-NTA beads, and incubated with murine testes homogenate. Immunoprecipitates were immunoblotted with the indicated antibodies. (Right panel) This western blot is identical to the one displayed in Fig 1B. (D) Cell lysates from (C) were immunoblotted for alpha-tubulin acetylation levels. Similar results observed with cell lysates from (B) (not shown).

Figure 2.3: Dysferlin requires its alpha-tubulin binding domains to bind HDAC6 and prevent alpha-tubulin deacetylation.

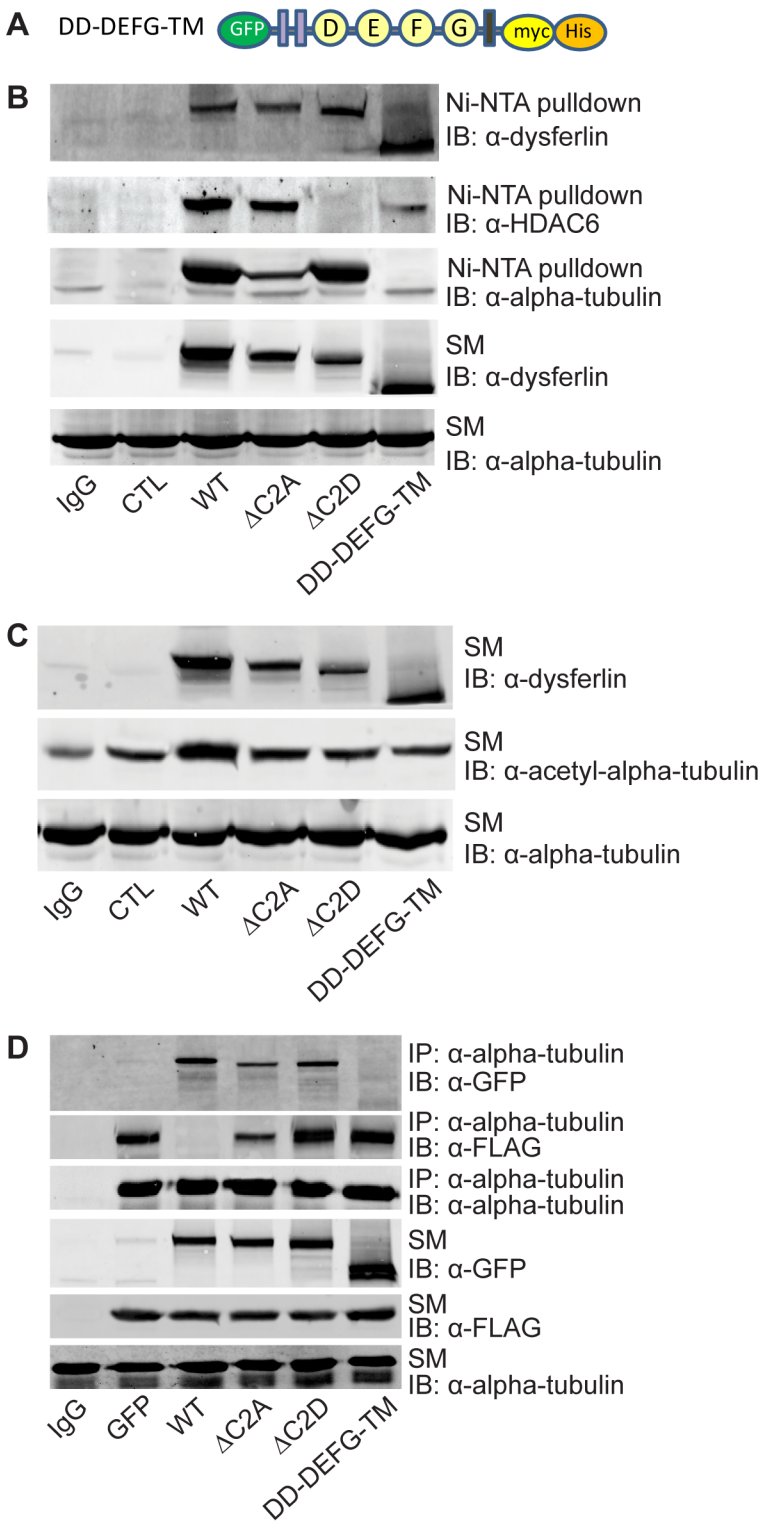

Figure 2.3: Dysferlin requires its alpha-tubulin binding domains to bind HDAC6 and prevent alpha-tubulin deacetylation.

(A) Schematic of dysferlin truncation construct (DD-DEFG-TM). (B) Wildtype dysferlin (WT), dysferlin deletion mutants ΔC2A and ΔC2D, or DD-DEFG-TM were transfected in HEK293T cells, pulled-down on Ni-NTA beads, incubated with murine testes homogenate and immunoblotted with the indicated antibodies. (C) Cell lysates from (B) were immunoblotted for alpha-tubulin acetylation levels. (D) FLAG-HDAC6 was co-transfected with wildtype dysferlin (WT), dysferlin deletion mutants (ΔC2A and ΔC2D), dysferlin truncation (DD-DEFG-TM) or GFP vector in HEK293T cells, immunoprecipitated with anti-alpha-tubulin antibodies, and immunoblotted with the indicated antibodies. As controls, cell lysates were immunoprecipitated without antibodies (CTL) or with anti-IgG antibodies (IgG).

Figure 2.4: Dysferlin expression increases alpha-tubulin acetylation in muscle cells

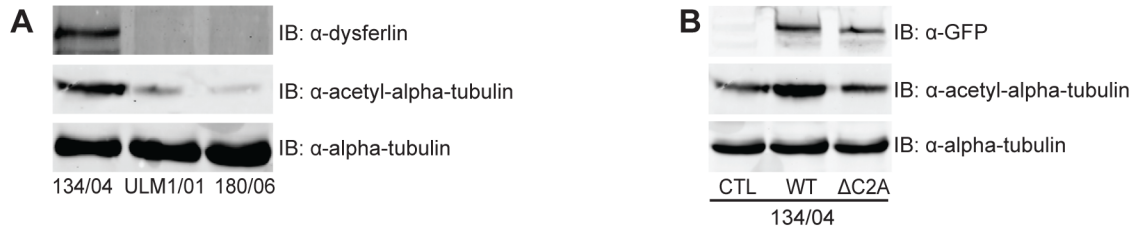

Figure 2.4: Dysferlin expression increases alpha-tubulin acetylation in muscle cells

(A) 134/04, 180/06 and ULM1/01 cell lysates were immunoblotted with anti-dysferlin and anti-acetylated alpha-tubulin antibodies. Alpha-tubulin was used as a loading control. (B) GFP-dysferlin wildtype (WT) or GFP-dysferlinΔC2A (ΔC2A) were transfected into 134/04 myoblasts. Transfected and untransfected (CTL) cell lysates were separated by SDS-PAGE and immunoblotted with the indicated antibodies.

Figure 2.5: Dysferlin expression increases resistance to microtubule depolymerization

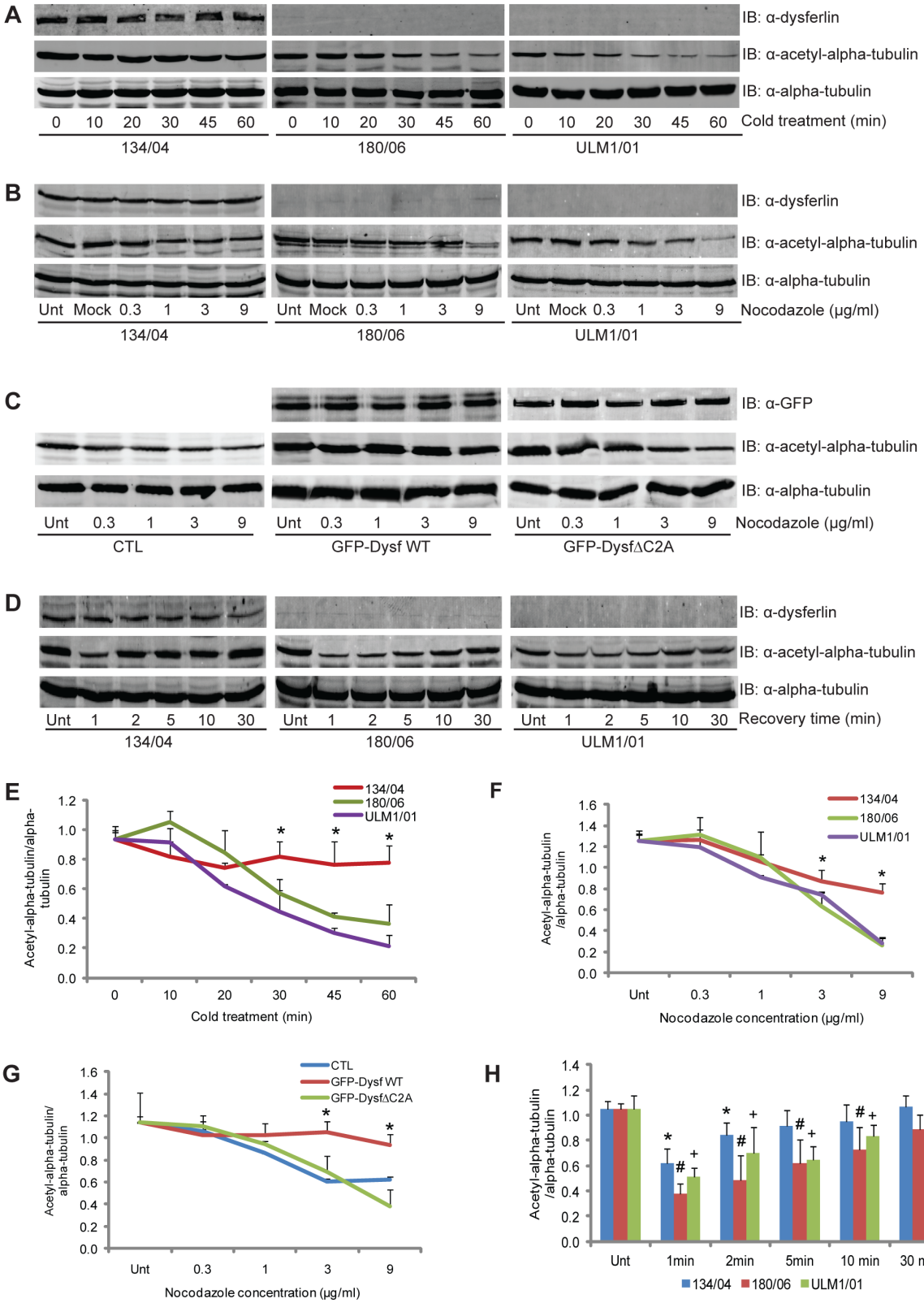

Figure 2.5: Dysferlin expression increases resistance to microtubule depolymerization.

(A) 134/04, 180/06 and ULM1/01 cells were incubated at 4°C for increasing lengths of time. Cell lysates were immunoblotted with the indicated antibodies. To equalize the baseline (0 min) acetylated alpha-tubulin levels in the 180/06 and ULM1/01 cells with those of the 134/04 cells, the intensity of the bands was linearly increased post-acquisition. (B) 134/04, 180/06 and ULM1/01 cells were untreated (Unt), mock-treated (Mock) or treated with increasing concentrations of Nocodazole. Cell lysates were immunoblotted with the indicated antibodies. To equalize the baseline (Unt) acetylated alpha-tubulin levels in the 180/06 and ULM1/01 cells with those of the 134/04 cells, the intensity of the bands was linearly increased post-acquisition. (C) GFP-dysferlin wildtype (GFP-Dysf WT) or GFP-dysferlinΔC2A (GFP-DysfΔC2A) were transfected into HEK293T cells. Transfected and untransfected (CTL) cells were treated with increasing concentrations of Nocodazole. Cell lysates were immunoblotted with the indicated antibodies. (D) 134/04, 180/06 and ULM1/01 cells were untreated (Unt) or treated with 2.5μg/ml Nocodazole, then the drug-containing media was replaced with fresh media and cells were allowed to recover for the indicated lengths of time. Cell lysates were immunoblotted with the indicated antibodies. To equalize the baseline (Unt) acetylated alpha-tubulin levels in the 180/06 and ULM1/01 cells with those of the 134/04 cells, the intensity of the bands was linearly increased post-acquisition. (E, F, G) The ratio of acetylated alpha-tubulin:alpha-tubulin at each time point or Nocodazole concentration was normalized to 134/04 levels to equalize starting values. * indicates that 134/04 values or GFP-Dysf WT values were significantly greater ($p<0.05$) than 180/06 and ULM1/01 levels (E, F) or CTL and ΔC2A levels (G), at the indicated time point or concentration. (H) The ratio of acetylated alpha-tubulin: alpha-tubulin was calculated for each time point and normalized to 134/04 levels to equalize starting values. *, # and + indicate that the value at the indicated time point is significantly different ($p<0.05$) than the Unt value for 134/04, 180/06, ULM1/01, respectively.

Figure 2.6: Dysferlin and acetylated alpha-tubulin levels increase during differentiation.

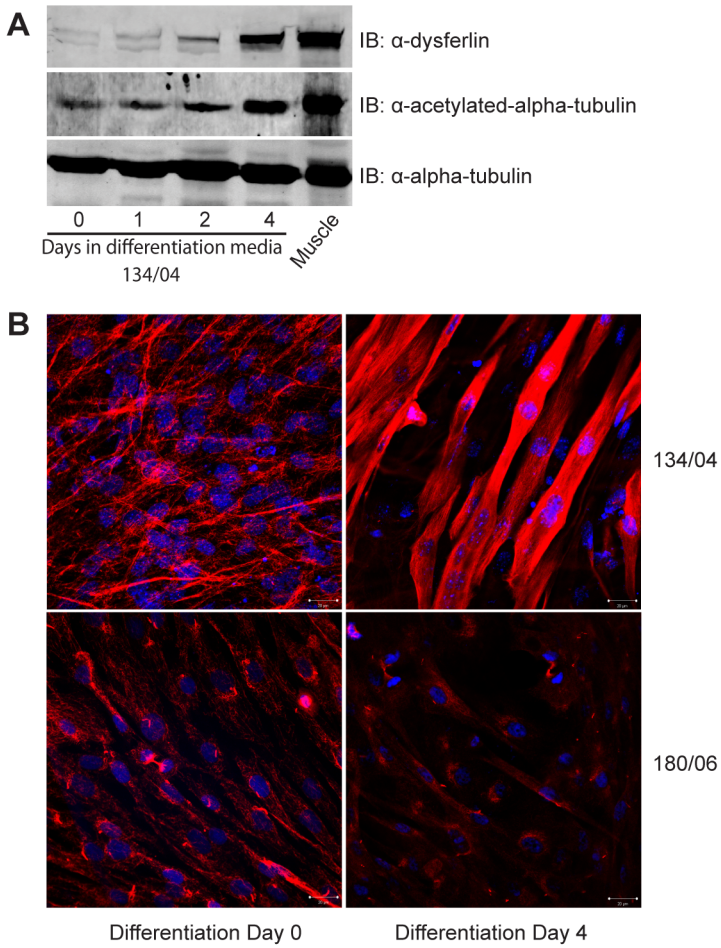

Figure 2.6: Dysferlin and acetylated alpha-tubulin levels increase during differentiation.

(A) 134/04 cells were cultured in differentiation media for the indicated number of days. Cell lysates from these cells and mouse skeletal muscle extract were immunoblotted with the indicated antibodies. (B) 134/04 cells and 180/06 cells were cultured in differentiation media for 0 days or 4 days to induce myotube formation. Cells were fixed and immunostained with anti-acetylated alpha-tubulin antibodies and DAPI. Images were captured at the same fluorescence intensity and gain to compare alpha-tubulin acetylation levels between cells. Scale bar: 20μm.

Figure 2.7: Effect of HDAC6 inhibition on myotube formation

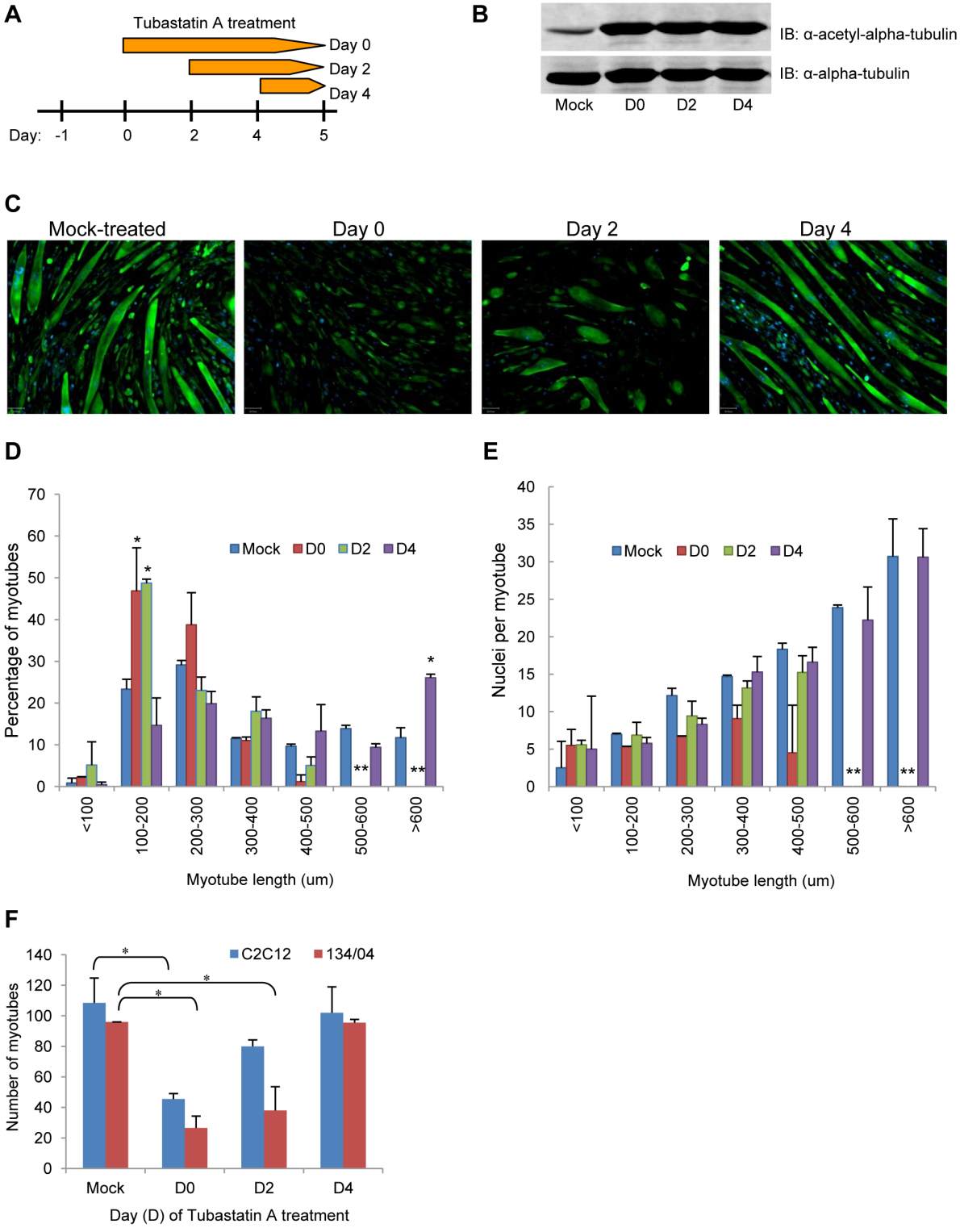

Figure 2.7: Effect of HDAC6 inhibition on myotube formation.

(A) C2C12 or 134/04 myoblasts were seeded in growth media on Day -1, then switched to differentiation media on Day 0. Cells were mock-treated (Mock) or treated with 7.5μM Tubastatin A beginning on different days post-induction of myogenic differentiation (Day 0, Day 2, Day 4). On Day 5, cells were fixed and stained with an anti-desmin antibody and DAPI. (B) Alpha-tubulin acetylation levels were assayed to confirm Tubastatin A efficacy. (C) Representative immunofluorescence images of desmin-stained myotubes in each treatment regime. Scale bar: 60μm. (D) Desmin-stained myotubes were categorized by their myotube length, and plotted against their relative number. (E) Desmin-stained myotubes were counted for their average number of nuclei and categorized by myotube length as in (D). * in (D) and (E) indicates $p<0.05$, significantly different from mock-treated myotubes in the same category. ** indicates that no myotubes were observed in the indicated category. (F) Absolute number of desmin-stained myotubes were counted and categorized by treatment regime. * indicates $p<0.05$, significantly different from Mock-treated. Shown here are results for C2C12 cells; similar results were obtained for 134/04 cells (not shown).

Supporting Information

Table S 2.1: Primers used for dysferlin C2 domain deletion constructs

Dysferlin C2 deletion construct	Deleted residues	Sequence of oligonucleotides (oligo)
ΔC2A	1-129	With 1 oligo 5'-ggcatggacgagctgtacaaggtgcccctgttcccgcccccct-3'
ΔC2B	215-349	With 2 oligos Forward: 5'-acatctagaaagctgctgtcagcgcctctggagagaaaagac-3' Reverse: 5'-ttcagaggggtcttttctctccagaggcgctgacagcagctttct-3'
ΔC2C	383-515	With 2 oligos Forward: 5'-ctgcgaggagcccacttctgccccacttttgggccctgctac-3' Reverse: 5'-gaggttgatgtagcagggcccaaaagtggggcagaagtgggctcc-3'
ΔC2D	1135-1265	With 1 oligo 5'-atgtccgtctccaccttgagcccgtcgggggagctgctggcc-3'
ΔC2E	1324-1462	With 2 oligos Forward: 5'-aacatctacatggttcctcagaaggagcccctcatccccatc-3' Reverse: 5'-ttcctcctggatggggatgaggggctccttctgaggaaccatgta-3'
ΔC2F	1561-1700	With 1 oligo 5'-ctcccagaagacccagccatcctcctccacctcttctgccag-3'
ΔC2G	1817-1965	With 2 oligos Forward: 5'-aggtttttcctgcgttgtattaagggctggtggccctgtgta-3' Reverse: 5'-ctcttctgctacacagggccaccagcccttaatacaacgcaggaa-3'
DD-DEFG-TM	1-870	DD-DEFG-TM cloning: with 2 oligos Forward: 5'-ccggaattcgctgaggggaagctgtct-3' Reverse: 5'-aagaatgcggccgcagctgaaggcttcac-3' eGFP cloning: with 2 oligos Forward: 5'-aaacttaagcttggtaccgag-3' Reverse: 5'-cagcatgaattccttgtacag-3'

List of primers used to clone dysferlin C2 deletion constructs from full-length dysferlin. Residues that were deleted from each construct are indicated. Deletion of the C2 domains coding region was performed by PCR mutagenesis using either the single or double mutagenic primers approach (see Materials and Methods).

CHAPTER 3

3 Modular dispensability of dysferlin C2 domains reveals rational design for mini-dysferlin molecules

3.1 Preface

Our group previously identified a patient with a lariat branch point mutation that caused natural exon-skipping of exon 32, which resulted in a truncated C2 domain within the dysferlin protein. Nevertheless, the aberrant protein presumably retained its functionality, as demonstrated by the patient's mild clinical phenotype. This observation suggested that some of dysferlin's C2 domains may be functionally redundant to the protein's function.

In this work, we studied the plasma membrane repair capacity and plasma membrane localization of mutant dysferlin constructs containing single C2 domain deletions, and demonstrated the modular dispensability of dysferlin's C2 domains. This study culminated in the identification of the minimal C2 domain requirement for a mini-dysferlin capable of sarcolemmal resealing and plasma membrane localization.

3.2 Abstract

Dysferlin is a large transmembrane protein composed of a C-terminal transmembrane domain, two DysF domains and seven C2 domains that mediate lipid and protein binding interactions. Recessive loss of function mutations in dysferlin lead to muscular dystrophies, for which no treatment is currently available. Dysferlin's large size precludes its encapsidation into an adeno-associated virus (AAV), the vector of choice for gene delivery to muscle. To design mini-dysferlin molecules suitable for AAV mediated gene transfer, we tested internally truncated dysferlin constructs, each lacking one of the seven C2 domains, for their ability to localize to the plasma membrane and to repair laser induced plasmalemmal wounds in dysferlin deficient human myoblasts. We demonstrate that dysferlin's C2B, C2C, C2D and C2E domains were dispensable for correct plasmalemmal localization. Furthermore, we show that the C2B, C2C, C2E domains, and to a lesser extent the C2D domain are dispensable for its membrane repair function. Based on these results, we designed small dysferlin molecules, which can localize to the plasma membrane, can reseal laser-induced plasmalemmal injuries and are small enough to be incorporated into AAV. These results lay ground for AAV mediated gene therapy experiments in dysferlin deficient mouse models.

3.3 Introduction

Dysferlin is a large type II transmembrane protein composed of two DysF domains and seven C2 domains (named C2A to C2G) that mediate lipid (Davis et al., 2002; Therrien et al., 2009) and protein binding interactions (Matsuda et al., 2001; Lennon et al., 2003; Huang et al., 2007; Cai et al., 2009; Azakir et al., 2010). The protein is predominantly expressed in skeletal and cardiac muscle, and is also found in placenta and monocytes (Bashir et al., 1998; De Luna et al., 2007; Vandre et al., 2007). Its subcellular localization is at the sarcolemma, at T-tubule membranes and in intracellular vesicular compartments of as yet unknown origin (Bansal et al., 2003; Klinge et al., 2010). Dysferlin mediates rapid calcium-dependent resealing of plasma membrane disruptions and is involved in the fusion of subsarcolemmal vesicles with the plasma membrane thus forming a membrane patch across the injury site (Bansal et al., 2003). Loss of dysferlin is responsible for the progressive, recessively inherited muscular dystrophies Limb-Girdle Muscular Dystrophy type 2B (LGMD2B) (Liu et al., 1998), Miyoshi Myopathy (Liu et al., 1998) and Distal Anterior Compartment Myopathy (Illa et al., 2001). There is currently no treatment for these debilitating diseases.

We previously reported an atypical case in a dysferlin-deficient family (Sinnreich et al., 2006). Two daughters exhibited a classical dysferlinopathy phenotype with disease onset in their teens caused by a homozygous null mutation in the *DYSF* gene. Both their parents were heterozygous for this null mutation, but their mother harboured a lariat branch point mutation leading to in-frame skipping of exon 32 on her second *DYSF* allele. This allele produced mRNA devoid of exon 32 (Sinnreich et al., 2006), which translates into an internally truncated dysferlin protein lacking part of the fourth C2 domain (C2D). Because the mother displayed only a very mild clinical phenotype, we hypothesized that this truncated protein retained some of its biological activity (Sinnreich et al., 2006). In the present study, we therefore designed a recombinant dysferlin construct lacking its 32nd exon, and showed that the internally truncated protein was indeed biologically active, as it restored the deficit in plasma membrane resealing in dysferlin-deficient myoblasts.

The observation of protein functionality despite truncation of part of the C2D domain

led us to ask the question which and how many of dysferlin's C2 domains may be dispensable. Such information would be important for a rational design of a functional mini-dysferlin molecule, which would be small enough to be incorporated into an adeno associated viral (AAV) vector for gene therapy purposes.
AAV is the current vector of choice for somatic gene therapy directed towards skeletal muscle due to high muscle tropism of certain AAV serotypes (Tang et al., 2010), long-term gene expression and the lack of human pathogenicity (Wu et al., 2010). However, AAV vectors have a small insert capacity (~4.6 kilobases, kb), precluding the insertion of full length dysferlin (6.2 kb of coding sequence alone) (Wu et al., 2010). Hence, the generation of functional mini-dysferlins suitable for AAV mediated gene transfer remains an important therapeutic goal. The identification of necessary domains to be included in such a mini-dysferlin molecule has not been addressed systematically so far, and a naturally occurring mini-dysferlin was unfortunately not able to alleviate the muscular dystrophy phenotype in dysferlin deficient mice (Lostal et al., 2012).

In this study, we characterized the functionality of internally truncated dysferlin constructs each lacking a subsequent C2 domain, and demonstrated that some C2 domains are dispensable for dysferlin's correct localization to the plasma membrane and importantly also for its ability to repair laser-induced plasmalemmal injuries in patient derived dysferlin deficient muscle cells. By recombinant generation of midi- and mini-dysferlins, we were able to determine the minimal C2 domain requirement for correct membrane localization and repair. The mini-dysferlin constructs generated are small enough to be incorporated into AAV vectors. Thus our results lay ground for AAV mediated gene therapy experiments in dysferlin deficient mouse models.

3.4 Results

Deletion of the 32nd exon does not affect dysferlin's membrane resealing activity

In a previous publication we described an atypical case of a mild dysferlinopathy phenotype in a patient harbouring a lariat branch point mutation leading to in-frame skipping of exon 32 (Sinnreich et al., 2006). We hypothesized that the resulting internally truncated dysferlin protein, devoid of a part of the C2D domain, retained sufficient biological activity to account for the mild phenotype. To test this theory, we

designed a recombinant dysferlin construct lacking its 32nd exon, harbouring an N-terminal GFP and a C-terminal c-myc tag (termed here dysferlinΔExon32) (Figure 3.1A).

Immunostaining for the extracellular c-myc epitope of the dysferlin construct demonstrated that dysferlinΔExon32 does localize to the plasma membrane in transfected C2C12 myoblasts (Figure 3.1B). Plasma membrane protein extraction of COS-7 cells transfected with dysferlinΔExon32 showed that 40.84% ± 8.9% of transfected dysferlinΔExon32 were targeted to the plasma membrane compared to wildtype (WT) dysferlin (Figure 3.1C and D).

We next assessed whether dysferlinΔExon32 can reverse the defect in plasma membrane resealing, which is intrinsic to the dysferlin-deficient human myoblast culture (ULM1/01). ULM1/01 cells transfected with a GFP vector could not reseal laser-induced plasmalemmal injuries. In contrast, transfection of dysferlinΔExon32 successfully restored plasma membrane resealing, similar to WT dysferlin (Figure 3.1D, E, F).

These results demonstrate that dysferlinΔExon32 retains its biological activity, as it localizes to the plasma membrane and reseals plasma membrane disruptions.

Dysferlin C2 domains exhibit modular dispensability

Deletion of dysferlin's 32nd exon results in an internal truncation of part of its C2D domain, and yet the protein can reseal laser-induced plasmalemmal injuries, suggesting a possible redundancy of certain dysferlin C2 domains. This led us to explore the membrane localization and resealing function of a recombinantly generated series of single C2 domain deletion mutants of dysferlin (Di Fulvio et al., 2011) (Figure 3.2A).

Immunostaining studies against the extracellular c-myc epitope of the dysferlinΔC2 constructs transfected into C2C12 cells showed plasmalemmal localization of dysferlin ΔC2B, ΔC2C, ΔC2D and ΔC2E. However, dysferlin ΔC2A, ΔC2F and ΔC2G did not exhibit staining at the plasma membrane (Figure 3.2B).

Similar results were obtained when plasma membrane proteins were extracted from COS-7 cells transfected with the dysferlinΔC2 constructs. Overexpressed dysferlin ΔC2B, ΔC2C, ΔC2D and ΔC2E were targeted to the plasma membrane, to a similar degree as overexpressed WT dysferlin. In contrast, less than 20% of overexpressed dysferlin

ΔC2A, ΔC2F and ΔC2G were targeted to the plasma membrane, as compared to WT dysferlin (Figure 3.2C and D).

To identify which of dysferlin's seven C2 domains could be involved in plasma membrane repair, the dysferlinΔC2 constructs were transfected into ULM1/01 dysferlin-deficient human myoblasts and plasma membrane resealing kinetics were determined after laser induced plasma membrane injury. Our results show that dysferlin ΔC2B, ΔC2C and ΔC2E were able to reseal laser-induced plasmalemmal injuries, whereas dysferlin ΔC2A, ΔC2F and ΔC2G were not (Figure 3.3A and B). Dysferlin ΔC2D was only partially able to restore the resealing function in the ULM1/01 myoblasts, even though it was targeted to the plasma membrane (Figure 3.2B, C, D).

Taken together, our results show that single deletion of dysferlin's C2B, C2C and C2E domains have no impact on dysferlin's capacity for plasmalemmal localization and resealing of laser-induced plasmalemmal injuries.

Mini-dysferlins are biologically active

Having demonstrated that dysferlin's C2B, C2C, C2E domains, and to a partial extent the C2D domain, were dispensable for dysferlin's role in membrane repair, we designed truncated forms of dysferlin lacking the C2B, C2C, C2E domains, termed midi-dysferlin 1, or additionally the C2D domain, termed midi-dysferlin 2 (Figure 3.4A).

These two constructs localized to the plasma membrane, as shown by immunofluorescence studies and Western blot analysis after plasma membrane protein extraction, when transfected into C2C12 and COS-7 cells, respectively (Figure 3.4B, C, D). Furthermore, the two midi-dysferlins were both able to restore the resealing deficit in dysferlin-deficient human myoblasts, to a similar extent as WT dysferlin (Figure 3.5), demonstrating that these two midi-dysferlins are biologically active.

By analyzing the midi-dysferlin constructs, we were able to assess which and how many of dysferlin's C2 domains may be dispensable for its function. However, the size of these constructs still surpasses the insert capacity of AAV vectors because they also include large interdomain sequences (see Figure 3.4A). Therefore, we designed mini-dysferlin constructs harbouring only the C2A, C2F and C2G domains, or only the C2A and C2G domains, in conjunction with the transmembrane domain. The mini-dysferlin constructs

differed in the use of the linker sequences connecting the C2A domain to the C2F or C2G domain (Figure 3.4A).

Only mini-dysferlin 1 and mini-dysferlin 3, which contained the linker sequence adjacent to the C2A domain, were correctly targeted to the plasma membrane (Figure 3.4 B, C, D) and effectively resealed laser-induced plasmalemmal injuries (Figure 3.5A and B). Mini-dysferlin 2 and mini-dysferlin 4, which contained linker sequences derived from the C-terminal C2 domains, were not efficiently targeted to the plasma membrane (15.83% ± 1.83% and 13.98% ± 0.86, respectively), when compared to WT dysferlin. (Figure 3.4 B, C, D).

These results demonstrate that mini-dysferlin 1 and mini-dysferlin 3 retain the same capability for plasmalemmal localization and plasma membrane repair as full-length dysferlin.

3.5 Discussion

We previously reported an atypically mild phenotype in a dysferlinopathy patient who was compound heterozygous for a *DYSF* null allele and an exon 32 skipping allele, the latter encoding an internally truncated protein (Sinnreich et al., 2006). This observation prompted other groups to design exon-skipping strategies as possible therapeutic options for dysferlin-deficient patients (Aartsma-Rus et al., 2010; Wein et al., 2010). Although skipping of dysferlin's exon 32 was successful on RNA level in cultured cells (Aartsma-Rus et al., 2010; Wein et al., 2010), the question remained whether a protein lacking the peptide sequence encoded by exon 32 would be functional. Here we show that a recombinantly generated dysferlin construct lacking exon 32 is capable of resealing the plasma membrane of injured dysferlin-deficient human myoblasts (Figure 3.1). Therefore, our studies support the rationale to pursue skipping of exon 32 as a potential therapeutic strategy for patients harbouring mutations in this particular exon.

The C2D domain contains five putative residues for calcium ion binding and coordination, two of which are included in the peptide encoded by exon 32 (Therrien et

al., 2006; Lek et al., 2010). Since the generated dysferlin protein lacking the peptide sequence encoded by exon 32 retains some of its function, as evidenced by plasmalemmal localization and repair, as well as by the mild muscular dystrophy phenotype of the patient described earlier, it can be assumed that the exon 32 encoded peptide sequence is relatively dispensable. This raised the question of whether the entire C2D domain is dispensable, and in this regard, whether any of the other dysferlin C2 domains are functionally redundant. Understanding functional redundancy of dysferlin's C2 domains is important, since this knowledge would allow generation of recombinant dysferlin molecules lacking dispensable domains in an attempt to rationally design a short dysferlin protein capable of being inserted into AAV vectors for therapeutic purposes. Although it has been suggested that larger genomes can be packaged into AAV vectors (Grieger et al., 2005; Allocca et al., 2008), in-depth analysis showed that regardless of the size of the plasmid encoded vector or the capsid type, the packaged AAV vector genomes can not exceed 5.2 kb in length (Wu et al., 2010) and that large vector genomes observed in the aforementioned studies (Grieger et al., 2005; Allocca et al., 2008), were probably generated through rare recombination events (Wu et al., 2010). Taking advantage of such recombination events, recently a trans-splicing approach was chosen, in which two dysferlin coding fragments were incorporated into two different AAV vectors, to recombine after dual AAV-mediated gene transfer generating the full-length protein, albeit at low levels (Lostal et al., 2010).

We deleted subsequent C2 domains from full-length dysferlin and tested these constructs for their plasma membrane localization and membrane repair capacity (Figure 3.2 and Figure 3.3). These experiments defined the C2 domain requirements for dysferlin membrane localization and membrane repair. We observed that deletion of the entire C2D domain allowed correct membrane localization but only partial membrane resealing, while the dysferlin construct lacking only the peptide encoded by exon 32 was comparable to WT dysferlin regarding membrane repair (Figure 3.1E).

Experiments with midi- and mini-dysferlin constructs defined the minimal C2 domain requirements for plasmalemmal localization and repair (Figure 3.4 and Figure 3.5). We observed that mini-dysferlins containing the linker sequence immediately adjacent to the C2A domain (aa143-217) retained their biological activity. The size of the generated

biologically active mini-dysferlins (mini-dysferlin 1: 1518nt, and mini-dysferlin 2: 2274 nt; nucleotide numbers are without the GFP- and c-myc tags) would be suitable for their incorporation into AAV vectors (Tang et al., 2010) thus overcoming the hurdle to AAV-mediated gene delivery presented by full-length dysferlin's large cDNA size.

Krahn and colleagues had identified a naturally occurring mini-dysferlin molecule, which encompasses the C2F, the C2G and the transmembrane domain (Krahn et al., 2010). This naturally occurring mini-dysferlin molecule had resealing activity of dysferlin deficient mouse myofibers in vitro but was not capable of alleviating the muscular dystrophy phenotype of dysferlin-deficient mice in vivo (Lostal et al., 2012). Of note, this mini-dysferlin lacked the C2A domain, which is known to interact with AHNAK (Huang et al., 2007), phospholipids (Davis et al., 2002; Therrien et al., 2009), alpha-tubulin (Azakir et al., 2010), to mediate lysosome fusion to the cell membrane in coronary arterial endothelial cells (Han et al., 2012), and which was necessary in our study for membrane localization and repair. It is thus conceivable that the mini-dysferlin molecules described in our study may be better suited for AAV mediated gene transfer into dysferlin-deficient mouse models.

In this paper, we demonstrate that dysferlin's repair function can be carried out by a shorter version of the protein, thus raising the possibility of replacing full-length dysferlin with a mini-dysferlin small enough to be incorporated into an AAV vector for gene therapy. This work should lay ground for future in vivo experiments to test the influence of these mini-dysferlins on the physiology and pathology of dysferlin-deficient mice.

3.6 Experimental Procedures

Cell Culture and Transfection

C2C12 murine myoblasts and Monkey Kidney Fibroblasts (COS-7) were purchased from ATCC (Burlington, Ontario) (ATCC number CRL-1573 and CRL-1651, respectively). The ULM1/01 myoblast culture was obtained from EuroBioBank, along with the required IRB approvals. Myoblast culture ULM1/01 harbours two null alleles: a C4819T (R1607X) substitution and a 5085delT (F1695LfsX48) deletion (Azakir et al., 2012).

ULM1/01 myoblast cultures were infected with a retroviral construct carrying the E6E7 early region from human papillomavirus type 16 to extend their life span as described previously (Azakir et al., 2012). Cell cultures were maintained in Dulbecco's modified Eagle's medium (DMEM; Sigma) containing 10% fetal bovine serum (FBS; Invitrogen). Where indicated, cells were transfected using 10µl of Lipofectamine 2000 (Invitrogen) or Polyethylenimine (PEI) (Sigma) and 4 µg of plasmid DNA/10 cm^2 culture dish, at 70% confluency.

Plasmids and constructs

A plasmid encoding N'-terminally GFP-tagged and C'-terminally-c-myc-tagged dysferlin (termed here wildtype dysferlin, WT) was a generous gift from Dr. K. Bushby, Newcastle. All dysferlin constructs described in this study (WT, dysferlinΔExon32, dysferlinΔC2, midi- and mini-dysferlins) were derived from the original plasmid and contain an N'-terminal GFP tag and a C'-terminal c-myc tag. C2-domain deletion mutants were cloned as previously described (Di Fulvio et al., 2011). The GFP-myc-tagged midi- and mini-dysferlin constructs were cloned from the full-length dysferlin construct. Briefly, deletion of the coding region of the C2 domains was performed by PCR mutagenesis using domain spanning oligonucleotides and the QuikChange Site-Directed Mutagenesis Kit (Stratagene) applying the double mutagenic primer approach. The procedure was performed according to the manufacturer's protocol. In short, the PCR reaction was: 95°C for 3min; 95°C for 15s, 65°C for 1min, 68°C for 12min (18 cycles); 68°C for 7min. The PCR product was digested with DpnI, cloned into DSC-B vector, and transformed into DH5alpha or XL10-Gold bacterial cells. Plasmid DNA was isolated by mini-preps (Qiagen) and subsequently sequenced. To generate the midi-dysferlin 2 construct, a PCR reaction was performed using the midi-dysferlin 1 plasmid (for primer sequences see Table 3.1).

Plasma Membrane Protein Extraction and Western Blotting

Proteins were extracted from cultured, confluent COS-7 cells using the plasma membrane protein extraction kit (BioVision). The procedure was performed according to the manufacturer's protocol. Briefly, cells were washed, homogenized and centrifuged at 700 g for 10 min at 4°C. The supernatant was centrifuged at 10,000 g for

30 min at 4°C. The resulting supernatant contained the cytosolic fraction and the pellet contained the total cellular membrane protein fraction. The plasma membrane proteins were further isolated from the pellet by gradient centrifugation. Proteins were separated by SDS-polyacrylamide gel electrophoresis and transferred onto a polyvinylidene difluoride (PVDF) membrane. Membranes were blocked for 1 h in buffer 1 (Tris-buffered saline containing 3% Top-Block, 0.05% sodium azide) and incubated for 16 h at 4°C with the indicated antibodies in buffer 2 (Tris-buffered saline containing 3% Top-Block, 0.05% sodium azide, 0.1% Tween 20). Antibodies against α-tubulin were purchased from Abcam, against dysferlin from Vector Laboratories (REACTOLAB, clone Ham1/7B6), against GFP from Invitrogen, against c-myc from BioMol International. The membranes were washed with buffer 2 and incubated for 1 h with secondary antibodies, Alexa Fluor 680 goat anti-mouse IgG (Invitrogen) or IRDye 800 goat anti-rabbit IgG (Jackson Laboratories), in buffer 2 (1:10,000 dilution). Membranes were washed in TBS and detected with Odyssey Infrared Imaging System (LI-COR). Densitometric analysis was performed using ImageJ v1.45s (National Institutes of Health, USA). Statistical analysis was performed using the Student's T-test. All experiments were performed in quadruplicates.

Immunofluorescence assays

Cells were grown on poly-D-lysine-coated coverslips in growth media. Cells were transfected with the indicated plasmids for 24 h. Unpermeabilized cells were incubated for 15 min at room temperature with anti-c-myc antibody, which recognizes an extracellular C-terminal epitope. Cells were washed and fixed with 4% paraformaldehyde (PFA) for 20 min, blocked for 15 min in 2% fish skin gelatin, 1% normal goat serum, 0.15% Triton X-100 in PBS and incubated for 1 h at room temperature with Cy3 AffiniPure Goat Anti-Mouse IgG (H+L) secondary antibody (Jackson Laboratories) and mounted on glass slides with FluorSave reagent (Calbiochem). Images were captured on a LSM 710 inverted confocal microscope (Zeiss) and analyzed using Zen 2009 LE software (Zeiss). All experiments were performed in triplicates.

Plasmalemmal Repair Assay

Human dysferlin-negative myoblasts (ULM1/01) were transfected with the indicated plasmids using Lipofectamine 2000. Plasma membrane injuries were performed as previously described (Azakir et al., 2012). Briefly, myoblasts were cultured in a Lab-Tek chambered coverglass coated with 4 µg/ml of poly-D-lysine. At time of injury, the medium was replaced with PBS containing 10 mM HEPES and 1.5 mM $CaCl_2$. The fluorescent dye FM4-64 (Invitrogen) was added to the solution at a concentration of 2.5 µM. Myoblast plasma membranes were injured with laser beams from a LSM 710 inverted confocal microscope (Zeiss) as described in (Azakir et al., 2012). Images were captured before injury (t = 0) and for 5 min after injury at 5-second intervals. The fluorescence intensity at the site of injury was measured using Zeiss 2009 software. At each time point, relative fluorescence values were determined by subtracting the background value and dividing the net increase in fluorescence by the fluorescence value at t = 0.

3.7 Acknowledgements

This study was supported by Myosuisse, Association Française contre les Myopathies (AFM), MDAC-ALS-CIHR Partnership and the Swiss National Science Foundation (SNF). We thank Muscle Tissue Culture Collection MTCC for providing the myoblast samples used in this study. The Muscle Tissue Culture Collection is part of the German network on muscular dystrophies (MD-NET, service structure S1, 01GM0601) funded by the German ministry of education and research (BMBF, Bonn, Germany). The Muscle Tissue Culture Collection is a partner of Eurobiobank (www.eurobiobank.org) and TREAT-NMD (www.treat-nmd.eu). We thank Dr. Bushby, Newcastle, for the GFP-cDNA. We thank Beat Erne for technical assistance.

3.8 Figures and Figure Legends

Figure 3.1: DysferlinΔExon32 retains its biological function.

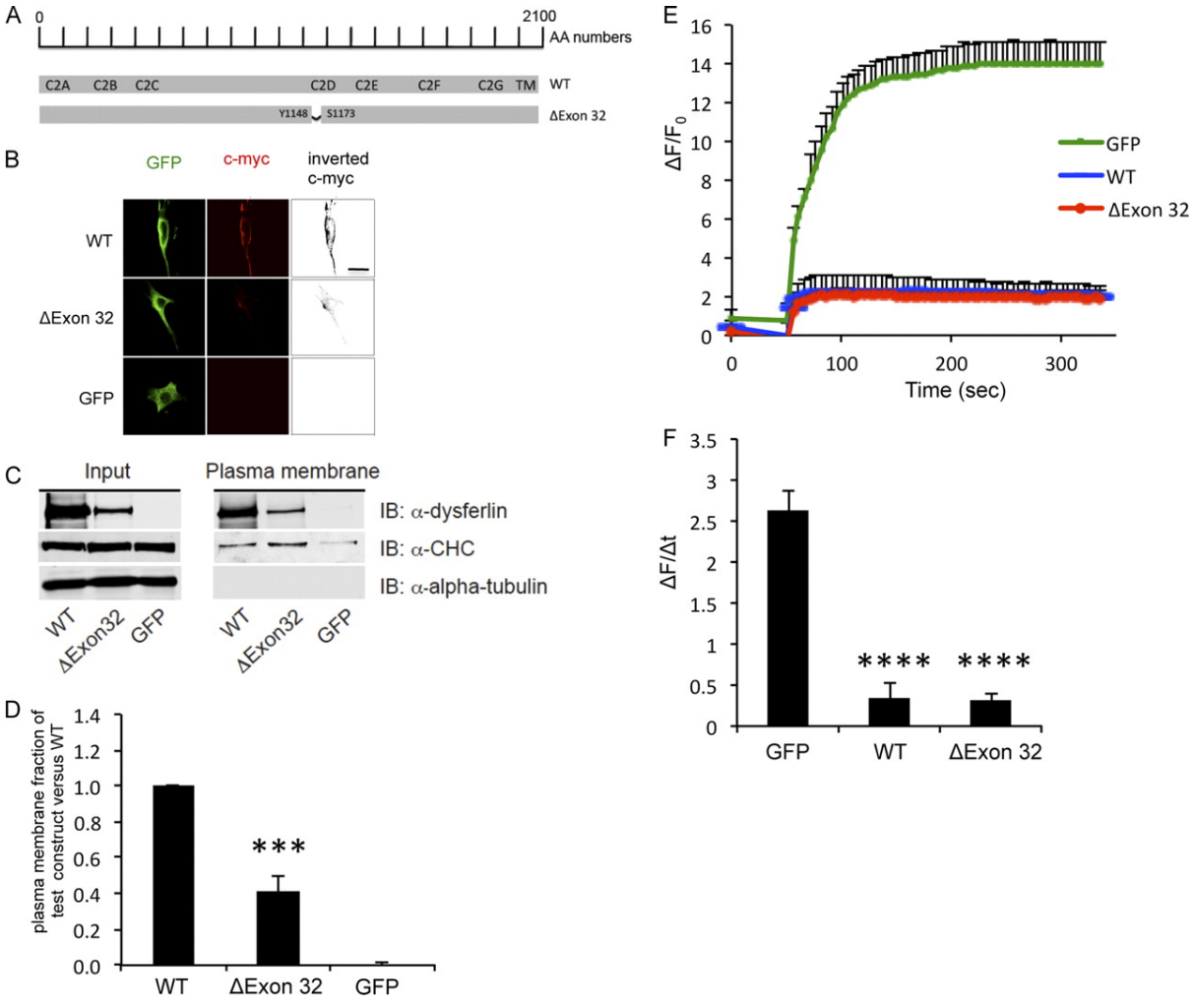

Figure 3.1: DysferlinΔExon32 retains its biological function. (A) Schematic representation of the ΔExon32 mutation in the dysferlin protein sequence, compared to wildtype (WT) dysferlin. AA numbers = amino acid enumeration. (B) Immunostaining against an extracellular c-myc dysferlin epitope (red) in C2C12 myoblasts demonstrates plasma membrane localization of overexpressed GFP-dysferlinΔExon32-myc construct (dysferlinΔExon32) and GFP-dysferlin-myc (WT), but not GFP vector alone (GFP). Immunostaining against GFP (green) and the GFP tag demonstrates total cellular expression of each construct. An inverted black and white image of c-myc (inverted c-myc) is represented on the right to better visualize the plasma membrane staining with the anti-myc antibody. Scale bar, 20 μm. (C) COS-7 cells were transfected with GFP, WT or dysferlinΔExon32. Western blots of plasma membrane protein extracts were stained with anti-dysferlin antibodies, with anti-α-tubulin antibodies as negative control and with anti-clathrin heavy chain antibodies (CHC) as positive control (n = 4). IB: immunoblot. (D) Graphical representation of (C) showing the ratio between the amounts of plasmalemmal dysferlin construct versus total dysferlin construct, compared to the ratio between the amounts of plasmalemmal WT dysferlin versus total WT dysferlin. (E) Plasma membrane repair assay was performed on the dysferlin deficient myoblast culture ULM1/01 transfected with GFP, WT or dysferlinΔExon32. Relative fluorescence intensity ($\Delta F/F_0$) over time following laser-induced injury is represented as means ± 1 SD. Numbers of individual measurements are as follows: for GFP (n = 12), for dysferlinΔExon32 (n=16) and for WT (n = 16). (F) Graphical representation of (E) depicting the change in relative fluorescence intensity after 5 min post-injury. Stars indicate that differences were statistically significant (***, $p < 0.001$; ****, $p < 0.0001$).

Figure 3.2: GFP-tagged dysferlin ΔC2B, ΔC2C, ΔC2D and ΔC2E localize to the plasma membrane.

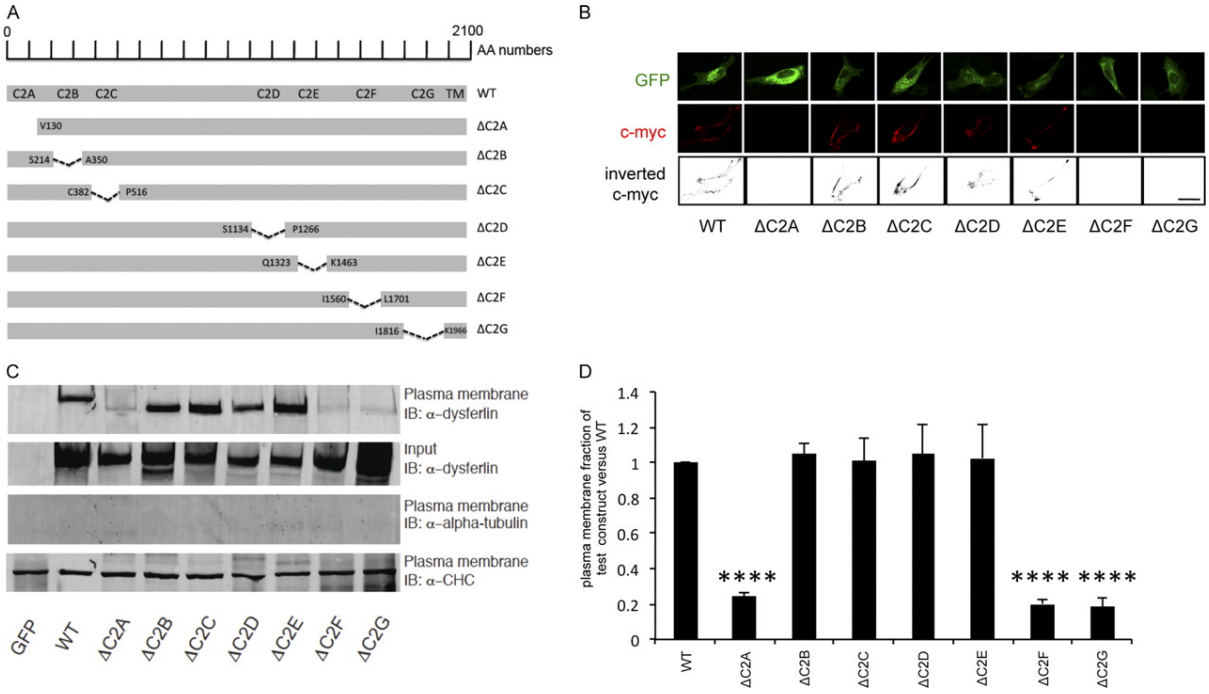

Figure 3.2: GFP-tagged dysferlin ΔC2B, ΔC2C, ΔC2D and ΔC2E localize to the plasma membrane. (A) Schematic representation of the deleted C2 domain regions in the dysferlin protein sequence compared to WT dysferlin. AA numbers = amino acid enumeration. (B) Immunostaining against the extracellular c-myc dysferlin epitope (red) in C2C12 myoblasts transfected with the indicated plasmids. Immunostaining against GFP (green) demonstrates cellular expression of each construct. An inverted black and white image of c-myc (inverted c-myc) is represented on the right to better visualize the plasma membrane staining with the anti-myc antibody. Scale bar 20 μm. (C) COS-7 cells were transfected with the indicated plasmids. Western blots of plasma membrane protein extracts were stained with anti-dysferlin antibodies, with anti-α-tubulin antibodies as negative control and with anti-clathrin heavy chain antibodies (CHC) as positive control (n = 4). (D) Graphical representation of (C) showing the ratio between the amount of plasmalemmal dysferlin construct versus total dysferlin construct, compared to the ratio between the amount of plasmalemmal WT dysferlin versus total WT dysferlin. Stars indicate that differences were statistically significant (****, $p < 0.0001$).

Figure 3.3: GFP-tagged dysferlin ΔC2B, ΔC2C and ΔC2E restore the defect in membrane repair of dysferlin deficient myoblasts.

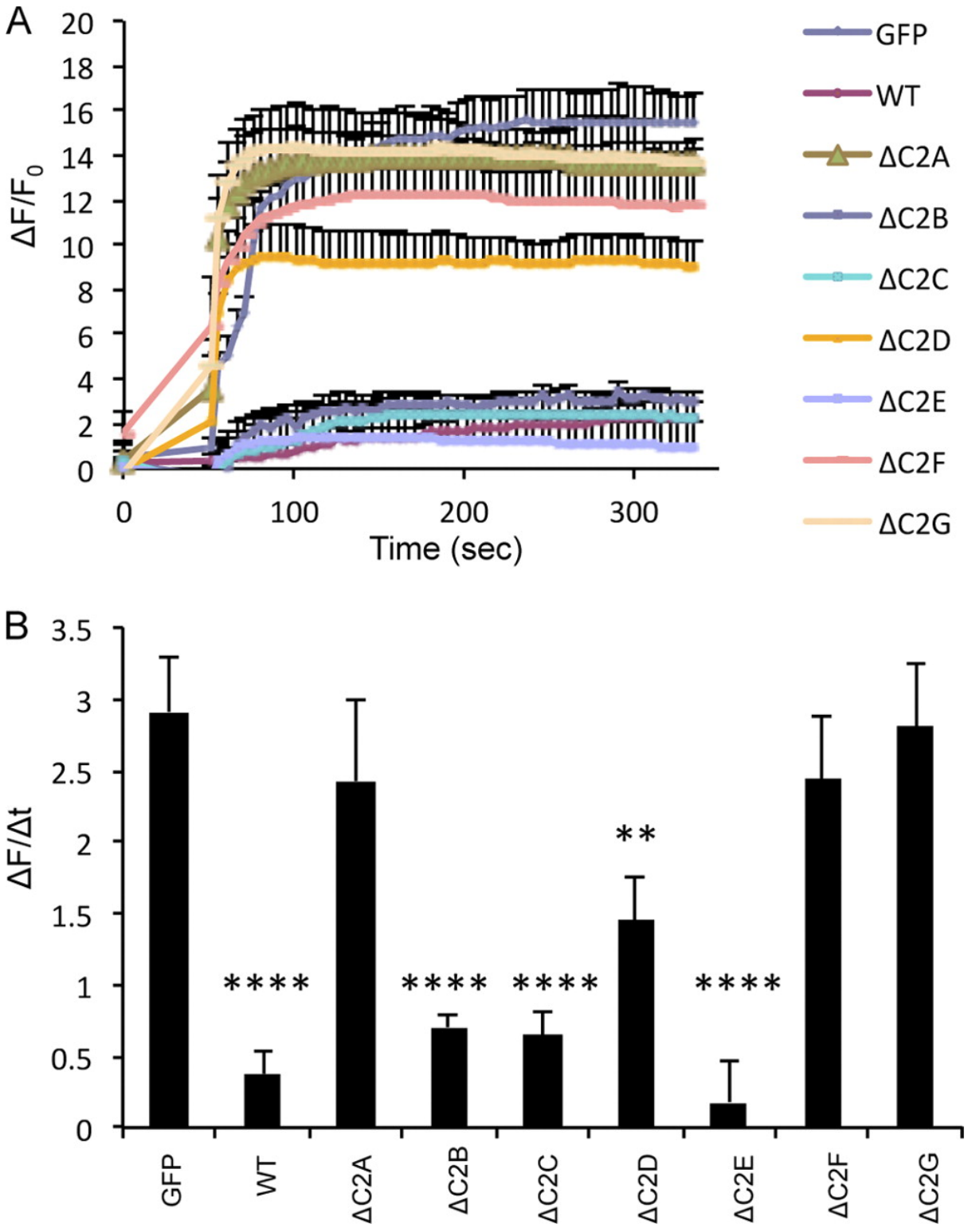

Figure 3.3: GFP-tagged dysferlin ΔC2B, ΔC2C and ΔC2E restore the defect in membrane repair of dysferlin deficient myoblasts. (A) Plasma membrane repair assay was performed on the dysferlin deficient myoblast culture ULM1/01 transfected with the indicated plasmids. Relative fluorescence intensity ($\Delta F/F_0$) over time following laser-induced injury is presented as means ± 1 SD. Numbers of individual measurements are as follows: for GFP (n = 12), for WT and ΔC2A to ΔC2G (n = 15 for each construct). (B) Graphical representation of (A) depicting the change in relative fluorescence intensity after 5 min post-injury. Stars indicate that differences were statistically significant (**, $p < 0.01$; ****, $p < 0.0001$).

Figure 3.4: Midi-dysferlin 1 and 2, and mini-dysferlin 1 and 3 localize to the plasma membrane.

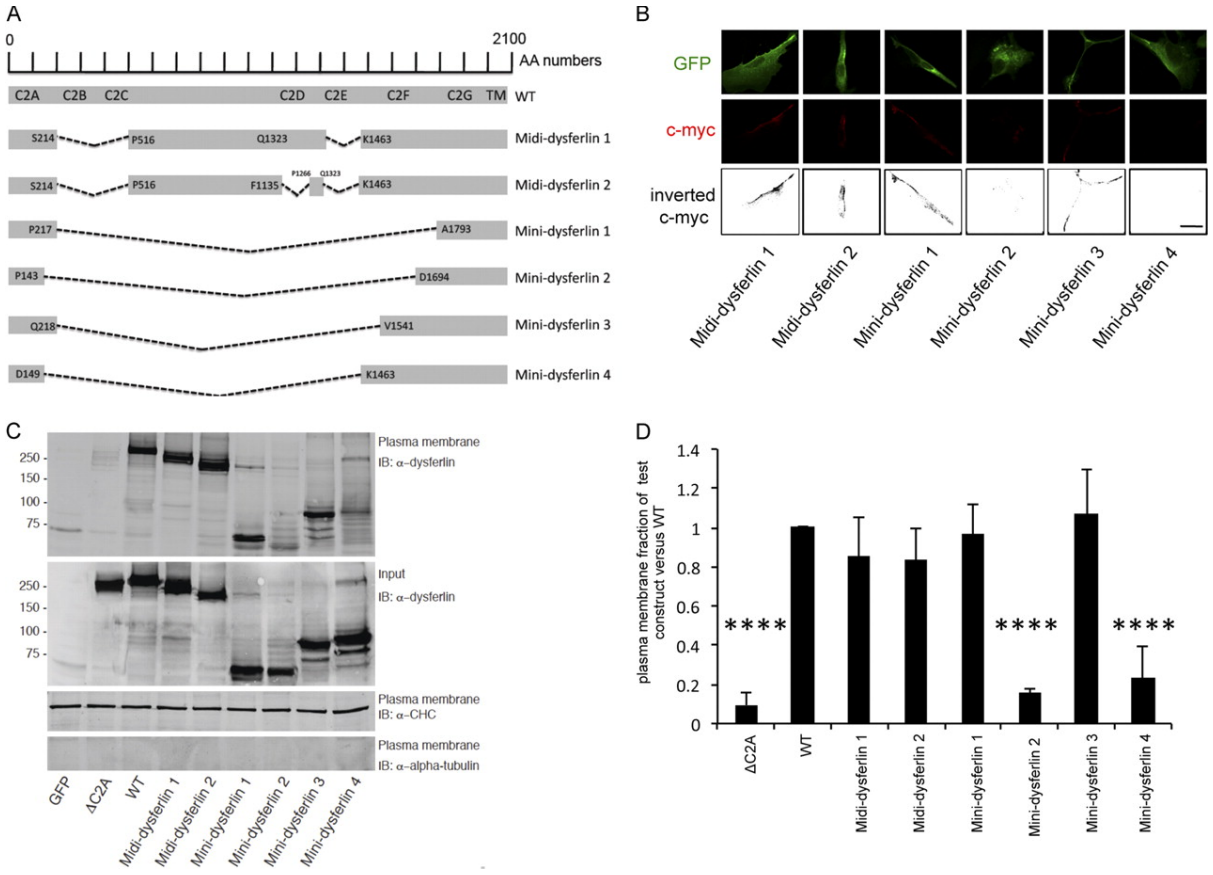

Figure 3.4: Midi-dysferlin 1 and 2, and mini-dysferlin 1 and 3 localize to the plasma membrane. (A) Schematic representation of the deleted AA regions in the dysferlin protein sequence compared to WT dysferlin. A short AA sequence adjacent to the C2A domain was used as the linker sequence in mini-dysferlins 1 and 3. A short amino sequence adjacent to the C2G or C2F domains were used as the linker sequence in mini-dysferlins 2 and 4, respectively. AA numbers = amino acid enumeration. (B) Immunostaining against the extracellular c-myc dysferlin epitope (red) in C2C12 myoblasts transfected with the indicated plasmids. Immunostaining against GFP (green) demonstrates total cellular expression of each construct. An inverted black and white image of c-myc (inverted c-myc) is represented on the right to better visualize the plasma membrane staining with the anti-myc antibody. Scale bar 20 μm. (C) COS-7 cells were transfected with the indicated plasmids. Western blots of plasma membrane protein extracts were stained with anti-dysferlin antibodies, with anti-α-tubulin antibodies as negative control and with anti-clathrin heavy chain (CHC) antibodies as a positive control (n = 4). (D) Graphical representation of (C) showing the ratio between the amounts of plasmalemmal dysferlin construct versus total dysferlin construct, compared to the ratio between the amounts of plasmalemmal WT dysferlin versus total WT dysferlin. Stars indicate that differences were statistically significant (****, $p < 0.0001$).

Figure 3.5: Midi-dysferlin 1 and 2, and mini-dysferlin 1 and 3 restore the defect in membrane repair.

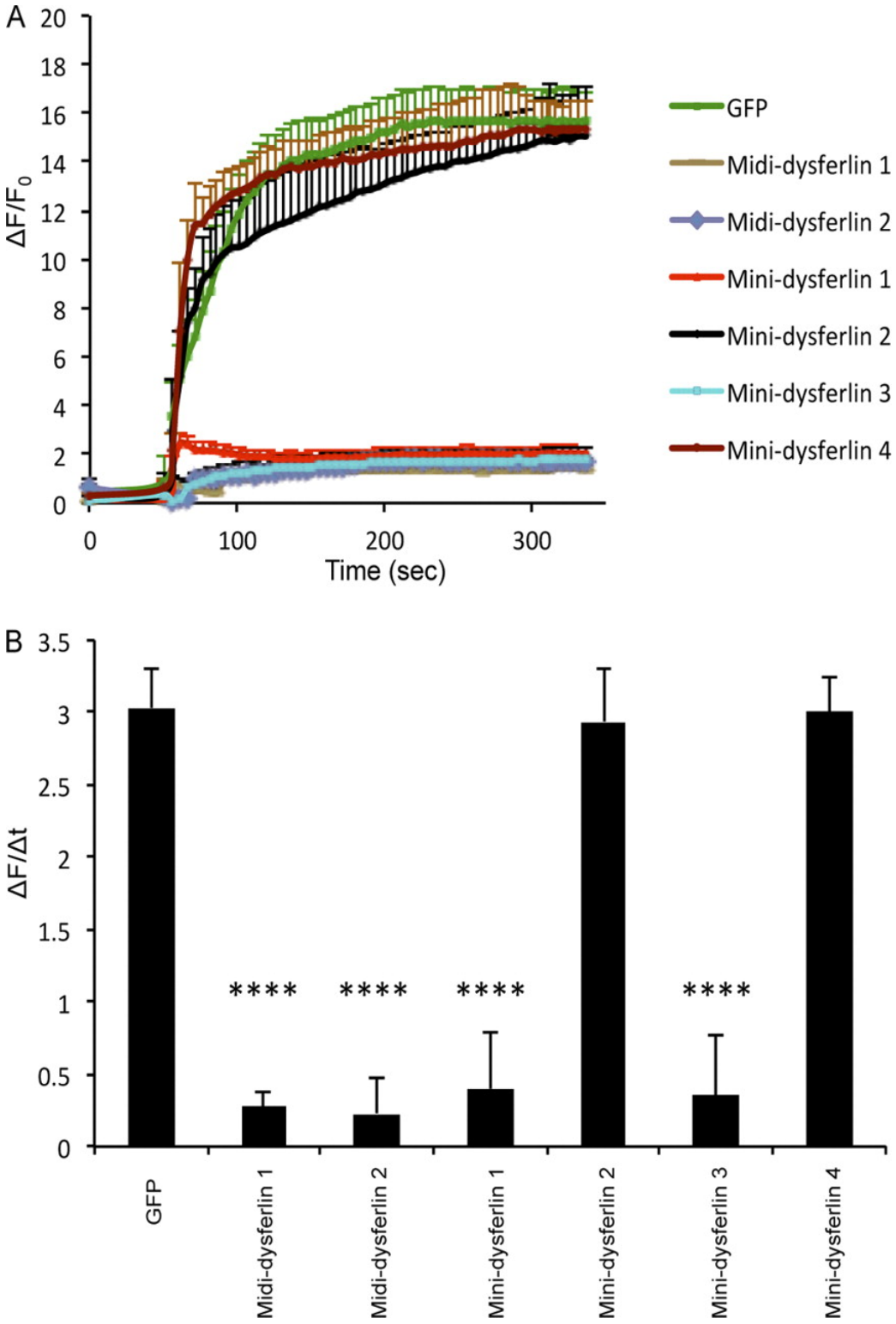

Figure 3.5: Midi-dysferlin 1 and 2, and mini-dysferlin 1 and 3 restore the defect in membrane repair. (A) Plasma membrane repair assay was performed on the dysferlin deficient myoblast culture ULM1/01 transfected with the indicated plasmids. Relative fluorescence intensity ($\Delta F/F_0$) over time following laser-induced injury is presented as means ± 1 SD. Numbers of individual measurements are as follows: for GFP (n = 15), for midi-dysferlin 1 and 2 (n = 20 for each construct), for mini-dysferlin 1 (n=24), for mini-dysferlin 2 (n=20), for mini-dysferlin 3 (n= 21), for mini-dysferlin 4 (n=18). (B) Graphical representation of (A) depicting the change in relative fluorescence intensity after 5 min post-injury. Stars indicate that differences were statistically significant (****, $p < 0.0001$).

Table 3. 1: Primers used for midi- and mini-dysferlin constructs

Dysferlin C2 deletion construct	Sequence of oligonucleotides (oligo)
Dysferlin ΔExon32	Forward: 5'-ATTTCCTGCATATTCGACTAT CCC TATGCCATCGTCTCC-3' Reverse: 5'-GGAGACGATGGCATAGGGATA GTCGAATATGCAGGAAAT-3'
Mini-dysferlin 1	Forward: 5'-ACTCCTCTGGAGCCCTCCCCGGACCAGCTCCGCCCCTCCCAGCTC- 3' Reverse: 5'-GAGCTGGGAGGGGCGGAGCTGGTCCGGGGAGGGCTCCAGAGGAGT- 3'
Mini-dysferlin 2	Forward: 5'-AAGCTGCTGTCAGACAAACCGGCCCTGGGGCGGCCTGGACCT-3' Reverse: 5'-AGGTCCAGGCCGCCCCAGGGCCGGTTTGTCTGACAGCAGCTT- 3'
Mini-dysferlin 3	Forward: 5'-CCCTCCCCGACTCTGCCTGACCTGGATAAGGAGCCCCTCATCCCCATCCAGGAG-3' Reverse: 5'-CTC CTG GAT GGG GAT GAG GGG CTC CTT ATC CAG GTC AGG CAG AGT CGG GGA GGG-3'
Mini-dysferlin 4	Forward: 5'-CTAGAAAGCTGCTGTCAGACAAACCGCAGGTGATTGGTGAATTTAAGGGCCTCTTC- 3' Reverse: 5'-GAAGAGGCCCTTAAATTCACCAATCACCTGCGG TTTGTCTGACAGCAGCTTTCTAG- 3'
Midi-dysferlin 1	Forward: 5'-ACATCTAGAAAGCTGCTGTCACCCACTTTTGGGCCCTGCTAC- 3' Reverse: 5'-GTAGCAGGGCCCAAAAGTGGGTGACAGCAGCTTTCTAGATGT- 3'
Midi-dysferlin 2	Forward: 5'-ATG TCC GTC TCC ACC TTG AGC CCG TCG GGG GAG CTG CTG GCC Reverse: 5'-GGC CAG CAG CTC CCC CGA CGG GCT CAA GGT GGA GAC GGA CAT- 3'

CHAPTER 4

4 Proteasomal inhibition restores biological function of missense mutated dysferlin in patient-derived muscle cells

4.1 Preface

Dysferlin-deficient patients demonstrate a total loss or marked reduction in the levels of dysferlin protein. This suggests that the mutated dysferlin protein produced is being rapidly degraded.

The majority of mutations leading to dysferlinopathies are caused by single point mutations, notably missense and nonsense mutations. From a logical standpoint, nonsense mutations, which encode premature stop codons resulting in truncated proteins, would be easily recognized by the cell's quality control system and sent for degradation. However, missense mutations still produce a full-length protein albeit with a single amino acid alteration. And yet they are nevertheless rapidly degraded. A study by Dr Cooper's group revealed that a single point mutation in dysferlin's FerI domain adjacent to the C2C domain (Lysine 344 Proline) resulted in increased endocytosis and degradation of the missense mutated protein (Evesson et al., 2010). Western blots of muscle biopsies from patients harbouring at least one missense mutation also showed absent or markedly reduced dysferlin protein levels (Therrien et al., 2006). These studies suggested that the severely reduced dysferlin levels observed in patients harbouring dysferlin missense mutations may be due to an increased degradation rate.

We theorized that not all missense mutations—which account for 29% of all dysferlinopathic alleles—would be located in critically conserved regions of the protein, thus raising the possibility that certain mis-sense mutations would be functional when salvaged from degradation. Studies on missense mutated cystathionine b-synthase (CBS) revealed that proteosomal inhibition, or induction of the folding chaperone Heat shock protein 70 (Hsp70), restored significant CBS enzymatic activity in yeast, in fibroblasts derived from homocystinuric patients and also in a mouse model for homocystinuria (Singh et al., 2010).

There are two major pathways for protein degradation, namely the proteosomal and lysosomal pathways.

Proteins destined for proteosomal degradation are tagged with specific ubiquitin chains via the ubiquitin cascade, which involves the sequential interactions between ubiquitin and three ubiquitin-associated enzymes: E1, E2 and E3. The ubiquitin-activating enzyme, E1, activates the ubiquitin moiety. E1 then transfers the ubiquitin to the active site of the ubiquitin-conjugating enzyme, E2. The ubiquitin-ligase enzyme, E3, specifically recognizes the protein targeted for degradation, and interacts with E2 to directly, or indirectly, transfer the ubiquitin via covalent linkage to a lysine residue of the target protein. The ubiquitin length (chains versus monomers) and linkage site (lysine 48, 63, 11, etc) act as signals for various destinations and pathways. The classical proteosomal degradation signal is a polyubiquitin chain on lysine 48.

Proteins destined for lysosomal degradation are also ubiquitinated via a different ubiquitin chain (the canonical signal being a lysine 63 polyubiquitin chain). These proteins traffic from the endosomal sorting compartment into multi-vesicular bodies, which subsequently fuse their contents to lysosomes, where lysosomal enzymes degrade the protein.

In the following work, we demonstrate that dysferlin is degraded via the proteosomal degradation pathway. Furthermore, we show that a specific dysferlin missense mutation, Arginine 555 Tryptophan, can be salvaged from degradation using proteosomal inhibitors and that the protein retains its functionality. This study provides proof of concept that proteosomal inhibition may be a possible novel therapeutic option for some dysferlin-deficient patients harbouring missense mutations.

4.2 Abstract

Dysferlin is a transmembrane protein implicated in surface membrane repair of muscle cells. Mutations in dysferlin cause the progressive muscular dystrophies Miyoshi myopathy, limb girdle muscular dystrophy 2B, and distal anterior compartment myopathy. Dysferlinopathies are inherited in an autosomal recessive manner, and many patients with this disease harbour missense mutations in at least one of their two pathogenic DYSF alleles. These patients have significantly reduced or absent dysferlin levels in skeletal muscle, suggesting that dysferlin encoded by missense alleles is rapidly degraded by the cellular quality control system. We reasoned that missense mutated dysferlin, if salvaged from degradation, might be biologically functional. We used a dysferlin-deficient human myoblast culture harbouring the common R555W missense allele and a DYSF-null allele, as well as control human myoblast cultures harbouring either two wildtype or two null alleles. We measured dysferlin protein and mRNA levels, resealing kinetics of laser-induced plasmalemmal wounds, myotube formation, and cellular viability after treatment of the human myoblast cultures with the proteasome inhibitors lactacystin or bortezomib (Velcade). We show that endogenous R555W missense mutated dysferlin is degraded by the proteasomal system. Inhibition of the proteasome by lactacystin or Velcade increases the levels of R555W missense mutated dysferlin. This salvaged protein is functional as it restores plasma membrane resealing in patient-derived myoblasts and reverses their deficit in myotube formation. Bortezomib and lactacystin did not cause cellular toxicity at the regimen used. Our results raise the possibility that inhibition of the degradation pathway of missense mutated dysferlin could be used as a therapeutic strategy for patients harbouring certain dysferlin missense mutations.

4.3 Introduction

Mutations in dysferlin are responsible for the progressive autosomal recessive muscular dystrophies Miyoshi myopathy (Liu et al., 1998), limb girdle muscular dystrophy type 2B (Bashir et al., 1998), and distal anterior compartment myopathy (Illa et al., 2001).

Dysferlin is a transmembrane protein composed of seven C2 domains and two DysF domains (Therrien et al., 2006), expressed predominantly in skeletal and cardiac muscle (Illa et al., 2001). Dysferlin is implicated in muscle surface membrane repair, as muscle fibers from dysferlin deficient mice are unable to efficiently repair membrane tears induced by laser injuries (Bansal et al., 2003). Dysferlin is important for myotube formation of cultured myoblasts as dysferlin-deficient myoblasts show impaired fusion in vitro (de Luna et al., 2006).

All pathogenic dysferlin mutations reported so far reduce protein expression levels in skeletal muscle (Therrien et al., 2006). This is the case for patients who harbour two DYSF-null alleles, or whose second pathogenic DYSF allele contains a missense mutation, and even for patients with two DYSF missense alleles (Therrien et al., 2006). Absence or strongly reduced levels of dysferlin in the case of missense mutations suggest that the dysferlin protein is sensitive to amino acid substitutions and is rapidly degraded by the quality control system of the cell (Therrien et al., 2006).

We reasoned that some of the eliminated missense mutated dysferlin might be functional if salvaged from degradation. Here we show that levels of endogenous R555W missense mutated dysferlin can be significantly increased through inhibition of the proteasomal system in cultured human myoblasts. The salvaged missense mutated protein is functional as it reverses plasma membrane resealing defects and restores impaired myotube formation.

As dysferlinopathies are recessively inherited, loss-of-function diseases, our results raise the possibility that inhibition of the degradation pathway of missense mutated

dysferlin could be used as a therapeutic strategy for patients harbouring certain dysferlin missense mutations.

4.4 Results

Characterization of Human Myoblast Cultures: DYSF Mutations and Protein Levels—The genotypes of the myoblast cultures used are summarized in Table 1. The control myoblast culture 134/04 containing two wildtype DYSF alleles shows normal dysferlin levels when grown to confluence and is capable of forming myotubes (Figure 4.1*A*), with increased dysferlin levels after fusion (Figure 4.1*B*) (De Luna et al., 2004). Desmin levels are known to increase upon myoblast fusion (Gard et al., 1980; De Luna et al., 2004) and are shown here for the control 134/04 myoblasts after 5 days in fusion medium (Figure 4.1*C*).

ULM1/01 cells carry two dysferlin-null alleles and thus do not express full-length dysferlin (Figure 4.1*B*). Myoblast cells 180/06 carry one dysferlin-null allele. Importantly, the second DYSF allele in the 180/06 cells harbours a missense mutation, exchanging arginine 555 for a tryptophan (R555W). This missense mutation has been described previously (Nguyen et al., 2005; Nguyen et al., 2007; Krahn et al., 2009; Liewluck et al., 2009) and represents the fourth most common missense mutation in the dysferlin gene, according to the Leiden muscular dystrophy Web site (den Dunnen, 1998). 180/06 myoblasts produce barely detectable amounts of dysferlin (Figure 4.1*B*).

The two mutant myoblast cell lines, ULM1/01 and 180/06, show impairment of myotube formation after 5 days in fusion medium (Figure 4.1*A*) and accordingly, express low levels of desmin compared with fused 134/04 control cells (Figure 4.1*C*). These results demonstrate that mutations resulting in absence or strong reduction of dysferlin impair myotube formation in the myoblast cultures ULM1/01 and 180/06.

Membrane Resealing in Untreated Myoblast Cultures— Upon induction of plasma membrane wounds, the dysferlin-deficient myoblasts ULM1/01 and 180/06 continuously accumulated the FM1-43 dye at the plasmalemmal injury site, demonstrating defective membrane repair (Figure 4.1*E*). Resealing kinetics of ULM1/01

and 180/06 did not differ from each other (Figure 4.1*D*). In contrast, wildtype 134/04 myoblasts were able to repair the induced injury rapidly, as shown by the lack of significant dye accumulation (Figure 4.1, *D* and *E*). These results confirm that the absence or severe reduction of dysferlin leads to defective plasmalemmal resealing in the myoblast cultures 180/06 and ULM1/01.

Proteasomal Inhibitors, but Not Lysosomal Inhibitors, Increase Missense Mutated Dysferlin Levels—We aimed to identify the cellular degradation pathway responsible for degradation of endogenous missense mutated dysferlin. Inhibition of the lysosomal pathway using chloroquine and controlled for by a dose-dependent increase in cathepsin D and LC3-II with dysferlin degradation. Proteasomal inhibition was demonstrated by an increase of ubiquitinated proteins with increasing concentrations of the inhibitor (Figure 4.2*B*). Levels of dysferlin in wildtype myoblasts increased moderately in presence of lactacystin. Importantly, lactacystin significantly increased dysferlin levels in a dose-dependent manner in 180/06 myoblasts harbouring the missense allele R555W (Figure 4.2, *B* and *C*). No immunoreactivity was detected in ULM1/01 myoblasts, which harbour two null alleles and are not able to generate a full-length dysferlin. Use of this myoblast culture as a negative control demonstrates the specificity of the dysferlin antibody used in this study, which recognizes a C-terminal epitope. Because no fulllength dysferlin protein is generated by the null alleles, increased dysferlin levels in the 180/06 myoblasts must stem from the missense allele.

Our results demonstrate that endogenous R555W missense mutated dysferlin is degraded by the proteasome rather than by lysosomes. Moreover, when immunoprecipitated, salvaged missense mutated dysferlin proved to be ubiquitinated and thereby destined for degradation by the proteasomal system (Figure 4.2*F*). These findings led us to explore the effects of the FDA-approved proteasomal inhibitor Velcade (bortezomib) on the degradation of dysferlin. Velcade is a reversible peptide boronate blocking the chymotrypsin-like activity of the proteasome (Adams et al., 2004). Velcade treatment slightly increased dysferlin accumulation in the wildtype 134/04 myoblasts (Figure 4.2*D*). Importantly, Velcade markedly increased dysferlin levels in 180/06 myoblasts, but not in ULM1/01 myoblasts (Figure 4.2, *D* and *E*). Salvaged R555W missense mutated dysferlin localized correctly to the plasma

membrane as demonstrated by staining of nonpermeabilized Velcade-treated 180/06 myoblasts with an antibody directed against the extracellular domain of dysferlin (Figure 4.3*A*).

To test whether Velcade would influence mRNA levels to a similar degree as protein levels, we performed quantitative RTPCR experiments on Velcade-treated 180/06 myoblasts. 10 nM Velcade led to a 23-fold increase in missense mutated dysferlin protein levels yet increased dysferlin mRNA levels by only 4-fold (Figure 4.3*B*).

Missense Mutated Dysferlin Can Rescue Membrane Resealing—To test whether the salvaged missense mutated dysferlin protein is biologically active, we tested myoblasts for their ability to reseal laser-induced plasmalemmal injuries under increasing concentrations of lactacystin or Velcade. Lactacystin-treated 180/06 cells successfully resealed their membrane injury in a dose-dependent manner, at concentrations as low as 8 uM, but optimally at 12 uM (Figure 4.4, *A* and *B*). Velcade treatment of 180/06 myoblasts likewise resulted in resealing of the membrane injury in a dose-dependent manner (Figure 4.4, *C* and *D*), at concentrations as low as 10 nM.

In contrast to 180/06 myoblasts, ULM1/01 myoblasts treated with up to 12 uM lactacystin or 50 nM Velcade were unable to reseal their membranes after injury (Supplemental Figure S4.1A and B). To demonstrate that the failure to reseal membrane disruptions in ULM1/01 myoblasts was due to the lack of dysferlin protein and was not an inherent problem of this specific myoblast culture, we transfected ULM1/01 cells with GFP-tagged human dysferlin. Expression of the GFP-dysferlin protein conferred plasma membrane resealing capabilities to those cells, indicating that membrane resealing was possible in these mutant myoblasts if provided with functional dysferlin (Supplemental Figure S4.1*C*).

These results demonstrate that: (i) missense mutated R555W dysferlin is biologically active and can reseal injured plasma membranes of cultured human myoblasts if rescued from proteasomal degradation and (ii) C-terminally truncated dysferlin forms, even if generated from either of the two null alleles (such proteins would escape

detection by the antibody used in this study), are not capable of resealing the plasma membrane.

Lactacystin or Velcade Treatment Reverses Impairment of Myotube Formation in Human Myoblasts Harbouring Missense Mutated Dysferlin—We next tested whether salvaged missense mutated dysferlin protein is able to reverse the fusion deficit of cultured myoblasts. Myoblast culture 180/06 harbouring the dysferlin missense allele was capable of myotube formation upon treatment with lactacystin (as low as 8 uM; Figure 4.5*A*) or Velcade (as low as 10 nM; Figure 4.5*G*).

The increase in desmin levels in the treated 180/06 cells paralleled those observed in 134/04 myotubes (Figure 4.5, *B*, *C*, *H*, and *I*). In contrast, ULM1/01 myoblasts did not fuse upon treatment with proteasomal inhibitors (Figure 4.5, *D* and *J*), and desmin levels remained unchanged (Figure 4.5, *E*, *F*, *K*, and *L*). These results indicate that missense mutated dysferlin protein salvaged by lactacystin or Velcade treatment is able to reverse the fusion deficit of cultured myoblasts.

Toxicity of Lactacystin and Velcade—Because induction of apoptosis is the proposed mechanism of action of proteasome inhibitors in the treatment of multiple myeloma (Sterz et al., 2008) we tested the toxicity of the inhibitors in the human myoblast cultures. We did not detect any appreciative cell death at concentrations that conferred efficient membrane resealing and myoblast fusion, even when cells were incubated for up to 5 days in the presence of either lactacystin (Figure 4.6, *A*–*C*) or Velcade (Figure 4.6, *D*–*F*). Toxicity was observed only at significantly higher concentrations of both drugs (20 uM for lactacystin and 500 nM for Velcade). Toxicity profiles of the proteasomal inhibitors were similar in all three human myoblast cultures.

Our results show that the use of proteasomal inhibitors under conditions necessary to salvage missense mutated dysferlin from degradation, to restore membrane resealing and to reverse the fusion deficit is devoid of toxicity in cultured human myoblasts.

4.5 Discussion

In certain genetic diseases, mutations may lead to only subtle protein-folding anomalies without rendering the protein biologically inactive, yet causing its enhanced degradation (Chaudhuri et al., 2006). Many dysferlinopathy patients harbour missense mutations in at least one of their two pathogenic DYSF alleles and show markedly reduced or undetectable dysferlin protein levels in skeletal muscle (Therrien et al., 2006). We hypothesized that such dysferlin missense mutations could give rise to a biologically functional protein if salvaged from degradation. In this proof-of-concept study we show that inhibition of the proteasome leads to a significant increase in protein levels of a dysferlin missense mutant in cultured human myoblasts (Figure 4.2). We further demonstrate that this missense mutated dysferlin protein is functional, able to restore plasmalemmal resealing (Figure 4.4), and able to reverse the fusion deficit of cultured human myoblasts (Figure 4.5). Our results indicate that the effect of proteasomal inhibition is largely due to the interference with the degradation of missense mutated dysferlin rather than due to the enhanced dysferlin mRNA expression. This is in line with a recent study (Belanto et al., 2010) in which a 10-fold increase in dysferlin mRNA obtained by dexamethasone treatment of C2C12 myoblasts was able to only double dysferlin protein levels. The above observations, therefore, suggest that the markedly increased levels of missense mutated dysferlin in our study are largely due to the inhibition of protein degradation, although we cannot exclude that the slight increase in dysferlin mRNA, through as yet unexplored mechanisms, may also play a role.

Our study has been performed with the common R555W DYSF allele. The R555W mutation lies in a polypeptide stretch between the C2C domain and the Dysf domain of the dysferlin protein, a region that may have low functional relevance. It is conceivable that many other dysferlin missense mutant proteins may retain their functional activity when salvaged from degradation. However, it is likely that some missense mutations lie in functionally more important dysferlin regions and that the biological activity of such mutated proteins might not be salvageable. It would therefore be important to systematically map dysferlin missense mutants for retention of their biological activity.
Velcade has been approved by the Federal Drug Administration (FDA) for treatment of multiple myeloma and mantle cell lymphoma (Bross et al., 2004). The antineoplastic effect is due to sensitization of tumor cells to apoptosis through interference with

degradation of proteins implicated in cell cycle control (Sterz et al., 2008) and through repression of NF-KB signaling by stabilization of the cytoplasmic inhibitor I-KB (Sterz et al., 2008). In the myoblast cultures used in this study, Velcade concentrations that allowed us to achieve membrane repair and myoblast fusion (10 nM) were not toxic even when cells were treated for 5 days. These concentrations are within the range at which Velcade confers its antineoplastic effect on multiple myeloma cells *in vitro* (Hideshima et al., 2001). It is therefore possible that concentrations of Velcade similar to those used for the treatment of patients with multiple myeloma would also influence the degradation of missense mutated dysferlin (Bross et al., 2004).

Therapeutic strategies aiming to influence the cellular misfolded protein response and/or the protein degradation pathways have been proposed for cystic fibrosis patients carrying the common cystic fibrosis transmembrane conductance regulator mutation deltaF508 (Ward et al., 1995). This mutant chloride channel protein is retained in the endoplasmatic reticulum but is functional when forced to reach the plasma membrane (Pedemonte et al., 2005). Further examples include the dominant negative mutations in caveolin-3, which cause sequestration in the Golgi apparatus of the wildtype caveolin-3 encoded by another allele. Treatment of cultured caveolin-3 mutant cells with proteasomal inhibitors allows the wildtype proteins to reach the plasma membrane (Galbiati et al., 2000). Also, members of the dystrophin glycoprotein complex, which become secondarily deficient in the absence of dystrophin, can be salvaged in a mouse model of dystrophinopathy and in muscle explants from Duchenne and Becker muscular dystrophy patients upon treatment with proteasomal inhibitors (Bonuccelli et al., 2007; Gazzerro et al., 2010). Currently, no causal pharmacological treatment is available for patients affected by the progressive and debilitating muscular dystrophies caused by dysferlin deficiency. Based on clinical observations of dysferlinopathy patients with internally truncated dysferlin molecules and mild phenotype (Sinnreich et al., 2006; Krahn et al., 2010), exon-skipping strategies have been developed (Aartsma-Rus et al., 2010; Wein et al., 2010), analogous to strategies currently tested in patients with dystrophinopathies (van Deutekom et al., 2007; Kinali et al., 2009). Other experimental treatment possibilities include the generation of small dysferlin molecules suitable for adeno-associated virus (AAV)-mediated gene delivery (Krahn et al., 2010), or expression of dysferlin coding fragments which recombine after

dual adeno-associated virus-mediated gene transfer to generate one transcript able to produce the full-length protein (Lostal et al., 2010). Stop codon read-through, using Ataluren (PTC124), has been suggested as a possible therapy for patients harbouring nonsense mutations (Wang et al., 2010), and cell based therapies have also been recently proposed using mesangioblasts (Diaz-Manera et al., 2010).

Because dysferlinopathies are recessively inherited, loss-of-function diseases, our observations suggest that it would be worth exploring the inhibition of the degradation pathway of missense mutated dysferlin as a possible therapeutic strategy for patients who harbour at least one missense dysferlin allele encoding a protein, which retains its function when salvaged from degradation. Because currently no available dysferlin-deficient mouse models carry dysferlin missense alleles (Bittner et al., 1999; Bansal et al., 2003; Ho et al., 2004), the proof of concept shown here should lay ground for the development of appropriate knock-in mouse models harbouring dysferlin missense alleles or for clinical trials in patients carrying dysferlin missense alleles encoding a salvageable protein.

4.6 Experimental Procedures

Cell Culture and Transfection—We obtained three human primary myoblast cultures from EuroBioBank, along with the required IRB approvals. Myoblast culture 134/04 contains two wildtype DYSF alleles. Myoblast culture 180/06 harbours one DYSF allele containing the missense mutation C1663T (R555W) and an additional null allele 3708delA (D1237TfsX24). Myoblast culture ULM1/01 harbours two null alleles: a C4819T (R1607X) substitution and a 5085delT (F1695LfsX48) deletion (see Table 4.1). All cells of the three myoblast cultures stained positive for desmin (data not shown). Myoblast cultures were infected with a retroviral construct carrying the E6E7 early region from human papillomavirus type 16 to extend their life span as described previously (Lochmuller et al., 1999). Myoblast cultures were maintained in Dulbecco's modified Eagle's medium (DMEM; Sigma) containing 10% fetal bovine serum (FBS; Invitrogen). Where indicated, cells were transfected with pEGFP-C1 (Clontech) and a plasmid encoding GFP-dysferlin (a gift from Dr. K. Bushby) using 10 ul of Lipofectamine 2000 (Invitrogen) and 4 ug of plasmid DNA/10cm^2 culture dish, at 70% confluence.

Cells were cultured for 24 h before treatment with lactacystin (Enzo Life Sciences), bortezomib (Velcade; Selleck Chemicals), chloroquine, or pepstatin/E64d (SigmaAldrich) at the indicated concentrations. These experiments were done in quadruplet.

For myotube formation, human myoblasts were cultured in DMEM containing 10% FBS. Near confluence, cells were switched to fusion medium containing 2% horse serum and the indicated concentrations of lactacystin or Velcade.

Protein Extraction and Western Blotting—Proteins were extracted from cultured, confluent myoblasts as described previously (Azakir et al., 2010). Proteins were separated on SDS-polyacrylamide gel and blotted onto a polyvinylidene difluoride (PVDF) membrane. Membranes were blocked for1h in buffer 1 (Tris-buffered saline containing 3% Top-Block, 0.05% sodium azide) and incubated for 16 h with the indicated antibody in buffer 2 (Tris-buffered saline containing 3% Top-Block, 0.05% sodium azide, 0.05% Tween 20). Monoclonal antibody against a-tubulin was purchased from Abcam; against dysferlin from Vector Laboratories (REACTOLAB, clone Ham1/7B6), against ubiquitin from Enzo Life Sciences, against LC3 from Cell Signaling. A polyclonal antibody against desmin was purchased from Sigma-Aldrich. The membranes were washed with buffer 2 and incubated for 1 h with secondary antibodies Alexa Fluor680 goat anti-mouse IgG (Invitrogen) or IRDye 800 goat antirabbit IgG (Jackson Laboratories) in buffer 2 (1:10,000 dilution). Membranes were washed in buffer 2 and detected with Odyssey Infrared Imaging System (LI-COR). Western blotting experiments were repeated at least three times. Densitometric analysis was performed using ImageJ (National Institutes of Health). Statistical analysis was performed using Student's t-test.

RNA Isolation, cDNA Synthesis, and Relative Quantitative Real-time PCR—Total cellular RNA was extracted using the RNeasy Mini kit (Qiagen). RNase-free DNase-treated RNA samples were reverse transcribed with random hexamers using the High Capacity cDNA Reverse Transcription kit (Applied Biosystems) according to the manufacturer's protocol. Primers for hypoxanthine-guanine phosphoribosyltransferase (HPRT)2 and dysferlin were purchased from Microsynth; HPRT_forward, TGA CCT TGA TTT ATT TTG

CAT ACC and HPRT_ reverse, CGA GCA AGA CGT TCA GTC CT; DYSF_forward, CAG TCC CAG AGA GTT CAC AGG and DYSF_reverse, CCA GGG AGA GCA GAA GCC A. Relative quantitative PCR was performed on a Real-Time PCR system Step One Plus AB Applied Biosystems in a 96-well microtiter plate using 2X FastSYBR Green Master mix (AB Applied Biosystems) and 300 pM-specific primer mix. To compensate for variable RNA and cDNA yields, the expression of HPRT was used as a control.

Immunoprecipitation and Immunocytochemistry—For immunoprecipitation assays, protein extracts of human myoblast cultures 180/06 were incubated with rabbit polyclonal antidysferlin antibody (Orbigen) and protein A-Sepharose for 16 h at 4 °C. Beads were washed extensively and prepared for Western blot analysis and probed with anti-ubiquitin antibody (Millipore).

For immunocytochemistry, 180/06 myoblasts were treated with 50 nM Velcade for 24 h, washed, and preincubated for 15 min with rabbit monoclonal anti-dysferlin antibody which recognizes an extracellular C-terminal epitope (Epitomics). Cells were washed and fixed for 20 min with 4% paraformaldehyde, blocked for 30 min with 1% normal goat serum, 2% of fish skin gelatin, and 0.2% Triton X-100 in PBS, and incubated with DyLight 488-Conjugated AffiniPure goat anti-rabbit IgG (H+L) (Jackson Laboratories) for 1 h and mounted on coverslips with Fluorsave reagent (Calbiochem).

DNA Analysis—DYSF alleles of myoblast cultures were verified by sequencing exons of interest as described in Therrien et al. (Therrien et al., 2006) using the following primer pairs: exon 18 forward, 5'-CGTGGCGTTCTTCTTTATACACTGAC-3' and exon 19 reverse, 5'-TGATTTATTCCCACTTTACAGCTGAGAC-3'; exon 34 forward, 5'-CAGCTTGTTTTGTCCTTGAGTCCTGCTA-3' and exon 34 reverse, 5'-CAGACATTCCTGATCCCCAAATTCTATTC-3'; exon 44 forward, 5'-CAGATCTCATGATACTTATTTACTATC-3', and exon 44 reverse, 5'-CTTCTAGAGCACTTGGTCCTTAACACAAC-3'; exon 46 forward, 5'-CATTTCCAATTCATTCTTTCGGTC-3' and exon 46 reverse, 5'-CCACCACTTACAAGCAATAACATCTC-3'.

Plasmalemmal Repair Assay—We developed this assay by modifying a protocol by Bansal et al. (Bansal et al., 2003) initially designed for mouse myofibers. Myoblasts were cultured in a Lab-Tek chambered coverglass (two wells) coated with 4 ug of poly-D-lysine. After 24 h, 70% confluent myoblasts were switched to PBS containing 10 mM HEPES and 1.5 mM CaCl2. The fluorescent dye FM1-43 or FM4-64 (both from Invitrogen) was added to the medium of the respective myoblast culture at a concentration of 2.5 uM. Myoblast plasma membranes were injured with a combination of three lasers (405 nm (30 mW), 458 nm (25 mW), 488 nm (25 mW)) for 4,000 cycles (lasting 50 s in total) on an LSM 710 inverted confocal microscope (Zeiss). Images were captured before injury (t = 0) and for 5 min after injury at 5-s intervals. The fluorescence intensity at the site of damage was measured using Zeiss 2009 software. At each time point, relative fluorescence values were determined by subtracting the background value and dividing the net fluorescence increase by the value of florescence at t = 0. Numbers of repeat plasmalemmal injuries are indicated in the legends alongside the respective experiments.

Cytotoxicity Assay—Cytotoxicity was determined using the MTT reagent (3-(4,5-dimethylthiazol-2-yl)-2,5-diphenyltetrazolium bromide) (Invitrogen) according to the manufacturer's instructions.

4.7 Acknowledgements

We thank Muscle Tissue Culture Collection for providing the myoblast samples used in this study. The Muscle Tissue Culture Collection is part of the German network on muscular dystrophies (MD-NET, service structure S1, 01GM0601) funded by the German Ministry of Education and Research (BMBF, Bonn, Germany). The Muscle Tissue Culture Collection is a partner of EuroBioBank and TREAT-NMD. We thank Dr. E. Shoubridge and Timothy Johns for help with the E6E7 retroviral infection of the human myoblast cultures; Dr. K. Bushby, Newcastle, for the GFP-cDNA; Beat Erne and Steven Salomon for technical assistance; and Drs. M. Filipowicz, J. Sinnreich, M. Rüegg, and J. Halter for helpful discussions.

4.8 Figures and Figure Legends

Figure 4.1: Characterization of the human myoblast cultures.

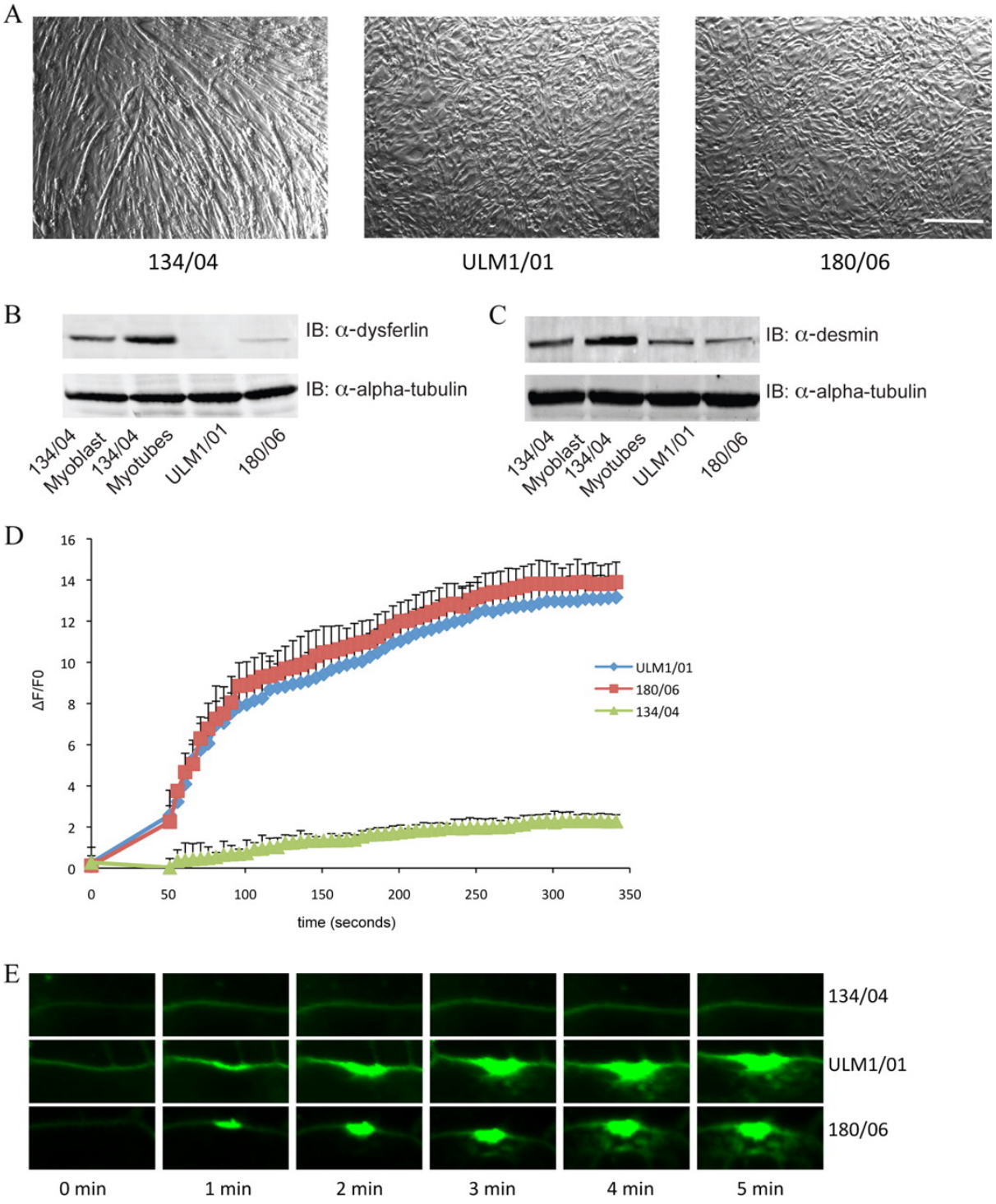

Figure 4.1: Characterization of the human myoblast cultures.

(A) Light microscopy image to show capability of myotube formation in 134/04, and impairment thereof in ULM1/01 and in 180/06 human myoblasts after five days in fusion media. Scale bar represents 250μm. (B) Western blot for dysferlin in 134/04 myoblasts and myotubes, and ULM1/01 and 180/06 myoblasts. The two null alleles in ULM1/01 cells introduce stop codons in exons 44 and 46, respectively. Truncated dysferlin proteins, if generated at all from either of these two null alleles, would lack the C2 domains F and G as well as the transmembrane domain. The anti-DYSF antibody used in this study recognizes polypeptides encoded by exon 54 (amino acids 2020-2037), and would thus not be able to recognize such potentially truncated proteins. 180/06 cells carry one null allele and the Arg555Trp missense allele. The bottom panel shows the level of alpha-tubulin as loading control of identical samples run on a parallel gel. IB: Immunoblot. (C) Western blot for desmin in 134/04 myoblasts and myotubes, and ULM1/01 and 180/06 myoblasts. The bottom panel shows the level of alpha-tubulin as loading control of identical samples run on a parallel gel. (D) Quantitative data of relative fluorescence intensity over time after laser-induced injury of 134/04 (green triangles, n=10), ULM1/01 (blue diamonds, n=10) and 180/06 (red squares, n=10) myoblasts, indicating defective plasma membrane resealing in ULM1/01 and 180/06 myoblasts and effective resealing in 134/04 myoblasts. Data are presented as means plus one standard deviation. (E) Membrane repair assay performed on human myoblast cultures 134/04, ULM1/01 and 180/06 in the presence of Ca^{2+}. The panel shows fluorescence accumulation of the FM1-43 dye over time. The lack of fluorescence intensity increase at the wound site in 134/04 myoblasts indicates that the injured plasma membrane has been resealed, whereas increased fluorescence intensity at the wound site of ULM1/01 and 180/06 myoblasts indicates impaired membrane resealing. Scale bar 1 μm.

Figure 4.2: Proteasomal inhibitors, but not lysosomal inhibitors, significantly increase protein levels of the dysferlin missense mutant Arg555Trp in cultured human myoblasts.

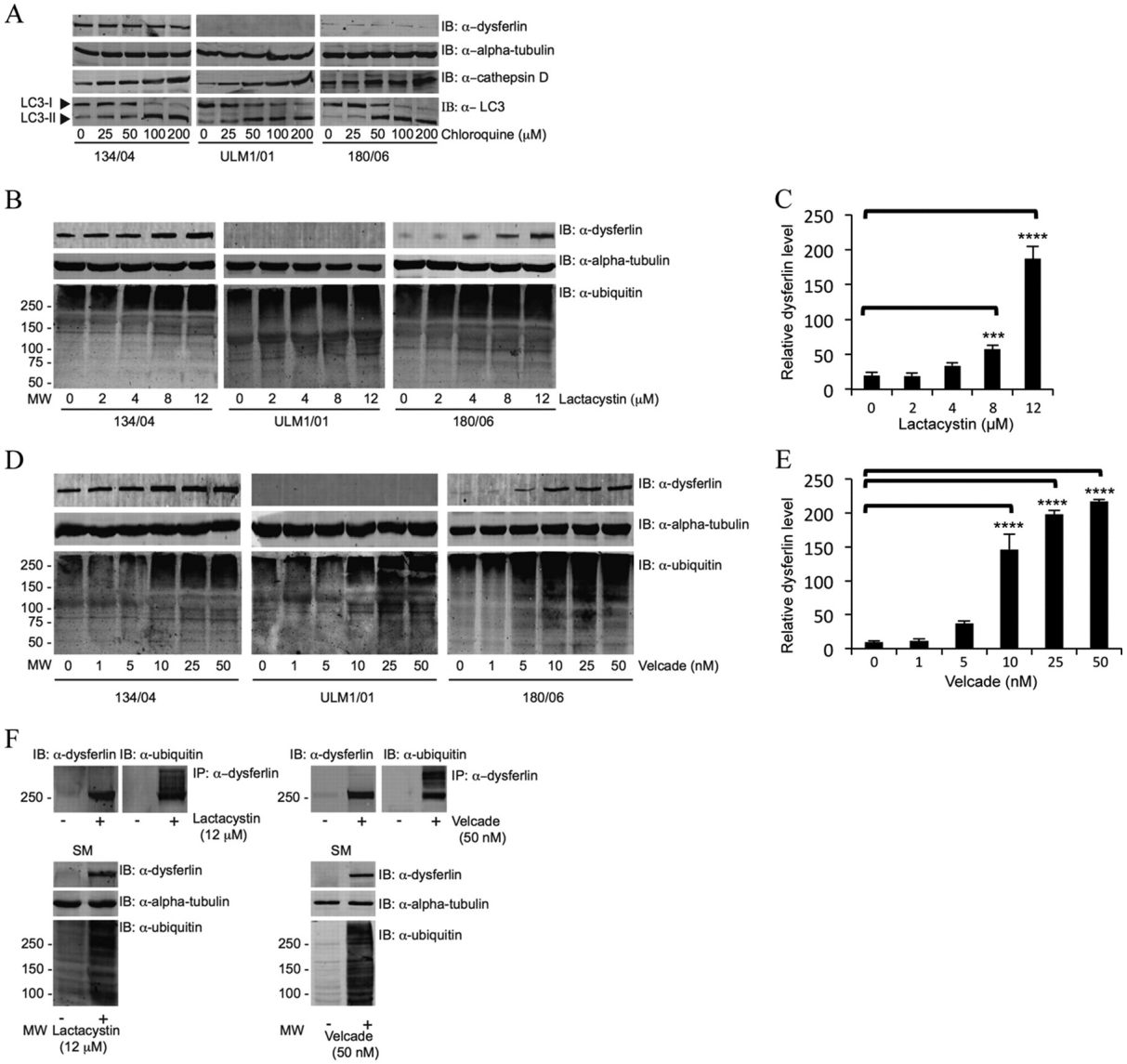

Figure 4.2: Proteasomal inhibitors, but not lysosomal inhibitors, significantly increase protein levels of the dysferlin missense mutant Arg555Trp in cultured human myoblasts. (A) Confluent cultures of 134/04, ULM1/01 and 180/06 myoblasts were treated with increasing concentrations of the lysosomal inhibitor chloroquine. Western blots of protein extracts were blotted with anti-cathepsin D and anti-LC3 antibodies to demonstrate successful lysosomal inhibition (lower panels) or with anti-dysferlin antibody to detect the expression of full-length dysferlin (upper panel). Alpha-tubulin was used as a loading control (middle panel). (B) and (D) Confluent cultures of 134/04, ULM1/01 and 180/06 myoblasts were treated with increasing concentrations of the proteasomal inhibitors Lactacystin (B) or Velcade (D). Western blots of protein extracts were stained with anti-ubiquitin antibodies to demonstrate successful proteasomal inhibition (lower panel), with anti-alpha-tubulin antibodies as a loading control (middle panel) and with anti-dysferlin antibodies to detect the expression of full length dysferlin (upper panel) (n=4). Dysferlin levels increase significantly in the myoblast culture 180/06 harbouring the Arg555Trp DYSF missense allele and to a lesser degree in the wildtype myoblast culture 134/04. Western Blot of ULM1/01 myoblasts which harbour two null alleles, not able to generate full-length dysferlin, demonstrates that the C-terminally directed anti-dysferlin antibody used in this study is specific to dysferlin. (C) and (E) y axis depicts the ratio between dysferlin and alpha-tubulin in 180/06 cells at each lactacystin (C) or Velcade (E) concentration normalized to the ratio between dysferlin and alpha-tubulin in 134/04 cells in absence of inhibitors. Stars indicate that differences were statistically significant (***: $p<0.001$, ****: $p<0.0001$). (F) Salvaged missense mutated dysferlin is ubiquitylated. Confluent cultures of 180/06 myoblasts were treated with proteasomal inhibitors Lactacystin or Velcade. Dysferlin was immunoprecipitated with rabbit polyclonal anti-dysferlin antibody and blotted with anti-ubiquitin antibody (see materials and methods). IP: Immunoprecipitation, IB: Immunoblot, SM: Standard Material, 5% of total protein loaded.

Figure 4.3: Velcade treatment leads to localization of missense mutated dysferlin to the plasma membrane and increases dysferlin mRNA.

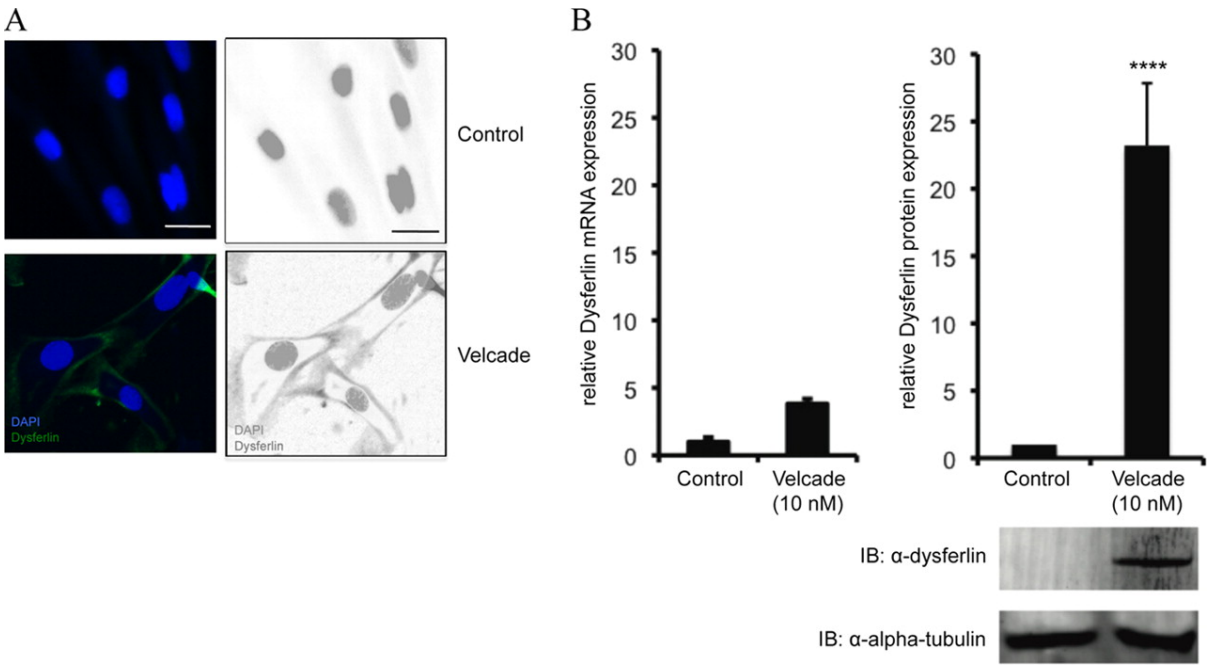

Figure 4.3: Velcade treatment leads to localization of missense mutated dysferlin to the plasma membrane and increases dysferlin mRNA. (A) Immunostaining against an extracellular dysferlin epitope in 180/06 myoblasts, carrying the Arg555Trp dysferlin missense allele, incubated for 24 hours with Velcade (50nM) demonstrates membrane localization of dysferlin (green), DAPI (blue). An inverted image in black and white is represented on the right to better visualize the plasma membrane staining with the anti-dysferlin antibody in the Velcade treated cells. Scale bar represents 50 μm. (B) Levels of dysferlin mRNA (left panel) increase four-fold after 24 hour incubation of 180/06 human myoblasts with 10nM Velcade. Levels of missense mutated dysferlin protein (right panel) increase 23-fold after 24 hours incubation of 180/06 human myoblasts with 10nM Velcade. Protein levels were measured by densitometric analysis using the Western blot shown. Stars indicate that differences were statistically significant (****: $p<0.0001$).

Figure 4.4: Missense mutated dysferlin can rescue defective membrane resealing.

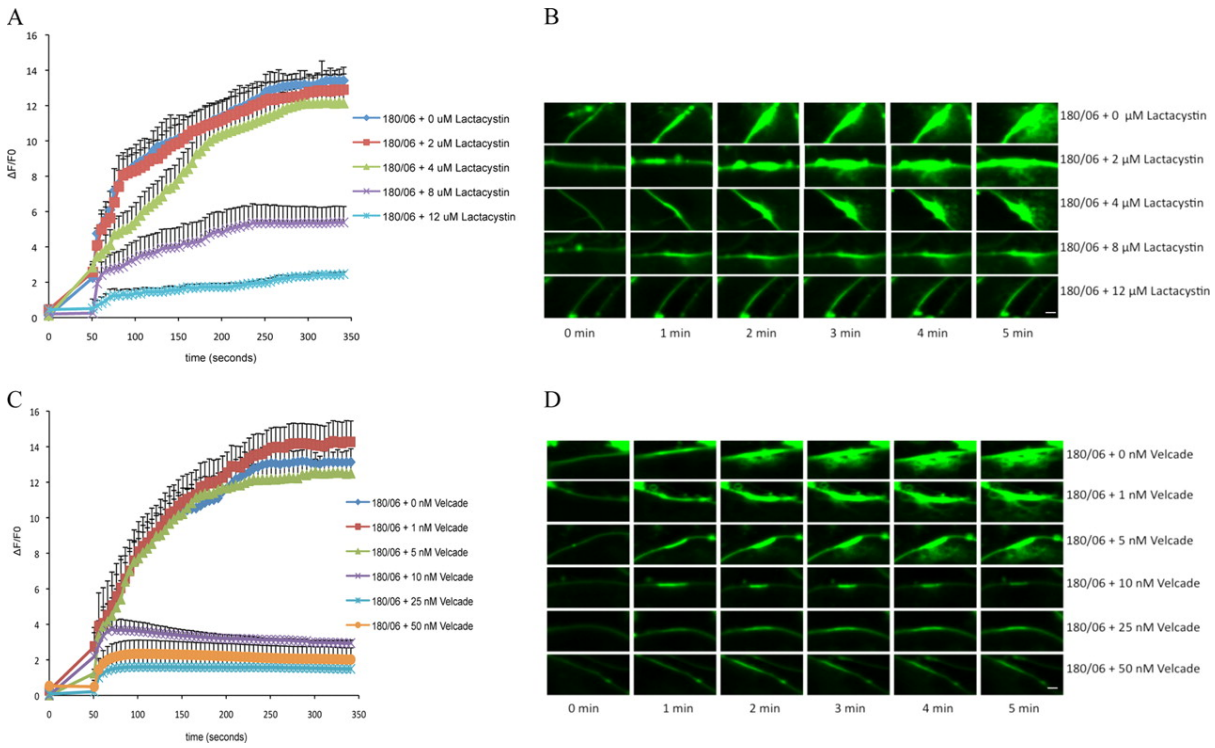

Figure 4.4: Missense mutated dysferlin can rescue defective membrane resealing. Plasma membrane repair assay performed on myoblast culture 180/06 which harbours a dysferlin missense allele Arg555Trp and a DYSF null allele. The laser-induced injury was performed after incubating the myoblasts for 24 hours with increasing concentrations of Lactacystin (A, B) or Velcade (C, D). Quantitative data of relative fluorescence intensity over time after laser-induced injury of 180/06 myoblasts treated with increasing concentrations of Lactacystin (A) or Velcade (C). Data are presented as means plus one standard deviation. Numbers of individual measurements are indicated as follows: for Lactacystin 0 μM (n=7), 2 μM (n=10), 4 μM (n=10), 8 μM (n=12), 12 μM (n=17); for Velcade 0 nM (n=7), 5 nM (n=10), 10 nM (n=12), 25 nM (n= 20), 50 nM (n=20). (B) and (D) show the fluorescence accumulation of the FM1-43 dye over time at the plasma membrane injury site after incubating the myoblasts for 24 hours with increasing concentrations of Lactacystin (B) or Velcade (D). Scale bar represents 1 μm.

Figure 4.5: Treatment with proteasome inhibitors induces myotube formation in myoblasts harbouring the dysferlin missense allele Arg555Trp

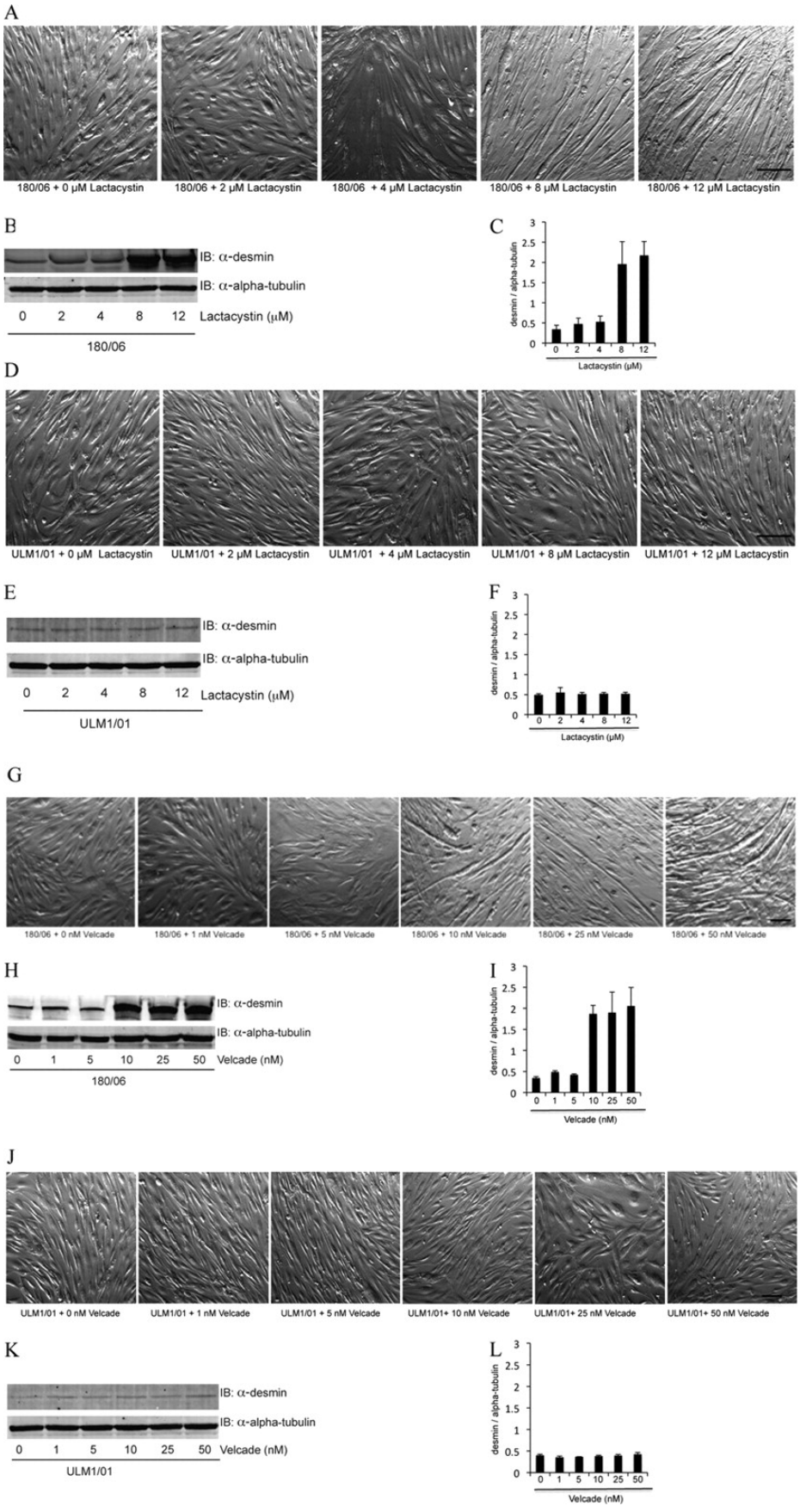

Figure 4.5: Treatment with proteasome inhibitors induces myotube formation in myoblasts harbouring the dysferlin missense allele Arg555Trp. Light microscopy images of human myoblasts 180/06 (A) and (G) and ULM1/01 (D) and (J) treated with increasing concentrations of Lactacystin (A) to (F) or Velcade (G) to (L) for 5 days in fusion media to induce myotube formation. Scale bar represents 50 μm. Desmin expression levels are shown as a marker for fusion, and alpha-tubulin levels represent loading controls of identical samples run on parallel gels (B), (E), (H), (K). Desmin levels were quantified in three independent experiments using Image J and were normalized to the levels of alpha-tubulin (C), (F), (I), (L). Data are presented as means plus one standard deviation. 180/06 myoblasts can fuse when treated with concentrations as low as 8 μM of Lactacystin or 10 nM of Velcade. ULM1/01 myoblasts remain unable to fuse irrespective of the concentrations of inhibitors used.

Figure 4.6: The concentrations of Lactacystin and Velcade used to achieve the biological effects are not toxic to the cultured human myoblasts

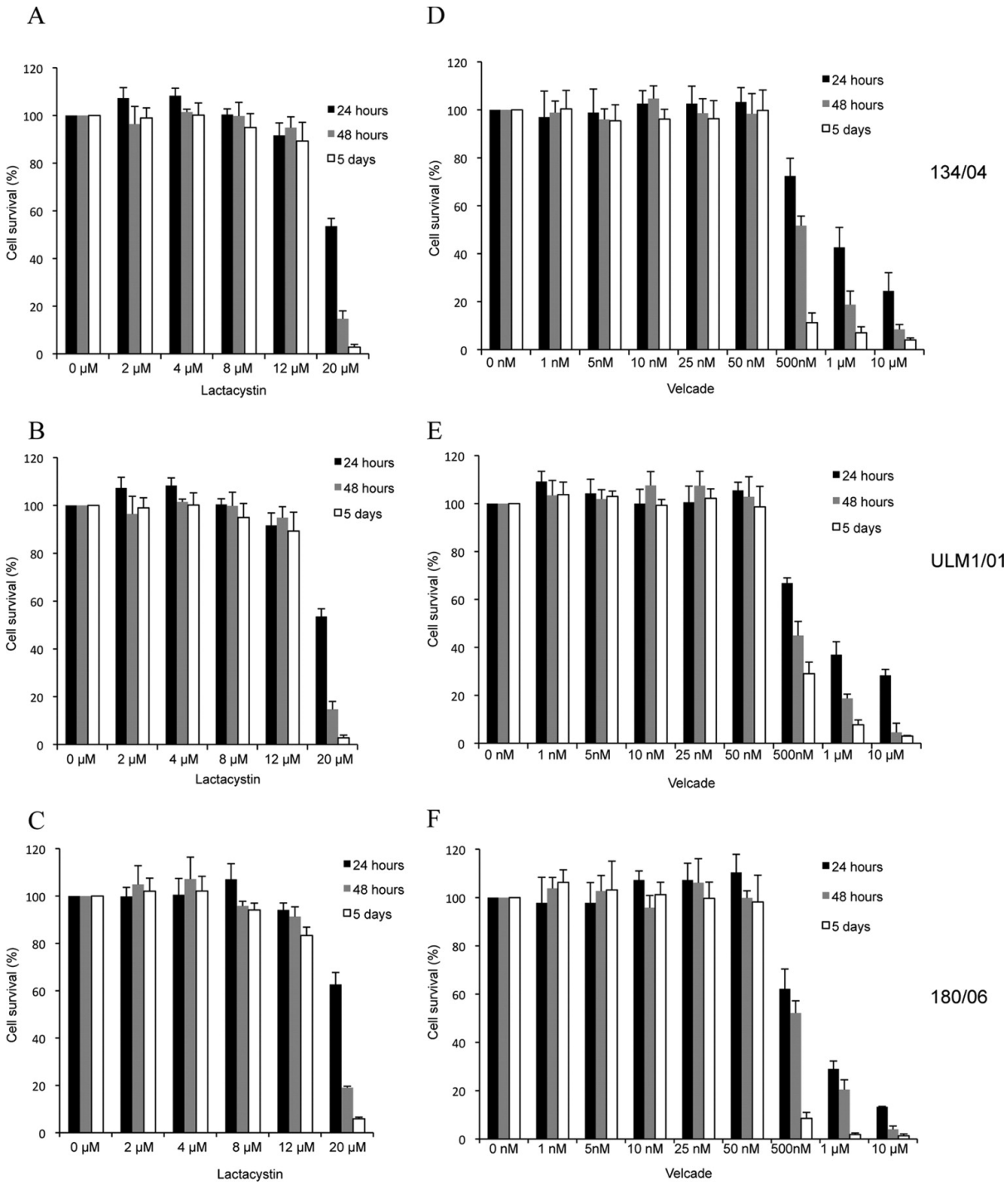

Figure 4.6: The concentrations of Lactacystin and Velcade used to achieve the biological effects are not toxic to the cultured human myoblasts. Cytotoxicity was measured in the human cultured myoblasts treated with increasing concentrations of Lactacystin (A), (B), (C) or Velcade (D), (E), (F) after 24 hours (black bars), 48 hours (grey bars) and 5 days (white bars). The Y-axis represents the percentage of surviving cells as compared to control cells without proteasomal inhibitor treatment. Data are presented as means plus one standard deviation.

Figure S 4.1: Membrane resealing failure in myoblasts harbouring two DYSF null alleles.

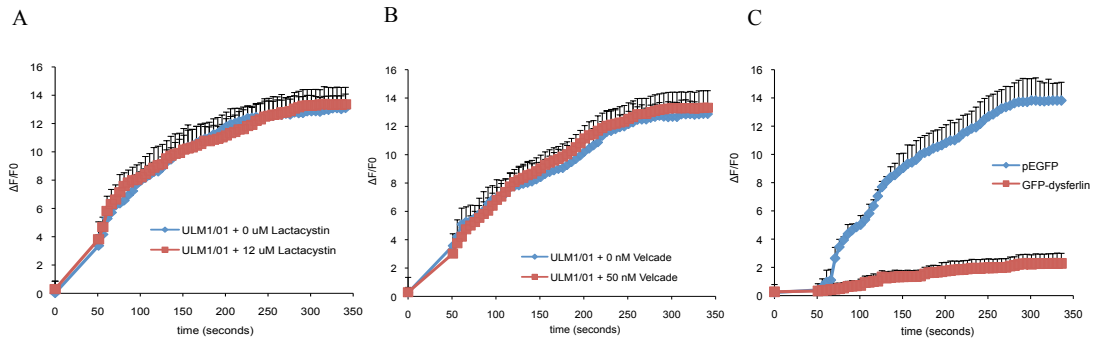

Figure S4.1: Membrane resealing failure in myoblasts harbouring two DYSF null alleles. Quantification of relative fluorescence intensity over time after laser-induced injury of ULM1/01 myoblasts (harbouring two null dysferlin alleles) treated with 12 μM Lactacystin (A) or 50 nM of Velcade (B) reveals no effect on plasmalemmal resealing kinetics. Transfection of these cells with GFP-dysferlin reinstates membrane resealing capability, measured with FM4-64 instead of FM1-43, so as not to interfere with the fluorescence emitted by the GFP epitope (C). Numbers of individual measurements are as follows: for Lactacystin: 0 μM (n= 8) and 12 μM (n= 12); for Velcade: 0 nM (n= 10) and 50 nM (n=10); for GFP (n=8) and GFP-dysferlin (n=12) Data are presented as means plus one standard deviation.

CHAPTER 5

5 Certain dysferlin missense mutations are intrinsically biologically active

5.1 Preface

Our proof-of-principle study presented in Chapter 4 suggests that certain dysferlin missense mutations may retain their biological activity if they are salvaged from proteasomal degradation. Missense mutations of the dysferlin gene account for 29% of the mutations and are located throughout the *DYSF* genome; they are found within individual C2 domains, fer domains, DysF domains and the transmembrane domain, as well as in linker regions between the domains. We theorized that in addition to the Arg555Trp mutation studied in Chapter 4, there might be other dysferlin missense mutations that retain their biological function when salvaged from proteasomal degradation. We designed recombinantly-generated missense mutated dysferlin cDNAs harbouring epitope tags, which were tested for correct plasmalemmal localization and their ability to reseal laser-induced membrane injuries. This study identified additional functional and nonfunctional dysferlin missense mutations, the results of which could be used to expand the repertoire of patients that may be amenable to Bortezomib (Velcade) treatment.

5.2 Abstract

Dysferlin is a large transmembrane protein involved in the plasma membrane repair of skeletal muscle cells. Recessively inherited mutations in dysferlin lead to muscular dystrophies, for which no treatment is currently available. Patients harbouring missense mutations in their dysferlin alleles have significant to total loss of their dysferlin protein. We recently showed that patient-derived myoblasts harbouring the Arg555Trp missense mutation retained functional activity when rescued from proteasomal degradation. We reasoned that other dysferlin missense mutations may also produce biologically active proteins, and used recombinantly-generated dysferlin molecules harbouring common missense mutations to screen for additional functional mutants. Using a plasma membrane localization assay and a plasma membrane repair assay, we showed that some dysferlin missense mutations (Val374Leu and Asp1837Asn) are intrinsically biologically active, whereas others (Arg959Trp, Pro1970Ser and Arg2042Cys) lack functionality when overexpressed by transient transfection, or when rescued from proteasomal degradation using the FDA-approved proteasomal inhibitor, Bortezomib (Velcade). These studies suggest that there may be a significant number of dysferlin missense mutations that may be amenable to proteasomal inhibition as a possible therapeutic strategy for dysferlinopathy patients harbouring missense mutations.

5.3 Introduction

Dysferlin is a large transmembrane protein implicated in calcium-dependent plasmalemmal repair of muscle cells. It localizes to the plasma membrane, to the T-tubules and to intracellular vesicles of as yet unidentified origin (Bansal et al., 2003; Klinge et al., 2010). Recessively-inherited mutations in the *DYSF* gene cause Limb girdle muscular dystrophy type 2B (LGMD2B) (Liu et al., 1998), Miyoshi Myopathy (Liu et al., 1998) and Distal anterior compartment myopathy (Illa et al., 2001). Single nucleotide substitutions in the *DYSF* gene resulting in missense and nonsense mutations similarly result in total loss of, or severe reduction in, dysferlin protein levels in skeletal muscle (Therrien et al., 2006). This suggests that dysferlin is highly sensitive to single residue mutations and is rapidly degraded.

We previously showed that dysferlin harbouring the missense mutation Arg555Trp can be salvaged from degradation in the proteasome, and that it retains its biological activity, as demonstrated by rescued plasmalemmal resealing kinetics, plasmalemmal localization and myotube formation, which are characteristic features of full-length dysferlin function (Azakir et al., 2012).

To date, there are over 130 pathogenic dysferlin missense mutations that have been reported in the Leiden Muscular Dystrophy database (den Dunnen, 1998). Using site-directed mutagenesis techniques on a full-length dysferlin construct, we designed numerous recombinant dysferlin missense mutations to test their ability to rescue plasmalemmal resealing in repair-defective patient-derived dysferlin-deficient myoblasts, as well as their ability to correctly localize at the plasma membrane. These two assays were chosen based on our prior study reporting a correlation between dysferlin's ability to localize at the plasma membrane and its ability to repair the plasma membrane (Azakir et al., 2012).

This study identified additional dysferlin mutations that are inherently functional, as well as certain dysferlin missense mutations that remain biologically inactive, even when expressed at sufficient levels. The results of this study will help to identify dysferlin-deficient patients harbouring missense mutations that may be amenable to

Velcade treatment. The identification of intrinsically inactive dysferlin missense mutations could lead to a further understanding of dysferlin function, structure and protein-lipid interactions through the characterization of critical dysferlin residues.

5.4 Results

Recombinant Dysferlin Arg555Trp is biologically active

When treated with the proteasomal inhibitor, Velcade, patient-derived myoblasts harbouring the dysferlin missense mutation, Arg555Trp, showed increased levels of biologically active dysferlin protein (Azakir et al., 2012). However, patient-derived myoblasts harbouring different *DYSF* missense mutations are not readily available. An alternative would be to use recombinantly-generated missense mutated dysferlin plasmids.

Using the recombinant full-length dysferlin vector harbouring an N-terminal GFP tag and C-terminal His-myc tags, we used site-directed mutagenesis to generate a GFP-dysferlin R555W-His-myc plasmid (GFP-DysfR555W), and showed that its protein levels were increased when transiently-transfected COS cells were treated with the proteasomal inhibitor, Velcade (Figure 5.1A, B).

To determine whether recombinant GFP-DysfR555W can rescue the membrane-resealing deficit present in dysferlin-deficient muscle cells, the recombinant protein was transiently transfected into patient-derived dysferlin-deficient myoblasts (ULM1/01, harbouring two DYSF nonsense alleles), then treated or not with 25nM Velcade and assayed for laser-induced plasmalemmal resealing kinetics. The results showed that both untreated and treated cells were able to restore plasma membrane resealing function (Figure 5.1C).

These results suggest that, similar to patient-derived dysferlin Arg555Trp myoblasts, recombinantly-generated dysferlin Arg555Trp protein also retains biological activity.

Velcade administration was intended to increase the protein amount to sufficient levels in order to observe any biological activity of the recombinant protein. However, this purpose seems to be sufficiently achieved by protein overexpression alone via transient transfection. These results suggest that Velcade treatment is not needed to discern whether the recombinant missense mutated dysferlin is intrinsically biologically active.

Certain dysferlin missense mutations lack biological activity, despite Velcade treatment

To validate our screening approach, we screened for a dysferlin missense mutation that lacked plasmalemmal localization and resealing abilities, even when overexpressed or treated with Velcade.

Dysferlin Arg959Trp has a point mutation within dysferlin's DysF domain. When transfected COS cells were treated with Velcade, the levels of GFP-DysfArg959Trp were not significantly altered (Figure 5.2A,B), despite efficient Velcade activity (as demonstrated by increased protein ubiquitination). Immunofluorescent assaying for plasmalemmal insertion revealed that in the absence or presence of Velcade treatment, GFP-DysfArg959Trp did not localize to the plasma membrane (Figure 5.2C,D). Nor was GFP-DysfArg959Trp able to rescue the plasma membrane resealing deficit when transfected into dysferlin-deficient myoblasts (Figure 5.2E). These results demonstrate that the overexpression system used is not providing false-positive results to our screening approach of missense mutated constructs.

Screening of additional mutations identified two more biologically inactive dysferlin missense mutations. The missense mutation Pro1970Ser is located at the C-terminal edge of the C2G domain. Velcade treatment of transfected COS cells revealed a significant increase in protein levels (Figure 5.2A,B). Yet despite this increase, GFP-DysfPro1970Ser failed to localize to the plasma membrane (Figure 5.2C,D) or to rescue plasma membrane resealing kinetics when overexpressed in dysferlin-deficient myoblasts (Figure 5.2E).

The missense mutation Arg2042Cys lies adjacent to, and intracellular to, the transmembrane domain. Velcade treatment of transfected COS cells revealed no change

in protein levels (Figure 5.2A,B). Although this mutant was able to localize to the plasma membrane (Figure 5.2C,D), it was unable to rescue to resealing deficit in the dysferlin-deficient muscle cells (Figure 5.2E).

These three dysferlin missense mutations demonstrate that even when expressed at high levels (by transient expression and/or by proteasomal inhibitor treatment) some dysferlin missense mutations are inherently biological inactive. They serve as examples validating the screening approach used in this study.

Certain dysferlin missense mutations are biologically active

We next identified two biologically active dysferlin missense mutations: Val374Leu and Asp1837Asn. Proteasomal inhibition did not significantly alter their protein levels (Figure 5.3A,B). Yet, they still showed similar plasmalemmal localization potential as wildtype dysferlin (Figure 5.3C,D) and demonstrated similar plasma membrane resealing kinetics as wildtype dysferlin (Figure 5.3E).

5.5 Discussion

Dysferlinopathies are caused by mutations in the DYSF gene. Single nucleotide substitutions comprise 72% of pathogenic dysferlin mutations; approximately 40% of these are missense mutations (den Dunnen, 1998). And yet, the vast majority of missense mutations result in little to no dysferlin protein being produced (Therrien et al., 2006). It is theorized that these subtle protein-folding aberrations lead to rapid degradation of the dysferlin protein.

Previously, we presented a dysferlin missense mutation (Arg555Trp) that, upon rescue from proteasomal degradation, demonstrated biological activity (Azakir et al., 2012). Proteasomal inhibition restored missense-mutated dysferlin protein levels in the patient-derived myoblasts, and the salvaged protein rescued the membrane resealing deficit, restored plasmalemmal localization and reestablished myotube formation (Azakir et al., 2012). In this study, a recombinantly-generated GFP-dysferlin construct harbouring the same Arg555Trp mutation also exhibited biological activity, as it

restored membrane resealing kinetics in a dysferlin-deficient myoblast cell line when overexpressed in the dysferlin-deficient myoblast cell line.

Theorizing that other dysferlin missense mutations could demonstrate similar biological capacity if salvaged from degradation, we tested multiple dysferlin missense mutations for their ability to localize to, and repair, the plasma membrane when treated with the proteasomal inhibitor, Velcade.

Certain dysferlin missense mutations are intrinsically biologically active

Similarly to wildtype dysferlin and missense mutated Arg555Trp, the Val374Leu and Asp1837Asn missense mutants were able to restore membrane resealing kinetics and localize correctly at the plasma membrane when overexpressed in dysferlin-deficient ULM1/01 muscle cells. These results demonstrate the potential existence of numerous intrinsically active missense mutated dysferlin proteins being harboured by patients that may be salvageable by proteasomal inhibitor treatment, thus giving further support to proteasomal inhibition as a novel therapeutic option for certain dysferlinopathy patients.

Unexpectedly, these two constructs—as well as the GFP-DysfArg555Trp construct—did not require proteasomal inhibitor treatment to demonstrate these functions, as was required in the patient-derived Arg555Trp muscle cell line. This is likely due to the use of an overexpression system: the amount of exogenous protein produced by the transfected plasmids far exceeded the amount of endogenous protein salvaged by Velcade treatment in the patient-derived muscle cell line. This suggests that if the protein can escape the cell's quality control system, certain missense mutations can correctly perform their functions (plasmalemmal localization and membrane repair, at least), as they are intrinsically biologically active. Lostal et al (2010) proposed that 10% dysferlin levels at the sarcolemma is sufficient for normal membrane resealing (Lostal et al., 2010). This expression level is far surpassed by the transfection levels achieved in this study. Nevertheless, overexpression alone is insufficient to restore dysferlin function of a missense mutated protein, as demonstrated by the biological inactivity of GFP-DysfArg959Trp, GFP-DysfPro1970Ser and GFP-DysfArg2042Cys, which showed no

improvement in membrane resealing kinetics or in plasmalemmal localization, even when treated with Velcade. These examples validate the use of recombinant proteins are screening tools for dysferlin activity, and demonstrate that proteasomal inhibitor treatment would not benefit all dysferlin-deficient patients.

Certain dysferlin missense mutations lack intrinsic biological active

Three dysferlin missense mutations used in this study, Arg959Trp, Pro1970Ser and Arg2042Cys, did not restore dysferlin function in the ULM1/01 dysferlin-deficient myoblasts. The inactivity of these mutated dysferlin proteins suggest that certain regions of the dysferlin protein are critical for its function or stability.

The Arg959Trp mutation lies within the DysF domain of the dysferlin protein. Although the function of this domain is currently unknown, structural studies of the inner DysF domain in the myoferlin homolog suggests that it may be important for providing structural stability to the protein (Patel et al., 2008). The DysF domain contains multiple structural motifs consisting of stacks of arginines and aromatic residues (Patel et al., 2008). These motifs are believed to orient the arginine side chain without preventing it from forming hydrogen bonds elsewhere, and have been shown to provide structural stability for the growth factor receptor gp130 or for the thrombospondin repeat domain (Bravo et al., 1998; Tan et al., 2002). Substitution of the arginine 959 residue in dysferlin's DysF domain with a bulky tryptophan could result in domain destabilization.

This study demonstrates that the proof-of-concept Arg555Trp missense mutation is not an isolated case, and that multiple dysferlin missense mutations may be amenable to Velcade treatment. Characterization of dysferlin's missense mutations could identify further subgroups of dysferlinopathy patients who may be responsive to Velcade treatment, and may also open the field to further investigation into dysferlin's molecular biology, to provide broaden insights into dysferlin's structure, stability and lipid/protein interactions.

5.6 Experimental Procedures

Cell Culture and Transfection— The human primary myoblast culture, ULM1/01, was obtained from EuroBioBank, along with the required IRB approvals. Myoblast culture ULM1/01 harbours two null alleles: a C4819T (R1607X) substitution and a 5085delT (F1695LfsX48) deletion. Cells were immortalized and characterized as previously described (Azakir et al., 2012). Myoblast cultures were maintained in Dulbecco's modified Eagle's medium (DMEM; Sigma) containing 10% fetal bovine serum (FBS; Invitrogen) and 1% Penicillin-Streptamycin. Where indicated, cells were transfected at 70% confluency with pEGFP-C1 (Clontech), and a plasmid encoding GFP-dysferlin (a gift from Dr. K. Bushby) or a plasmid encoding a GFP-dysferlin missense mutation, using Lipofectamine 2000 (Invitrogen) in a 1:1.5 DNA:Lipofectamine 2000 ratio (for myoblasts) or 2mg/ml polyethylenimine (PEI, Sigma) in a 1:1 DNA:PEI ratio (for COS cells). Cells were cultured for 24 h before treatment with Velcade (Selleck Chemicals) at the indicated concentrations. Experiments were done at least in triplicate.

Plasmids and constructs

A plasmid encoding N'-terminally GFP-tagged and C'-terminally-c-myc-tagged dysferlin (WT) was a generous gift from Dr. K. Bushby, Newcastle. All dysferlin missense mutated constructs described in this study were derived from the original plasmid and contain an N-terminal GFP tag and C-terminal His-myc tags. Missense mutants were cloned from 50ng of the WT plasmid using the QuikChange Site-Directed Mutagenesis Kit (Agilent) as per the manufacturer's instructions. Briefly, the PCR conditions were: 95°C for 3min; 95°C for 15s, 65°C for 1min, 68°C for 12min (18 cycles); 68°C for 7min. The PCR product was digested with DpnI for 3 hours and transformed into DH5alpha or XL10-Gold bacterial cells. Plasmid DNA was isolated by mini-preps (Qiagen) and subsequently sequenced (for primer sequences see Table 5.1).

Protein Extraction and Western Blotting—Proteins were extracted in lysis buffer (10mM HEPES pH 7.4, 1% Triton X-100, protease inhibitor cocktail (Roche)) and sonicated 3x3seconds (burst power of 4) at 4°C with icing between bursts. Extracts were incubated for 20-30minutes at 4°C with rocking, then centrifuged at 13000rpm for 15minutes at 4°C. Protein concentrations of the supernatants were determined by BCA assay (Pierce). Proteins were separated on a SDS-polyacrylamide gel and transferred onto a polyvinylidene difluoride (PVDF) membrane. Membranes were blocked for

30min in buffer 1 (Tris-buffered saline containing 3% Top-Block, 0.05% sodium azide) and incubated overnight with the indicated antibody in buffer 2 (Tris-buffered saline containing 3% Top-Block, 0.05% sodium azide, 0.1% Tween 20). Mouse monoclonal antibody against dysferlin came from Vector Laboratories (REACTOLAB, clone Ham1/7B6), against ubiquitin from EnzoLifeSciences. Rabbit polyclonal antibodies against alpha-tubulin were purchased from Abcam. The membranes were washed with Tris-buffered saline containing 0.1% Tween 20 (TBST) and incubated for 45min-1hr with secondary antibodies Alexa Fluor680 goat anti-mouse IgG (Invitrogen) or IRDye 800 goat anti-rabbit IgG (Jackson Laboratories) in buffer 2 (1:10,000 dilution). Membranes were washed in TBST, rinsed in TBS and detected with Odyssey Infrared Imaging System (LI-COR). Western blotting experiments were repeated at least three times. Densitometric analysis was performed using ImageJ (National Institutes of Health). Statistical analysis was performed using Student's t-test.

Immunofluorescence assays—Transiently transfected ULM1/01 cells were washed twice in warm OptiMEM (Gibco), incubated for 15min with mouse monoclonal anti-c-myc antibody (Developmental Studies Hybridoma Bank), which recognizes the extracellular epitope tag of the dysferlin construct. Cells were washed with warm OptiMEM, fixed for 20 min with 4% paraformaldehyde and washed with PBS. Cells were blocked for 30 min with blocking buffer (1% normal goat serum, 2% of fish skin gelatin, and 0.15% Triton X-100 in PBS) and incubated with rabbit polyclonal anti-GFP antibody (Invitrogen) for 1h in blocking buffer, washed and incubated with DyLight 488-Conjugated AffiniPure goat anti-rabbit IgG (H+L) (Jackson Laboratories) and Cy3-Conjugated AffiniPure goat anti-mouse IgG (H+L) (Jackson Laboratories) for 45min, washed, stained with DAPI (1:10000) for five minutes and mounted on glass slides with Fluorsave reagent (Calbiochem). Images were captured on a LSM 710 inverted confocal microscope (Zeiss) and analyzed using Zen 2009 LE software (Zeiss) and ImageJ (NIH). All experiments were performed in triplicates.

Plasmalemmal Repair Assay—This assay was adapted for myoblasts from a protocol by Bansal et al (Bansal et al., 2003) initially designed for mouse myofibers. ULM1/01 myoblasts were cultured in a Lab-Tek chambered coverglass (two wells) coated with 0.03% gelatin. At 70% confluency, cells were transfected with GFP, GFP-dysferlin

wildtype or GFP-dysferlin missense mutated cDNA. After 5hours, media was changed and cells were treated with the indicated Velcade concentration overnight. For the injuries, media was switched to PBS pH 7.4 containing 10 mM HEPES pH 7.4 and 1.5mM $CaCl_2$. The fluorescent dye FM1-43 (2.5uM, Invitrogen) was added to the media. Myoblast plasma membranes were injured with a combination of three lasers (405 nm (30 mW), 458 nm (25 mW), 488 nm (25 mW)) for 4,000 cycles (lasting 80 s in total) on an LSM 710 inverted confocal microscope (Zeiss). Images were captured before injury (t = 0) and for 5 min after injury at 5-s intervals. The fluorescence intensity at the site of damage was measured using Zeiss 2010 software. At each time point, relative fluorescence values were determined by subtracting the background value and dividing the net fluorescence increase by the value of florescence at t = 0. Numbers of repeat plasmalemmal injuries are as follows: WT=24, GFP=16, R555W (0nM Velcade)=12, R555W (25nM Velcade)=16, V374L=20, R959W=21, D1837N=17, P1970S=18, R2042C=13.

5.7 Acknowledgements

We thank Muscle Tissue Culture Collection for providing the myoblast samples used in this study. The Muscle Tissue Culture Collection is part of the German network on muscular dystrophies (MD-NET, service structure S1, 01GM0601) funded by the German Ministry of Education and Research (BMBF, Bonn, Germany). The Muscle Tissue Culture Collection is a partner of EuroBioBank and TREAT-NMD. We thank Dr. E. Shoubridge and Timothy Johns for help with the E6E7 retroviral infection of the human myoblast cultures; Dr. K. Bushby, Newcastle, for the GFP-cDNA; Steven Salomon (Montreal, Canada) for construction of the recombinant dysferlin missense mutations; and Beat Erne (Basel, Switzerland) for technical assistance.

5.8 Figures and Figure Legends

Figure 5.1: Recombinant dysferlin Arg555Trp is biologically active

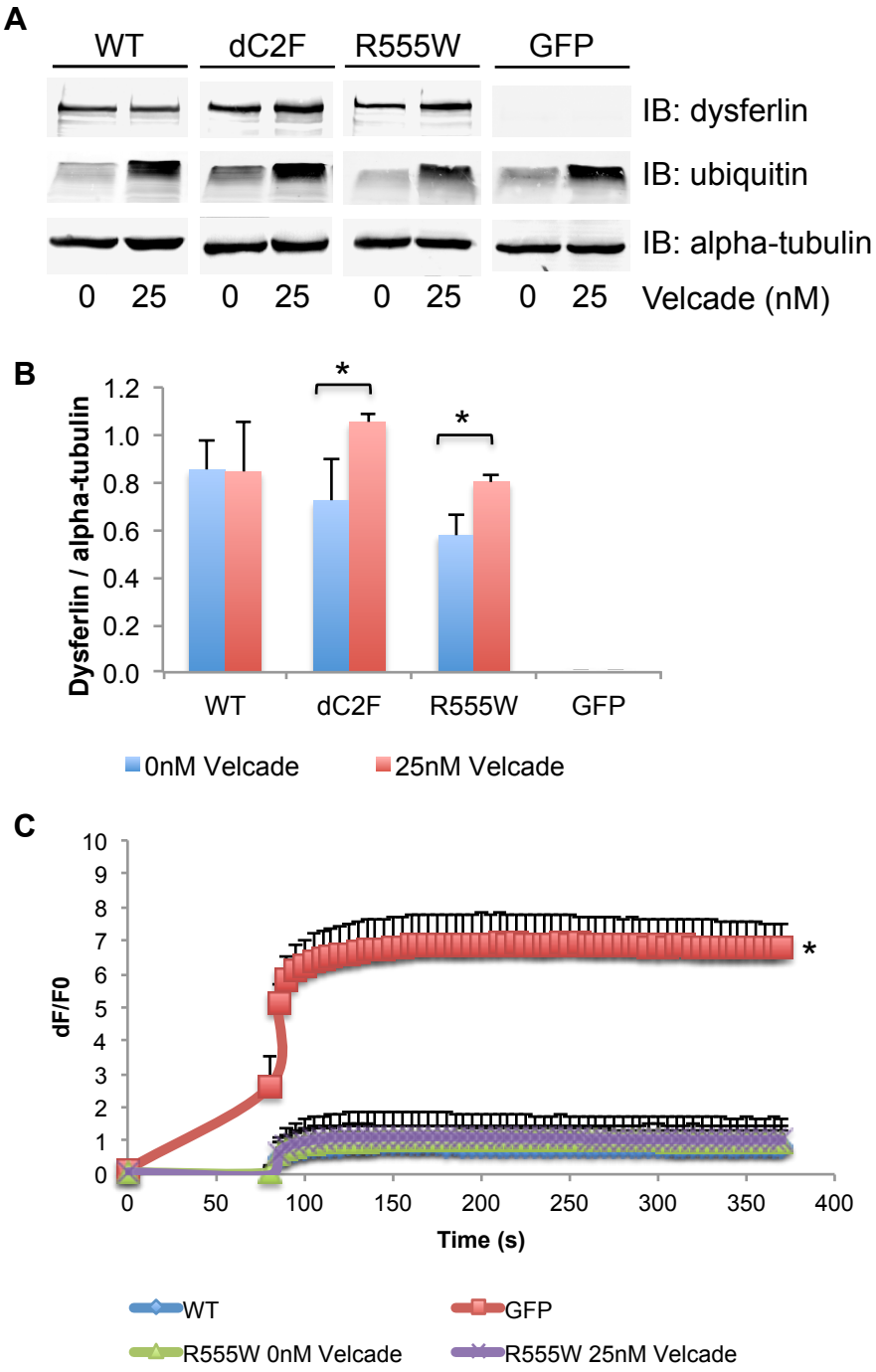

Figure 5.1: Recombinant dysferlin Arg555Trp (R555W) is biologically active.
(A) COS-7 cells were transfected with GFP, WT, dysferlinΔC2F or dysferlinR555W and treated with 0nM or 25nM Velcade. Western blots of protein extracts were stained with anti-dysferlin antibodies, and with anti-ubiquitin antibodies as positive control for Velcade treatment efficacy. Anti-alpha-tubulin antibodies were used as a loading control. (B) Quantification of dysferlin content over alpha-tubulin levels. * $p<0.05$. (C) Plasma membrane repair assay was performed on the dysferlin-deficient myoblast culture ULM1/01 transfected with GFP, WT or dysferlinR555W, treated with 0nM or 25nM Velcade. Relative fluorescence intensity ($\Delta F/F_0$) over time following laser-induced injury is represented as means + standard deviation. * $p<0.0005$, resealing kinetics are significantly different from WT resealing kinetics.

Figure 5.2: Certain dysferlin missense mutations lack biological activity

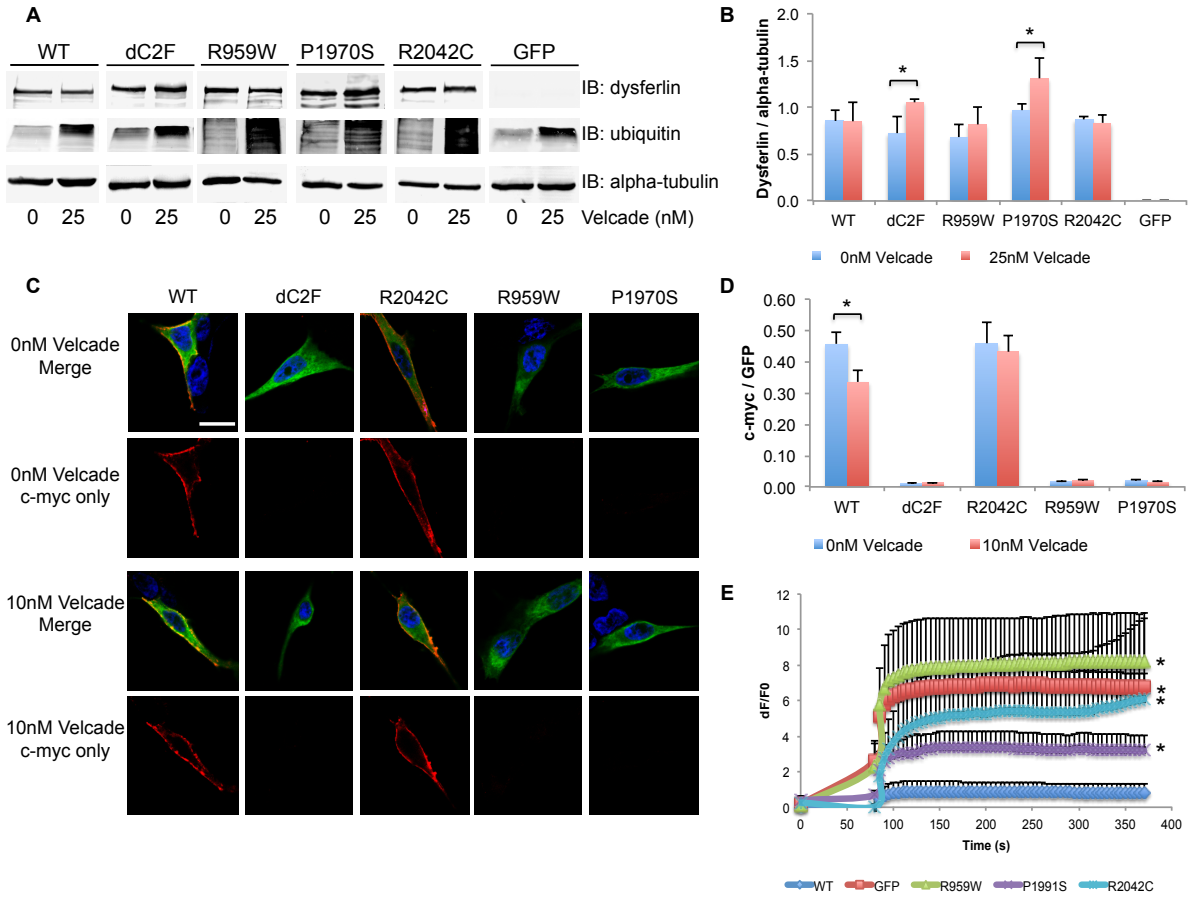

Figure 5.2: Certain dysferlin missense mutations lack biological activity.

(A) COS-7 cells were transfected with GFP, WT, dysferlinΔC2F, dysferlinR959W, dysferlinR2042C or dysferlinP1970S. Western blots of protein extracts were stained with anti-dysferlin antibodies, and with anti-ubiquitin antibodies as positive control for Velcade treatment efficacy. Anti-alpha-tubulin antibodies were used as a loading control. (B) Quantification of dysferlin content over alpha-tubulin levels. * $p<0.05$. (C) Immunostaining against the extracellular c-myc epitope on the dysferlin construct (red) in ULM1/01 myoblasts transfected with GFP, WT, dysferlinΔC2F, dysferlinR959W, dysferlinR2042C or dysferlinP1970S. Immunostaining against GFP (green) demonstrates cellular expression of each construct. Lower panel showing c-myc staining only is included to better visualize the plasma membrane staining. Scale bar = 10 μm. (D) Quantification of plasmalemmally-inserted dysferlin (c-myc) over dysferlin content (GFP). ** $p<0.005$. Error bars are reported as mean + SEM. (E) Plasma membrane repair assay was performed on the dysferlin-deficient myoblast culture ULM1/01 transfected with GFP, WT, dysferlinR959W, dysferlinR2042C or dysferlinP1970S. Relative fluorescence intensity ($\Delta F/F_0$) over time following laser-induced injury is represented as means + standard deviation. * $p<0.0005$, resealing kinetics are significantly different from WT resealing kinetics.

Figure 5.3: Certain dysferlin missense mutations are intrinsically biologically active

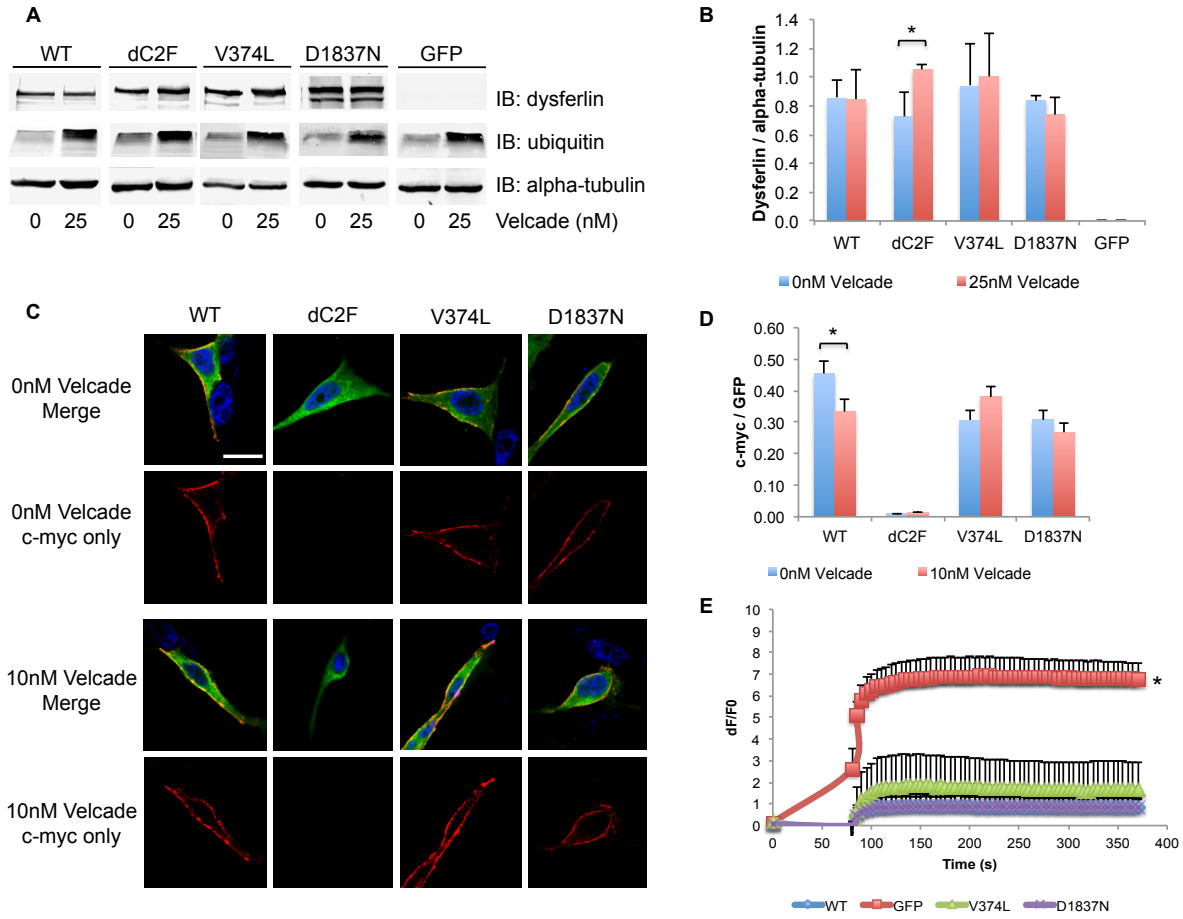

Figure 5.3: Certain dysferlin missense mutations are intrinsically biologically active. (A) COS-7 cells were transfected with GFP, WT, dysferlinΔC2F, dysferlinV374L or dysferlinD1837N. Western blots of protein extracts were stained with anti-dysferlin antibodies, and with anti-ubiquitin antibodies as positive control for Velcade treatment efficacy. Anti-alpha-tubulin antibodies were used as a loading control. (B) Quantification of dysferlin content over alpha-tubulin levels. * $p<0.05$. (C) Immunostaining against the extracellular c-myc epitope on the dysferlin construct (red) in ULM1/01 myoblasts transfected with GFP, WT, dysferlinΔC2F, dysferlinV374L or dysferlinD1837N. Immunostaining against GFP (green) demonstrates cellular expression of each construct. Lower panel showing c-myc staining only is included to better visualize the plasma membrane staining. Scale bar = 10 μm. (D) Quantification of plasmalemmally-inserted dysferlin (c-myc) over dysferlin content (GFP) * $p<0.05$. Error bars are reported as mean + SEM. (E) Plasma membrane repair assay was performed on the dysferlin-deficient myoblast culture ULM1/01 transfected with GFP, WT, dysferlinV374L or dysferlinD1837N. Relative fluorescence intensity ($\Delta F/F_0$) over time following laser-induced injury is represented as means + standard deviation. * $p<0.0005$, resealing kinetics are significantly different from WT resealing kinetics.

Table 5. 1: Primers used for missense mutated dysferlin constructs

Dysferlin missense mutation	Sequence of oligonucleotides (oligo)
R555W	Forward: 5'-GCT TAT CGT GGC TGG CTT CTG CTC TCC-3' Reverse: 5'-CAG GGA GAG CAG AAG CCA GCC ACG ATA AGC-3'
V374L	Forward: 5'- GCCCACAGGCCTAGCCCTGCGAGGAG -3' Reverse: 5'- CTCCTCGCAGGGCTAGGCCTGTGGGC -3'
R959W	Forward: 5'- GAG AAC CAG ACC TGG CTT CCC GGA GGC CAG -3' Reverse: 5'- CTG GCC TCC CGG AAG CCA GGT CTG GTT CTC -3'
P1970S	Forward: 5'- GAAGGGCTGGTGGTCCTGTGTAGCAGAAGAG -3' Reverse: 5'- CTCTTCTGCTACACAGGACCACCAGCCCTTC -3'
D1837N	Forward: 5'- GAGAAGATGAGCAACATTTATGTGAAAGGTTG -3' Reverse: 5'- CAACCTTTCACATAAATGTTGCTCATCTTCTC -3'
R2042C	Forward: 5'- ATC CTG TGG CGG TGT TTC CGG TGG GCC ATC -3' Reverse: 5'- GAT GGC CCA CCG GAA ACA CCG CCA CAG GAT -3'

CHAPTER 6

6 General Discussion

Dysferlinopathies are an incurable recessively inherited form of muscular dystrophy with a serious personal and socio-economic impact. Finding treatments or a cure for dysferlinopathies is imperative.

At the commencement of this thesis, the only clinical treatments for dysferlinopathies were symptomatic, primarily through anti-inflammatory medications, which often aggravated the disease rather than relieved the symptoms. Research into exon skipping for dysferlinopathies was in its infancy (Wein et al., 2010), adeno-associated viral therapies using full-length dysferlin were not very promising (Lostal et al., 2010), and a naturally occurring minidysferlin provided proof-of-principle potential for minidysferlin design (Krahn et al., 2010).

To understand how a gene leads to the disease, one must understand its biological mechanisms in order to gain insight as to how molecular alterations can lead to the pathology. Dysferlin's role in the membrane patch repair complex was acknowledged within five years of its discovery in 1998 (Bansal et al., 2003). However it was only in 2006 that dysferlin 's role was expanded to include myogenesis (de Luna et al., 2006). At the onset of this study, dysferlin was also implicated in calcium signaling (Covian-Nares et al., 2010), endothelial cell adhesion and angiogenesis (Sharma et al., 2010) and endothelial trafficking of membrane bound proteins (Leung et al., 2011).

This study investigated the molecular biology of dysferlin's C2 domains, plasmalemmal localization, membrane repair function, degradation pathway and involvement in myogenesis. Insights gleaned from these studies led to the rational design of minidysferlins suitable for AAV encapsidation, a novel pharmacological treatment option and further validation for exon skipping strategies for the treatment of dysferlinopathies.

6.1 Objectives and Summary of the Results

The following summarizes the results and conclusions made according to the objectives laid out in Chapter 1.

6.1.1 The dysferlin, alpha-tubulin, HDAC6 triad interaction provides insights into microtubule acetylation and myogenesis in muscle cells

Objective I - *To determine the significance of dysferlin's interaction with alpha-tubulin, as was previously described by our research group following a liquid-chromatography-mass spectrometry analysis of the dysferlin interactome.*

Shortly before the onset of this thesis study, our research group had used liquid-chromatography-tandem mass spectrometry to characterize the dysferlin interactome. A candidate dysferlin binding partner, alpha-tubulin, was shown to interact with dysferlin in its soluble (monomeric tubulin) and polymerized (microtubule) forms (Azakir et al., 2010). Microtubules are highly modified, for instance by acetylation, which led us to our study of HDAC6, the alpha-tubulin deacetylating enzyme, as a potential companion protein to this interaction. This study identified HDAC6 as a novel dysferlin interacting protein and showed the importance of dysferlin's C2 domains as protein binding modules for this triad interaction: binding HDAC6 via its C2D domain and binding alpha-tubulin via its C2A and C2B domains.

We showed that dysferlin expression increased the alpha-tubulin acetylation levels in muscle cells. Increased microtubule acetylation promotes microtubule stability, as demonstrated by increased resistance to Nocodazole-induced depolymerization and cold-induced depolymerization in the dysferlin-expressing muscle cells. Dysferlin expression also promoted faster microtubule recovery from depolymerization, resulting in more microtubules being repolymerized, stabilized and consequently post-translationally modified by acetylation. These results suggest that dysferlin may act as an inhibitor of HDAC6-mediated microtubule acetylation in muscle cells.

Given that differentiated muscle cells express higher levels of microtubule acetylation than undifferentiated myoblasts, we studied the effect of increased microtubule acetylation on muscle cell differentiation in dysferlin-expressing cells using the HDAC6 inhibitor Tubastatin. Results showed that when HDAC6 was inhibited early during differentiation, myotube formation was impaired. Conversely, HDAC6 inhibition in differentiated myotubes promoted myotube elongation. Given that dysferlin expression

is upregulated during myotube formation, these results suggest that temporal regulation of dysferlin may be important for proper myogenesis. Specifically, that later expression of dysferlin would promote myotube formation and elongation through increased microtubule acetylation, whereas early expression of dysferlin would promote premature microtubule hyperacetylation by way of inhibiting HDAC6, which would impair myotube formation.

The results would this study would recommend the use of promoters that are expressed at later stages of muscle differentiation, such as C5-12 (Spangenburg et al., 2004) and the human α-skeletal actin promoter (Evans et al., 2008), and would caution against the use of promoters expressed early in muscle development, such as CMV and CAG (Evans et al., 2008). This information could be useful in the future development of AAV-encapsidated dysferlin constructs.

6.1.2 Functional redundancy of dysferlin's C2 domains

Objective II – *To determine if there is functional redundancy between dysferlin's seven C2 domains in their ability to localize to and repair the muscle plasma membrane.*

Characterization of dysferlin's C2 domains currently consists of calcium dependent and independent phospholipid interactions, specifically with phosphatidylserine, phosphatidylinositol 4-phosphate or phosphatidylinositol 4,5-bisphosphate (Davis et al., 2002; Therrien et al., 2009). Protein interactions mediated by dysferlin's C2 domains included dysferlin C2A binding to MG53 dimers (Matsuda et al., 2012) and AHNAK (Huang et al., 2007); alpha-tubulin binding via dysferlin's C2A and C2B domains (Azakir et al., 2010); and HDAC6 binding to dysferlin's C2D domain, the latter being the newest addition as demonstrated in Chapter 2.

In Chapter 3, we investigated the functionality of dysferlin's C2 domains for plasmalemmal localization and resealing kinetics by individually deleting each C2 domain from a full-length dysferlin construct and transfecting the deleted constructs into dysferlin-deficient cells. This study revealed that dysferlin's C2A, C2F and C2G domains are essential for correct plasmalemmal localization and efficient resealing of

plasmalemmal injuries. However, deletion of dysferlin's C2B, C2C and C2E domains did not affect plasmalemmal localization and resealing kinetics, indicating that these domains are functionally redundant for at least these two of dysferlin's functions. Dysferlin's C2D domain, on the other hand, was not required for plasmalemmal localization, but its deletion affected the resealing kinetics; cells transfected with the GFP-DysfΔC2D construct did not reseal as efficiently as wildtype dysferlin. It is possible that the C2D domain is required to interact with a membrane repair protein, but this would not seem to be crucial given that mini-dysferlins lacking the C2D domain are still able to efficiently reseal the plasma membrane.

6.1.2.1 Rationale for the pursuit of exon skipping therapy for dysferlinopathies

Construction of midi-dysferlins having their C2 domains deleted, but without affecting the linker regions between them, demonstrated that multi-C2 domain deletions do not impair overall dysferlin function (for plasmalemmal localization and resealing). This suggests that dysferlin's C2 domains are independently folded domains, which agrees with the literature.

Furthermore, it suggests that removal of these entire domains would not be pathogenic, which would support the skipping of C2 domain-encoding exons. Our study of the functionality of a dysferlin construct lacking its 32nd exon, which was based on an observation of a mildly affected dysferlinopathic patient with a natural in frame skipping of the 32nd exon (Sinnreich et al., 2006), would further support this notion. As presented in Chapter 3, skipping of an exon encoding part of the C2D domain still allowed the truncated construct to localize to the plasma membrane although at lower efficiency than wildtype dysferlin. It did not impair the construct's ability to repair plasmalemmal disruptions with similar kinetics to wildtype dysferlin, which could correlate with the mild phenotype observed in the patient.

Additionally, the demonstration of functionality of the mini-dysferlins presented in Chapter 3 demonstrated that large deletions of entire coding sequences (for instance, from the C2B domain through to the C2F domain) can be tolerated by the protein.

This study supports the rationale for pursuing skipping of exon 32 as a potential therapeutic strategy for patients harbouring mutations in this particular exon. Coupled with the reports that several of dysferlin's exons (exons 19, 24, 30, 32, 34 and 49) are skippable using antisense oligonucelotides (AONS) (Aartsma-Rus et al., 2010; Santos et al., 2010; Wein et al., 2010), exon skipping for dysferlinopathies will likely become a more prominent topic in the coming years.

A consideration to bear in mind is that exon skipping would be an individually tailored therapeutic strategy, given that *DYSF* mutations are located throughout the gene and that patients often harbour two different pathological alleles (since dysferlinopathies are recessively inherited). Yet, because these diseases are recessively inherited, only one missense-mutated allele would theoretically need to be corrected for.

6.1.2.2 Rationale for the pursuit of AAV-mediated gene therapy for dysferlinopathies

Objective III – *To determine if a small mini-dysferlin can be generated that retains the functionality of full-length dysferlin, which would be small enough to encapsidate within an adeno-associated viral vector.*

The generation of a mini-dysferlin is required for effective AAV-mediated encapsidation. At the onset of this study, it was unclear whether a severely truncated dysferlin protein would still be functional. Within a year of commencing this thesis, Krahn et al demonstrated the *in vitro* muscle fiber resealing potential of a naturally occurring mini-dysferlin molecule, which encompassed the C2F, C2G and the transmembrane domain (Krahn et al., 2010).

Very recently, a study was published demonstrating that it was not full-length dysferlin being recruited to sites of membrane injury. In fact, it was a dysferlin fragment—consisting of the C2F, C2G and transmembrane domain—that was acting at the site of injury. Dr Cooper's group showed that upon injury, MG53 is recruited to and disperses around sites of injury (Lek et al., 2013). Full-length dysferlin is cleaved by calpain, releasing a 72 kDa C-terminal dysferlin fragment (dysferlin-C72), and vesicles adorned

with this minidysferlin accumulated at the site of injury (Lek et al., 2013). Upon dysferlin-C72's arrival, it and MG53 intercalated in a tight ring around the injury site and mediated membrane repair (Lek et al., 2013).

Dysferlin-C72 and the mini-dysferlin construct from Levy's group are quite similar, both having dysferlin's C2F-C2G-TM region. However, Levy's mini-dysferlin construct was unable to alleviate the muscular dystrophy phenotype of dysferlin-deficient mice *in vivo* (Lostal et al., 2012). Notably, this construct lacked the C2A domain, which the results of Chapter 3 showed to be required for plasma membrane localization and resealing, as well as for calcium dependent phospholipid binding and multiple protein interactions as demonstrated in previous studies by our laboratory and others (Davis et al., 2002; Huang et al., 2007; Therrien et al., 2009; Azakir et al., 2010; Matsuda et al., 2012). We reason that the mini-dysferlin molecules described in Chapter 3, which contain the C2A, C2F and/or C2G domains, may be better suited for AAV-mediated gene therapy.

One advantage AAV-mediated gene therapy has over exon skipping is that it does not require tailoring to each patient's mutation(s). However, studies are required to determine whether the mini-dysferlins described in Chapter 3 would be able to alleviate the dystrophic features. Lostal et al pointed out that *in vitro* resealing assays might not fully reflect the ability of a dysferlin construct to reverse or improve the *in vivo* dystrophic phenotype (Lostal et al., 2012). This emphasizes the fact that although loss of membrane repair capabilities in dysferlin-deficient muscle is an essential role of dysferlin, it may not be the only role or the only contributing factor to the development of dystrophic muscles. Studies on dysferlin-deficient human and mouse muscle/cultured muscle cells/monocytes point towards other influencing factors, such as the upregulation of the inflammasome and its activation (Rawat et al., 2010), which includes (among others) the upregulation of Thrombospondin-1 (De Luna et al., 2010) and pro-inflammatory NFκB signaling (Cohen et al., 2012), increased monocyte phagocytosis (Nagaraju et al., 2008), increased dendritic cell-T cell activation via the inadvertent release of co-stimulatory signals from the compensatory Rab27A/Slp2a endocytosic trafficking in muscle cells (Kesari et al., 2008) and increased expression of complement factors (Han et al., 2010).

A standard concern for gene therapy is possible immunogenicity from the gene delivery system. AAV ensures the lowest immunogenicity of the viral vectors; however, several human clinical trials with AAV revealed that the host's immune system generates antibodies against the AAV vector used (Manno et al., 2006; Mingozzi et al., 2007; Sterz et al., 2008), which precludes the effectiveness of any subsequent injections. Similar effects have been reported in canine Duchenne muscular dystrophy studies, but a short course of immunosuppression was sufficient to allow long-term expression of the recombinant protein (Wang et al., 2007; Wang et al., 2007). Studies are ongoing into modifying AAV serotypes to be less immunogenic or to contain the combined features of two different serotypes (Evans et al., 2008; Koo et al., 2011; Bowles et al., 2012). There are also concerns that the introduction of a dysferlin protein that is essentially novel to the dysferlinopathic system may result in an immune response against the 'foreign' protein.

6.1.3 Wildtype and missense mutated dysferlin are degraded in the proteasome

Objective IV – *To determine the degradation pathway(s) of wildtype dysferlin and missense-mutated dysferlin.*

At the onset of this thesis, dysferlin's degradation pathway was not fully characterized. One study determined that dysferlin is a short-lived protein, with a half-life of four to six hours (Evesson et al., 2010). The authors suggested that missense-mutated (Leu344Pro) dysferlin and dysferlinΔC2C were degraded by ER-associated degradation (ERAD) via the ubiquitin-proteasome system; however, the data presented in that paper was difficult to interpret. Another study proposed that wildtype dysferlin was primarily degraded by the ERAD ubiquitin-proteasome system, whereas a missense-mutated (Leu1341Pro) dysferlin was degraded by both the ubiquitin-proteasome system and the autophagy-lysosomal system (Fujita et al., 2007). However, this study was performed using an overexpression system, which likely caused non-physiological 'overflow' from the ERAD system into the lysosomal pathway.

In Chapter 4 of this thesis, we showed that both endogenous full-length dysferlin and endogenous missense-mutated Arg555Trp are degraded by the ubiquitin-proteasome system, and are not degraded by the lysosomal system to a detectable degree.

6.1.3.1 Therapeutic potential of proteasomal inhibitors for dysferlinopathies

The study presented in Chapter 4 offers proof-of-principle for the potential of proteasomal inhibition as a novel treatment strategy for dysferlinopathies.

Velcade (registered name for bortezomib) is a Federal Drug Administration (FDA)-approved drug currently in clinical use for the treatment of multiple myelomas and mantle cell lymphoma (Adams, 2004; Bross et al., 2004). In multiple myelomas, Velcade selectively induces apoptosis of cancer cells by preventing the degradation of proteins implicated in cell cycle control and surival, such as the NF-kB inhibitor, IkB (Obeng et al., 2006). NF-kB is a transcription factor that promotes cell survival and cell proliferation. Cancers prefer to degrade IkB, thus keeping NF-kB constitutively active. The proteasomal inhibitor, Velcade, stabilizes IkB, thus promoting cancer cell apoptosis.

Multiple myeloma cells are particularly sensitive to Velcade treatment. The antineoplastic doses used for multiple myeloma treatment were shown to be too low to affect normal cells (Hideshima et al., 2001). These doses correlate with the Velcade concentrations used to promote dysferlin rescue from proteasomal degradation used in Chapter 4. Velcade concentrations that allowed for rescued membrane repair and myoblast fusion (10 nM) were not toxic even when cells were treated for 5 days. It is therefore possible that concentrations of Velcade similar to those used for the treatment of patients with multiple myeloma would also influence the degradation of missense mutated dysferlin.

Proteasomal inhibition has also been proposed for other diseases caused by point mutations. In cystic fibrosis, the chloride channel protein bears the mutation ΔF508 (a single nucleotide deletion) (Ward et al., 1995), causing it to be retained in the endoplasmic reticulum and subsequently degraded. However, treatment with

proteasomal inhibition demonstrated that the mutated protein preserved its functionality when allowed to reach the plasma membrane (Pedemonte et al., 2005). A similar scenario is observed when missense mutated caveolin-3 is freed from its sequestration at the Golgi apparatus and permitted to reach the plasma membrane (Galbiati et al., 2000). These examples lend credence to the possibility of treating missense mutated dysferlin with proteasomal inhibitors.

However, the results of Chapter 5 suggest that not all patients would benefit from this treatment, as suggested by the Arg959Trp, Pro1970Ser and Arg2042Cys missense mutations. Patients would first have to be screened to ascertain if their mutation(s) would be benefitted by Velcade treatment, most likely by *in vitro* membrane resealing assays performed on cultured biopsy-derived myoblasts.

6.1.4 Certain dysferlin missense mutations are intrinsically biologically active

Objective V – *To determine whether missense-mutated dysferlin retains its biological activity, despite being flagged for degradation by the cell's quality control system.*

It is believed that dysferlin is very sensitive to single point mutations, given that they account for 71% of *DYSF* mutations and result in loss of, or severe reduction in, dysferlin protein levels. A study revealed that the missense mutation Leu344Pro showed increased protein internalization from the plasma membrane (~1.5 hours, compared to 3 hours for wildtype dysferlin) and increased protein lability when compared to wildtype dysferlin (Evesson et al., 2010). This suggests that missense-mutated dysferlin is rapidly degraded by the ubiquitin-proteasome system. However, it was uncertain whether missense mutated dysferlin was degraded because it was nonfunctional or because it was too quickly recognized by the cell's quality control system.

In Chapter 4, we presented a dysferlin missense mutation (Arg555Trp) that, upon salvage from proteasomal degradation, demonstrated biological activity; it rescued the membrane-resealing deficit, restored plasmalemmal localization and rescued the impairment in myotube formation. Study of additional dysferlin missense mutation-

harbouring constructs revealed that this is not a solitary case: dysferlin missense mutations Val374Leu and Asp1837Asn also demonstrated intrinsic functionality, as they were able to restore membrane resealing kinetics in dysferlin-deficient muscle cells. Furthermore, they demonstrated correct plasmalemmal localization when expressed in dysferlin-deficient muscle cells.

These constructs did not require proteasomal inhibitor treatment to demonstrate these functions, as was required in the patient-derived muscle cell line. This is likely due to the use of an overexpression system: the amount of exogenous protein produced by the transfected plasmids far exceeded the amount of endogenous protein salvaged by Velcade treatment in the patient-derived muscle cell line. This suggests that if the protein can escape the cell's quality control system, certain missense mutations can correctly perform their functions (plasmalemmal localization and membrane repair, at least), as they are intrinsically biologically active. This suggests that one needs to increase the dysferlin protein level to a sufficient threshold for it to have a measurable effect on functional outcome measures; Lostal et al propose that 10% dysferlin levels at the sarcolemma is sufficient for normal membrane resealing (Lostal et al., 2010). This expression level is far surpassed by the transfection levels achieved in this study.

6.1.5 Not all dysferlin missense mutations are intrinsically biologically active

Not all dysferlin missense mutations are intrinsically active, as demonstrated by the Arg959Trp, Pro1970Ser and Arg2042Cys missense mutated constructs. Even when overexpressed in dysferlin-deficient muscle cells, these mutations were unable to rescue membrane resealing kinetics, nor localize correctly at the plasma membrane (except for Arg2042Cys), regardless of Velcade treatment. These three mutated constructs validate the studies performed in Chapter 5, showing that increasing dysferlin levels is not sufficient to show protein activity of missense mutated dysferlin. These studies also demonstrate that proteasomal inhibitor treatment would not benefit all dysferlin-deficient patients, and suggest that personalized screening of each patient's mutation(s) would be needed to assess the applicability of proteasomal inhibition as a beneficial treatment option.

6.2 Outlook

The two functional mini-dysferlins presented in Chapter 3 are currently being examined in a gene therapy study using a mouse model of dysferlinopathy in our laboratory. This will assess whether these mini-dysferlins can ameliorate the muscular dystrophy phenotype present in these mice.

Swiss Medic has approved the proof-of-concept study presented in Chapter 4 for a clinical trial study to assess whether Velcade administration increases dysferlin protein levels in skeletal muscle of dysferlinopathy patients harbouring the Arg555Trp mutation. These trials represent the first dysferlin-directed therapeutic option available to patients with dysferlin deficiency. To decrease the side effects of proteasomal inhibition, our research group is pursuing the identification and inhibition of the E3 ubiquitin ligase(s) that targets dysferlin for proteasomal degradation. Our research group will continue to characterize the functionality of common dysferlin missense mutations, in order to increase the list of number of patients who may be helped by Velcade treatment. These characterization studies could also open the field to further investigation into dysferlin's molecular biology, to provide new insights into dysferlin's structure, stability and lipid/protein interactions.

References

Aartsma-Rus, A., Singh, K. H., Fokkema, I. F., Ginjaar, I. B., van Ommen, G. J., den Dunnen, J. T. and van der Maarel, S. M. (2010). Therapeutic exon skipping for dysferlinopathies? Eur J Hum Genet *18*(8): 889-894.

Achanzar, W. E. and Ward, S. (1997). A nematode gene required for sperm vesicle fusion. J Cell Sci *110 (Pt 9)*: 1073-1081.

Acsadi, G., Dickson, G., Love, D. R., Jani, A., Walsh, F. S., Gurusinghe, A., Wolff, J. A. and Davies, K. E. (1991). Human dystrophin expression in mdx mice after intramuscular injection of DNA constructs. Nature *352*(6338): 815-818.

Adams, J. (2004). The development of proteasome inhibitors as anticancer drugs. Cancer Cell *5*(5): 417-421.

Adams, J. and Kauffman, M. (2004). Development of the proteasome inhibitor Velcade (Bortezomib). Cancer Invest *22*(2): 304-311.

Akhmanova, A., Hoogenraad, C. C., Drabek, K., Stepanova, T., Dortland, B., Verkerk, T., Vermeulen, W., Burgering, B. M., De Zeeuw, C. I., Grosveld, F. and Galjart, N. (2001). Clasps are CLIP-115 and -170 associating proteins involved in the regional regulation of microtubule dynamics in motile fibroblasts. Cell *104*(6): 923-935.

Allocca, M., Doria, M., Petrillo, M., Colella, P., Garcia-Hoyos, M., Gibbs, D., Kim, S. R., Maguire, A., Rex, T. S., Di Vicino, U., Cutillo, L., Sparrow, J. R., Williams, D. S., Bennett, J. and Auricchio, A. (2008). Serotype-dependent packaging of large genes in adeno-associated viral vectors results in effective gene delivery in mice. J. Clin. Invest. *118*(5): 1955-1964.

Azakir, B. A., Di Fulvio, S., Kinter, J. and Sinnreich, M. (2012). Proteasomal inhibition restores biological function of mis-sense mutated dysferlin in patient-derived muscle cells. J Biol Chem *287*(13): 10344-10354.

Azakir, B. A., Di Fulvio, S., Salomon, S., Brockhoff, M., Therrien, C. and Sinnreich, M. (2012). Modular dispensability of dysferlin C2 domains reveals rational design for mini-dysferlin molecules. J Biol Chem *287*(33): 27629-27636.

Azakir, B. A., Di Fulvio, S., Therrien, C. and Sinnreich, M. (2010). Dysferlin interacts with tubulin and microtubules in mouse skeletal muscle. PLoS One *5*(4): e10122.

Bansal, D. and Campbell, K. P. (2004). Dysferlin and the plasma membrane repair in muscular dystrophy. Trends Cell Biol *14*(4): 206-213.

Bansal, D., Miyake, K., Vogel, S. S., Groh, S., Chen, C. C., Williamson, R., McNeil, P. L. and Campbell, K. P. (2003). Defective membrane repair in dysferlin-deficient muscular dystrophy. Nature *423*(6936): 168-172.

Bashir, R., Britton, S., Strachan, T., Keers, S., Vafiadaki, E., Lako, M., Richard, I., Marchand, S., Bourg, N., Argov, Z., Sadeh, M., Mahjneh, I., Marconi, G., Passos-Bueno, M. R., Moreira Ede, S., Zatz, M., Beckmann, J. S. and Bushby, K. (1998). A gene related to Caenorhabditis elegans spermatogenesis factor fer-1 is mutated in limb-girdle muscular dystrophy type 2B. Nat Genet *20*(1): 37-42.

Bazzaro, M., Lin, Z., Santillan, A., Lee, M. K., Wang, M. C., Chan, K. C., Bristow, R. E., Mazitschek, R., Bradner, J. and Roden, R. B. (2008). Ubiquitin proteasome system stress underlies synergistic killing of ovarian cancer cells by bortezomib and a novel HDAC6 inhibitor. Clin Cancer Res *14*(22): 7340-7347.

Belanto, J. J., Diaz-Perez, S. V., Magyar, C. E., Maxwell, M. M., Yilmaz, Y., Topp, K., Boso, G., Jamieson, C. H., Cacalano, N. A. and Jamieson, C. A. (2010). Dexamethasone induces dysferlin in myoblasts and enhances their myogenic differentiation. Neuromuscul Disord *20*(2): 111-121.

Benaud, C., Gentil, B. J., Assard, N., Court, M., Garin, J., Delphin, C. and Baudier, J. (2004). AHNAK interaction with the annexin 2/S100A10 complex regulates cell membrane cytoarchitecture. J Cell Biol *164*(1): 133-144.

Bernatchez, P. N., Acevedo, L., Fernandez-Hernando, C., Murata, T., Chalouni, C., Kim, J., Erdjument-Bromage, H., Shah, V., Gratton, J. P., McNally, E. M., Tempst, P. and Sessa, W. C. (2007). Myoferlin regulates vascular endothelial growth factor receptor-2 stability and function. J Biol Chem *282*(42): 30745-30753.

Bernatchez, P. N., Sharma, A., Kodaman, P. and Sessa, W. C. (2009). Myoferlin is critical for endocytosis in endothelial cells. Am J Physiol Cell Physiol *297*(3): C484-492.

Bertos, N. R., Gilquin, B., Chan, G. K., Yen, T. J., Khochbin, S. and Yang, X. J. (2004). Role of the tetradecapeptide repeat domain of human histone deacetylase 6 in cytoplasmic retention. J Biol Chem *279*(46): 48246-48254.

Beurg, M., Michalski, N., Safieddine, S., Bouleau, Y., Schneggenburger, R., Chapman, E. R., Petit, C. and Dulon, D. (2010). Control of exocytosis by synaptotagmins and otoferlin in auditory hair cells. J Neurosci *30*(40): 13281-13290.

Beurg, M., Safieddine, S., Roux, I., Bouleau, Y., Petit, C. and Dulon, D. (2008). Calcium- and otoferlin-dependent exocytosis by immature outer hair cells. J Neurosci *28*(8): 1798-1803.

Bittner, R. E., Anderson, L. V., Burkhardt, E., Bashir, R., Vafiadaki, E., Ivanova, S., Raffelsberger, T., Maerk, I., Hoger, H., Jung, M., Karbasiyan, M., Storch, M., Lassmann, H., Moss, J. A., Davison, K., Harrison, R., Bushby, K. M. and Reis, A. (1999). Dysferlin deletion in SJL mice (SJL-Dysf) defines a natural model for limb girdle muscular dystrophy 2B. Nat Genet *23*(2): 141-142.

Bonuccelli, G., Sotgia, F., Capozza, F., Gazzerro, E., Minetti, C. and Lisanti, M. P. (2007). Localized treatment with a novel FDA-approved proteasome inhibitor blocks the degradation of dystrophin and dystrophin-associated proteins in mdx mice. Cell Cycle *6*(10): 1242-1248.

Bowles, D. E., McPhee, S. W., Li, C., Gray, S. J., Samulski, J. J., Camp, A. S., Li, J., Wang, B., Monahan, P. E., Rabinowitz, J. E., Grieger, J. C., Govindasamy, L., Agbandje-McKenna, M., Xiao, X. and Samulski, R. J. (2012). Phase 1 gene therapy for Duchenne muscular dystrophy using a translational optimized AAV vector. Mol Ther *20*(2): 443-455.

Bravo, J., Staunton, D., Heath, J. K. and Jones, E. Y. (1998). Crystal structure of a cytokine-binding region of gp130. EMBO J *17*(6): 1665-1674.

Brose, N., Petrenko, A. G., Sudhof, T. C. and Jahn, R. (1992). Synaptotagmin: a calcium sensor on the synaptic vesicle surface. Science *256*(5059): 1021-1025.

Bross, P. F., Kane, R., Farrell, A. T., Abraham, S., Benson, K., Brower, M. E., Bradley, S., Gobburu, J. V., Goheer, A., Lee, S. L., Leighton, J., Liang, C. Y., Lostritto, R. T., McGuinn, W. D., Morse, D. E., Rahman, A., Rosario, L. A., Verbois, S. L., Williams, G., Wang, Y. C. and Pazdur, R. (2004). Approval summary for bortezomib for injection in the treatment of multiple myeloma. Clin Cancer Res *10*(12 Pt 1): 3954-3964.

Burghes, A. H., Logan, C., Hu, X., Belfall, B., Worton, R. G. and Ray, P. N. (1987). A cDNA clone from the Duchenne/Becker muscular dystrophy gene. Nature *328*(6129): 434-437.

Butler, K. V., Kalin, J., Brochier, C., Vistoli, G., Langley, B. and Kozikowski, A. P. (2010). Rational design and simple chemistry yield a superior, neuroprotective HDAC6 inhibitor, tubastatin A. J Am Chem Soc *132*(31): 10842-10846.

Cai, C., Weisleder, N., Ko, J. K., Komazaki, S., Sunada, Y., Nishi, M., Takeshima, H. and Ma, J. (2009). Membrane repair defects in muscular dystrophy are linked to altered interaction between MG53, caveolin-3, and dysferlin. J Biol Chem *284*(23): 15894-15902.

Cenacchi, G., Fanin, M., De Giorgi, L. B. and Angelini, C. (2005). Ultrastructural changes in dysferlinopathy support defective membrane repair mechanism. J Clin Pathol *58*(2): 190-195.

Chaudhuri, T. K. and Paul, S. (2006). Protein-misfolding diseases and chaperone-based therapeutic approaches. FEBS J *273*(7): 1331-1349.

Cirak, S., Arechavala-Gomeza, V., Guglieri, M., Feng, L., Torelli, S., Anthony, K., Abbs, S., Garralda, M. E., Bourke, J., Wells, D. J., Dickson, G., Wood, M. J., Wilton, S. D., Straub, V., Kole, R., Shrewsbury, S. B., Sewry, C., Morgan, J. E., Bushby, K. and Muntoni, F. (2011). Exon skipping and dystrophin restoration in patients with Duchenne muscular dystrophy after systemic phosphorodiamidate morpholino oligomer treatment: an open-label, phase 2, dose-escalation study. Lancet *378*(9791): 595-605.

Cohen, T. V., Cohen, J. E. and Partridge, T. A. (2012). Myogenesis in dysferlin-deficient myoblasts is inhibited by an intrinsic inflammatory response. Neuromuscul Disord *22*(7): 648-658.

Coura Rdos, S. and Nardi, N. B. (2007). The state of the art of adeno-associated virus-based vectors in gene therapy. Virol J *4*: 99.

Covian-Nares, J. F., Koushik, S. V., Puhl, H. L., 3rd and Vogel, S. S. (2010). Membrane wounding triggers ATP release and dysferlin-mediated intercellular calcium signaling. J Cell Sci *123*(Pt 11): 1884-1893.

Davis, D. B., Delmonte, A. J., Ly, C. T. and McNally, E. M. (2000). Myoferlin, a candidate gene and potential modifier of muscular dystrophy. Hum Mol Genet *9*(2): 217-226.

Davis, D. B., Doherty, K. R., Delmonte, A. J. and McNally, E. M. (2002). Calcium-sensitive phospholipid binding properties of normal and mutant ferlin C2 domains. J Biol Chem *277*(25): 22883-22888.

Davletov, B. A. and Sudhof, T. C. (1993). A single C2 domain from synaptotagmin I is sufficient for high affinity Ca2+/phospholipid binding. J Biol Chem *268*(35): 26386-26390.

De Luna, N., Freixas, A., Gallano, P., Caselles, L., Rojas-Garcia, R., Paradas, C., Nogales, G., Dominguez-Perles, R., Gonzalez-Quereda, L., Vilchez, J. J., Marquez, C., Bautista, J., Guerrero, A., Salazar, J. A., Pou, A., Illa, I. and Gallardo, E. (2007). Dysferlin expression in monocytes: a source of mRNA for mutation analysis. Neuromuscul Disord *17*(1): 69-76.

De Luna, N., Gallardo, E. and Illa, I. (2004). In vivo and in vitro dysferlin expression in human muscle satellite cells. J Neuropathol Exp Neurol *63*(10): 1104-1113.

De Luna, N., Gallardo, E., Sonnet, C., Chazaud, B., Dominguez-Perles, R., Suarez-Calvet, X., Gherardi, R. K. and Illa, I. (2010). Role of thrombospondin 1 in macrophage inflammation in dysferlin myopathy. J Neuropathol Exp Neurol *69*(6): 643-653.

de Luna, N., Gallardo, E., Soriano, M., Dominguez-Perles, R., de la Torre, C., Rojas-Garcia, R., Garcia-Verdugo, J. M. and Illa, I. (2006). Absence of dysferlin alters myogenin expression and delays human muscle differentiation "in vitro". J Biol Chem *281*(25): 17092-17098.

de Morree, A., Hensbergen, P. J., van Haagen, H. H., Dragan, I., Deelder, A. M., t Hoen, P. A., Frants, R. R. and van der Maarel, S. M. (2010). Proteomic analysis of the dysferlin protein complex unveils its importance for sarcolemmal maintenance and integrity. PLoS One *5*(11): e13854.

Demonbreun, A. R., Fahrenbach, J. P., Deveaux, K., Earley, J. U., Pytel, P. and McNally, E. M. (2011). Impaired muscle growth and response to insulin-like growth factor 1 in dysferlin-mediated muscular dystrophy. Hum Mol Genet *20*(4): 779-789.

den Dunnen, J. (1998, March 29, 2013). Leiden Muscular Database Pages. Dysferlin (DYSF) DYSF130329. from http://www.dmd.nl/dysf_home.html.

Di Fulvio, S., Azakir, B. A., Therrien, C. and Sinnreich, M. (2011). Dysferlin interacts with histone deacetylase 6 and increases alpha-tubulin acetylation. PLoS One *6*(12): e28563.

Diaz-Manera, J., Touvier, T., Dellavalle, A., Tonlorenzi, R., Tedesco, F. S., Messina, G., Meregalli, M., Navarro, C., Perani, L., Bonfanti, C., Illa, I., Torrente, Y. and Cossu, G. (2010). Partial dysferlin reconstitution by adult murine mesoangioblasts is sufficient for full functional recovery in a murine model of dysferlinopathy. Cell Death Dis *1*: e61.

Doherty, K. R., Cave, A., Davis, D. B., Delmonte, A. J., Posey, A., Earley, J. U., Hadhazy, M. and McNally, E. M. (2005). Normal myoblast fusion requires myoferlin. Development *132*(24): 5565-5575.

Doherty, K. R., Demonbreun, A. R., Wallace, G. Q., Cave, A., Posey, A. D., Heretis, K., Pytel, P. and McNally, E. M. (2008). The endocytic recycling protein EHD2 interacts with myoferlin to regulate myoblast fusion. J Biol Chem *283*(29): 20252-20260.

England, S. B., Nicholson, L. V., Johnson, M. A., Forrest, S. M., Love, D. R., Zubrzycka-Gaarn, E. E., Bulman, D. E., Harris, J. B. and Davies, K. E. (1990). Very mild muscular dystrophy associated with the deletion of 46% of dystrophin. Nature *343*(6254): 180-182.

Evans, V., Foster, H., Graham, I. R., Foster, K., Athanasopoulos, T., Simons, J. P., Dickson, G. and Owen, J. S. (2008). Human apolipoprotein E expression from mouse skeletal muscle by electrotransfer of nonviral DNA (plasmid) and pseudotyped recombinant adeno-associated virus (AAV2/7). Hum Gene Ther *19*(6): 569-578.

Evesson, F. J., Peat, R. A., Lek, A., Brilot, F., Lo, H. P., Dale, R. C., Parton, R. G., North, K. N. and Cooper, S. T. (2010). Reduced plasma membrane expression of dysferlin mutants is attributed to accelerated endocytosis via a syntaxin-4-associated pathway. J Biol Chem *285*(37): 28529-28539.

Fujita, E., Kouroku, Y., Isoai, A., Kumagai, H., Misutani, A., Matsuda, C., Hayashi, Y. K. and Momoi, T. (2007). Two endoplasmic reticulum-associated degradation (ERAD) systems for the novel variant of the mutant dysferlin: ubiquitin/proteasome ERAD(I) and autophagy/lysosome ERAD(II). Hum Mol Genet *16*(6): 618-629.

Galbiati, F., Volonte, D., Minetti, C., Bregman, D. B. and Lisanti, M. P. (2000). Limb-girdle muscular dystrophy (LGMD-1C) mutants of caveolin-3 undergo ubiquitination and proteasomal degradation. Treatment with proteasomal inhibitors blocks the dominant negative effect of LGMD-1C mutanta and rescues wild-type caveolin-3. J Biol Chem *275*(48): 37702-37711.

Gard, D. L. and Lazarides, E. (1980). The synthesis and distribution of desmin and vimentin during myogenesis in vitro. Cell *19*(1): 263-275.

Gazzerro, E., Assereto, S., Bonetto, A., Sotgia, F., Scarfi, S., Pistorio, A., Bonuccelli, G., Cilli, M., Bruno, C., Zara, F., Lisanti, M. P. and Minetti, C. (2010). Therapeutic potential of proteasome inhibition in Duchenne and Becker muscular dystrophies. Am J Pathol *176*(4): 1863-1877.

Geeraert, C., Ratier, A., Pfisterer, S. G., Perdiz, D., Cantaloube, I., Rouault, A., Pattingre, S., Proikas-Cezanne, T., Codogno, P. and Pous, C. (2010). Starvation-induced hyperacetylation of tubulin is required for the stimulation of autophagy by nutrient deprivation. J Biol Chem *285*(31): 24184-24194.

Gregorevic, P., Allen, J. M., Minami, E., Blankinship, M. J., Haraguchi, M., Meuse, L., Finn, E., Adams, M. E., Froehner, S. C., Murry, C. E. and Chamberlain, J. S. (2006). rAAV6-microdystrophin preserves muscle function and extends lifespan in severely dystrophic mice. Nat Med *12*(7): 787-789.

Grieger, J. C. and Samulski, R. J. (2005). Packaging capacity of adeno-associated virus serotypes: impact of larger genomes on infectivity and postentry steps. J. Virol. *79*(15): 9933-9944.

Grozdanovic, Z., Gosztonyi, G. and Gossrau, R. (1996). Nitric oxide synthase I (NOS-I) is deficient in the sarcolemma of striated muscle fibers in patients with Duchenne muscular dystrophy, suggesting an association with dystrophin. Acta Histochem *98*(1): 61-69.

Guerin, C. M. and Kramer, S. G. (2009). RacGAP50C directs perinuclear gamma-tubulin localization to organize the uniform microtubule array required for Drosophila myotube extension. Development *136*(9): 1411-1421.

Gumerson, J. D. and Michele, D. E. (2011). The dystrophin-glycoprotein complex in the prevention of muscle damage. J Biomed Biotechnol *2011*: 210797.

Gundersen, G. G., Khawaja, S. and Bulinski, J. C. (1989). Generation of a stable, posttranslationally modified microtubule array is an early event in myogenic differentiation. J Cell Biol *109*(5): 2275-2288.

Haggarty, S. J., Koeller, K. M., Wong, J. C., Grozinger, C. M. and Schreiber, S. L. (2003). Domain-selective small-molecule inhibitor of histone deacetylase 6 (HDAC6)-mediated tubulin deacetylation. Proc Natl Acad Sci U S A *100*(8): 4389-4394.

Han, R. and Campbell, K. P. (2007). Dysferlin and muscle membrane repair. Curr Opin Cell Biol *19*(4): 409-416.

Han, R., Frett, E. M., Levy, J. R., Rader, E. P., Lueck, J. D., Bansal, D., Moore, S. A., Ng, R., Beltran-Valero de Bernabe, D., Faulkner, J. A. and Campbell, K. P. (2010). Genetic ablation of complement C3 attenuates muscle pathology in dysferlin-deficient mice. J Clin Invest *120*(12): 4366-4374.

Han, W. Q., Xia, M., Xu, M., Boini, K. M., Ritter, J. K., Li, N. J. and Li, P. L. (2012). Lysosome fusion to the cell membrane is mediated by the dysferlin C2A domain in coronary arterial endothelial cells. J. Cell. Sci. *125*(Pt 5): 1225-1234.

Hara, Y., Balci-Hayta, B., Yoshida-Moriguchi, T., Kanagawa, M., Beltran-Valero de Bernabe, D., Gundesli, H., Willer, T., Satz, J. S., Crawford, R. W., Burden, S. J., Kunz, S., Oldstone, M. B., Accardi, A., Talim, B., Muntoni, F., Topaloglu, H., Dincer, P. and Campbell, K. P. (2011). A dystroglycan mutation associated with limb-girdle muscular dystrophy. N Engl J Med *364*(10): 939-946.

Herrick, D. Z., Sterbling, S., Rasch, K. A., Hinderliter, A. and Cafiso, D. S. (2006). Position of synaptotagmin I at the membrane interface: cooperative interactions of tandem C2 domains. Biochemistry *45*(32): 9668-9674.

Hideshima, T., Richardson, P., Chauhan, D., Palombella, V. J., Elliott, P. J., Adams, J. and Anderson, K. C. (2001). The proteasome inhibitor PS-341 inhibits growth, induces apoptosis, and overcomes drug resistance in human multiple myeloma cells. Cancer Res *61*(7): 3071-3076.

Ho, M., Post, C. M., Donahue, L. R., Lidov, H. G., Bronson, R. T., Goolsby, H., Watkins, S. C., Cox, G. A. and Brown, R. H., Jr. (2004). Disruption of muscle membrane and phenotype divergence in two novel mouse models of dysferlin deficiency. Hum Mol Genet *13*(18): 1999-2010.

Hoffman, E. P., Rao, D. and Pachman, L. M. (2002). Clarifying the boundaries between the inflammatory and dystrophic myopathies: insights from molecular diagnostics and microarrays. Rheum Dis Clin North Am *28*(4): 743-757.

Hohaus, A., Person, V., Behlke, J., Schaper, J., Morano, I. and Haase, H. (2002). The carboxyl-terminal region of ahnak provides a link between cardiac L-type Ca2+ channels and the actin-based cytoskeleton. FASEB J *16*(10): 1205-1216.

Holt, K. H. and Campbell, K. P. (1998). Assembly of the sarcoglycan complex. Insights for muscular dystrophy. J Biol Chem *273*(52): 34667-34670.

Huang, Y., de Morree, A., van Remoortere, A., Bushby, K., Frants, R. R., den Dunnen, J. T. and van der Maarel, S. M. (2008). Calpain 3 is a modulator of the dysferlin protein complex in skeletal muscle. Hum Mol Genet *17*(12): 1855-1866.

Huang, Y., Laval, S. H., van Remoortere, A., Baudier, J., Benaud, C., Anderson, L. V., Straub, V., Deelder, A., Frants, R. R., den Dunnen, J. T., Bushby, K. and van der Maarel, S. M. (2007). AHNAK, a novel component of the dysferlin protein complex, redistributes to the cytoplasm with dysferlin during skeletal muscle regeneration. FASEB J *21*(3): 732-742.

Hubbert, C., Guardiola, A., Shao, R., Kawaguchi, Y., Ito, A., Nixon, A., Yoshida, M., Wang, X. F. and Yao, T. P. (2002). HDAC6 is a microtubule-associated deacetylase. Nature *417*(6887): 455-458.

Illa, I., Serrano-Munuera, C., Gallardo, E., Lasa, A., Rojas-Garcia, R., Palmer, J., Gallano, P., Baiget, M., Matsuda, C. and Brown, R. H. (2001). Distal anterior compartment myopathy: a dysferlin mutation causing a new muscular dystrophy phenotype. Ann Neurol *49*(1): 130-134.

Johnson, C. P. and Chapman, E. R. (2010). Otoferlin is a calcium sensor that directly regulates SNARE-mediated membrane fusion. J Cell Biol *191*(1): 187-197.

Kaverina, I., Krylyshkina, O. and Small, J. V. (1999). Microtubule targeting of substrate contacts promotes their relaxation and dissociation. J Cell Biol *146*(5): 1033-1044.

Kesari, A., Fukuda, M., Knoblach, S., Bashir, R., Nader, G. A., Rao, D., Nagaraju, K. and Hoffman, E. P. (2008). Dysferlin deficiency shows compensatory induction of Rab27A/Slp2a that may contribute to inflammatory onset. Am J Pathol *173*(5): 1476-1487.

Kinali, M., Arechavala-Gomeza, V., Feng, L., Cirak, S., Hunt, D., Adkin, C., Guglieri, M., Ashton, E., Abbs, S., Nihoyannopoulos, P., Garralda, M. E., Rutherford, M., McCulley, C., Popplewell, L., Graham, I. R., Dickson, G., Wood, M. J., Wells, D. J., Wilton, S. D., Kole, R., Straub, V., Bushby, K., Sewry, C., Morgan, J. E. and Muntoni, F. (2009). Local restoration of dystrophin expression with the morpholino oligomer AVI-4658 in Duchenne

muscular dystrophy: a single-blind, placebo-controlled, dose-escalation, proof-of-concept study. Lancet Neurol *8*(10): 918-928.

Klinge, L., Harris, J., Sewry, C., Charlton, R., Anderson, L., Laval, S., Chiu, Y. H., Hornsey, M., Straub, V., Barresi, R., Lochmuller, H. and Bushby, K. (2010). Dysferlin associates with the developing T-tubule system in rodent and human skeletal muscle. Muscle Nerve *41*(2): 166-173.

Klinge, L., Laval, S., Keers, S., Haldane, F., Straub, V., Barresi, R. and Bushby, K. (2007). From T-tubule to sarcolemma: damage-induced dysferlin translocation in early myogenesis. Faseb J *21*(8): 1768-1776.

Kobayashi, Y. M., Rader, E. P., Crawford, R. W., Iyengar, N. K., Thedens, D. R., Faulkner, J. A., Parikh, S. V., Weiss, R. M., Chamberlain, J. S., Moore, S. A. and Campbell, K. P. (2008). Sarcolemma-localized nNOS is required to maintain activity after mild exercise. Nature *456*(7221): 511-515.

Koo, T., Malerba, A., Athanasopoulos, T., Trollet, C., Boldrin, L., Ferry, A., Popplewell, L., Foster, H., Foster, K. and Dickson, G. (2011). Delivery of AAV2/9-microdystrophin genes incorporating helix 1 of the coiled-coil motif in the C-terminal domain of dystrophin improves muscle pathology and restores the level of alpha1-syntrophin and alpha-dystrobrevin in skeletal muscles of mdx mice. Hum Gene Ther *22*(11): 1379-1388.

Koo, T., Okada, T., Athanasopoulos, T., Foster, H., Takeda, S. and Dickson, G. (2011). Long-term functional adeno-associated virus-microdystrophin expression in the dystrophic CXMDj dog. J Gene Med *13*(9): 497-506.

Kovacs, J. J., Murphy, P. J., Gaillard, S., Zhao, X., Wu, J. T., Nicchitta, C. V., Yoshida, M., Toft, D. O., Pratt, W. B. and Yao, T. P. (2005). HDAC6 regulates Hsp90 acetylation and chaperone-dependent activation of glucocorticoid receptor. Mol Cell *18*(5): 601-607.

Krahn, M., Beroud, C., Labelle, V., Nguyen, K., Bernard, R., Bassez, G., Figarella-Branger, D., Fernandez, C., Bouvenot, J., Richard, I., Ollagnon-Roman, E., Bevilacqua, J. A., Salvo, E., Attarian, S., Chapon, F., Pellissier, J. F., Pouget, J., Hammouda el, H., Laforet, P., Urtizberea, J. A., Eymard, B., Leturcq, F. and Levy, N. (2009). Analysis of the DYSF mutational spectrum in a large cohort of patients. Hum Mutat *30*(2): E345-375.

Krahn, M., Wein, N., Bartoli, M., Lostal, W., Courrier, S., Bourg-Alibert, N., Nguyen, K., Vial, C., Streichenberger, N., Labelle, V., DePetris, D., Pecheux, C., Leturcq, F., Cau, P., Richard, I. and Levy, N. (2010). A naturally occurring human minidysferlin protein repairs sarcolemmal lesions in a mouse model of dysferlinopathy. Sci Transl Med *2*(50): 50ra69.

Krajacic, P., Hermanowski, J., Lozynska, O., Khurana, T. S. and Lamitina, T. (2009). C. elegans dysferlin homolog fer-1 is expressed in muscle, and fer-1 mutations initiate altered gene expression of muscle enriched genes. Physiol Genomics *40*(1): 8-14.

Krylyshkina, O., Kaverina, I., Kranewitter, W., Steffen, W., Alonso, M. C., Cross, R. A. and Small, J. V. (2002). Modulation of substrate adhesion dynamics via microtubule targeting requires kinesin-1. J Cell Biol *156*(2): 349-359.

Kunkel, L. M., Hejtmancik, J. F., Caskey, C. T., Speer, A., Monaco, A. P., Middlesworth, W., Colletti, C. A., Bertelson, C., Muller, U., Bresnan, M., Shapiro, F., Tantravahi, U., Speer, J., Latt, S. A., Bartlett, R., Pericak-Vance, M. A., Roses, A. D., Thompson, M. W., Ray, P. N., Worton, R. G., Fischbeck, K. H., Gallano, P., Coulon, M., Duros, C., Boue, J., Junien, C., Chelly, J., Hamard, G., Jeanpierre, M., Lambert, M., Kaplan, J. C., Emery, A., Dorkins, H., McGlade, S., Davies, K. E., Boehm, C., Arveiler, B., Lemaire, C., Morgan, G. J., Denton, M. J., Amos, J., Bobrow, M., Benham, F., Boswinkel, E., Cole, C., Dubowitz, V., Hart, K., Hodgson, S., Johnson, L., Walker, A., Roncuzzi, L., Ferlini, A., Nobile, C., Romeo, G., Wilcox, D. E., Affara, N. A., Ferguson-Smith, M. A., Lindolf, M., Kaariainen, H., de la Chapelle, A., Ionasescu, V., Searby, C., Ionasescu, R., Bakker, E., van Ommen, G. J., Pearson, P. L., Greenberg, C. R., Hamerton, J. L., Wrogemann, K., Doherty, R. A., Polakowska, R., Hyser, C., Quirk, S., Thomas, N., Harper, J. F., Darras, B. T. and Francke, U. (1986). Analysis of deletions in DNA from patients with Becker and Duchenne muscular dystrophy. Nature *322*(6074): 73-77.

Ledig, S., Ropke, A. and Wieacker, P. (2010). Copy number variants in premature ovarian failure and ovarian dysgenesis. Sex Dev *4*(4-5): 225-232.

Lek, A., Evesson, F. J., Lemckert, F. A., Redpath, G. M., Lueders, A. K., Turnbull, L., Whitchurch, C. B., North, K. N. and Cooper, S. T. (2013). Calpains, Cleaved Mini-DysferlinC72, and L-Type Channels Underpin Calcium-Dependent Muscle Membrane Repair. J Neurosci *33*(12): 5085-5094.

Lek, A., Lek, M., North, K. N. and Cooper, S. T. (2010). Phylogenetic analysis of ferlin genes reveals ancient eukaryotic origins. BMC Evol Biol *10*: 231.

Lennon, N. J., Kho, A., Bacskai, B. J., Perlmutter, S. L., Hyman, B. T. and Brown, R. H., Jr. (2003). Dysferlin interacts with annexins A1 and A2 and mediates sarcolemmal wound-healing. J Biol Chem *278*(50): 50466-50473.

Leung, C., Shaheen, F., Bernatchez, P. and Hackett, T. L. (2012). Expression of myoferlin in human airway epithelium and its role in cell adhesion and zonula occludens-1 expression. PLoS One *7*(7): e40478.

Leung, C., Utokaparch, S., Sharma, A., Yu, C., Abraham, T., Borchers, C. and Bernatchez, P. (2011). Proteomic identification of dysferlin-interacting protein complexes in human vascular endothelium. Biochem Biophys Res Commun *415*(2): 263-269.

Leung, C., Yu, C., Lin, M. I., Tognon, C. and Bernatchez, P. (2013). Expression of Myoferlin in Human and Murine Carcinoma Tumors: Role in Membrane Repair, Cell Proliferation, and Tumorigenesis. Am J Pathol.

Liewluck, T., Pongpakdee, S., Witoonpanich, R., Sangruchi, T., Pho-Iam, T., Limwongse, C., Thongnoppakhun, W., Boonyapisit, K., Sopassathit, V., Phudhichareonrat, S., Suthiponpaisan, U., Raksadawan, N., Goto, K., Hayashi, Y. K. and Nishino, I. (2009). Novel DYSF mutations in Thai patients with distal myopathy. Clin Neurol Neurosurg *111*(7): 613-618.

Liu, J., Aoki, M., Illa, I., Wu, C., Fardeau, M., Angelini, C., Serrano, C., Urtizberea, J. A., Hentati, F., Hamida, M. B., Bohlega, S., Culper, E. J., Amato, A. A., Bossie, K., Oeltjen, J.,

Bejaoui, K., McKenna-Yasek, D., Hosler, B. A., Schurr, E., Arahata, K., de Jong, P. J. and Brown, R. H., Jr. (1998). Dysferlin, a novel skeletal muscle gene, is mutated in Miyoshi myopathy and limb girdle muscular dystrophy. Nat Genet *20*(1): 31-36.

Lochmuller, H., Johns, T. and Shoubridge, E. A. (1999). Expression of the E6 and E7 genes of human papillomavirus (HPV16) extends the life span of human myoblasts. Exp Cell Res *248*(1): 186-193.

Lompre, A. M., Hadri, L., Merlet, E., Keuylian, Z., Mougenot, N., Karakikes, I., Chen, J., Atassi, F., Marchand, A., Blaise, R., Limon, I., McPhee, S. W., Samulski, R. J., Hajjar, R. J. and Lipskaia, L. (2013). Efficient transduction of vascular smooth muscle cells with a translational AAV2.5 vector: a new perspective for in-stent restenosis gene therapy. Gene Ther.

Lostal, W., Bartoli, M., Bourg, N., Roudaut, C., Bentaib, A., Miyake, K., Guerchet, N., Fougerousse, F., McNeil, P. and Richard, I. (2010). Efficient recovery of dysferlin deficiency by dual adeno-associated vector-mediated gene transfer. Hum Mol Genet *19*(10): 1897-1907.

Lostal, W., Bartoli, M., Roudaut, C., Bourg, N., Krahn, M., Pryadkina, M., Borel, P., Suel, L., Roche, J. A., Stockholm, D., Bloch, R. J., Levy, N., Bashir, R. and Richard, I. (2012). Lack of correlation between outcomes of membrane repair assay and correction of dystrophic changes in experimental therapeutic strategy in dysferlinopathy. PLoS One *7*(5): e38036.

Makarova, O., Kamberov, E. and Margolis, B. (2000). Generation of deletion and point mutations with one primer in a single cloning step. Biotechniques *29*(5): 970-972.

Manno, C. S., Pierce, G. F., Arruda, V. R., Glader, B., Ragni, M., Rasko, J. J., Ozelo, M. C., Hoots, K., Blatt, P., Konkle, B., Dake, M., Kaye, R., Razavi, M., Zajko, A., Zehnder, J., Rustagi, P. K., Nakai, H., Chew, A., Leonard, D., Wright, J. F., Lessard, R. R., Sommer, J. M., Tigges, M., Sabatino, D., Luk, A., Jiang, H., Mingozzi, F., Couto, L., Ertl, H. C., High, K. A. and Kay, M. A. (2006). Successful transduction of liver in hemophilia by AAV-Factor IX and limitations imposed by the host immune response. Nat Med *12*(3): 342-347.

Marg, A., Schoewel, V., Timmel, T., Schulze, A., Shah, C., Daumke, O. and Spuler, S. (2012). Sarcolemmal repair is a slow process and includes EHD2. Traffic *13*(9): 1286-1294.

Marty, N. J., Holman, C. L., Abdullah, N. and Johnson, C. P. (2013). The C2 Domains of Otoferlin, Dysferlin, and Myoferlin Alter the Packing of Lipid Bilayers. Biochemistry.

Matsuda, C., Hayashi, Y. K., Ogawa, M., Aoki, M., Murayama, K., Nishino, I., Nonaka, I., Arahata, K. and Brown, R. H., Jr. (2001). The sarcolemmal proteins dysferlin and caveolin-3 interact in skeletal muscle. Hum Mol Genet *10*(17): 1761-1766.

Matsuda, C., Miyake, K., Kameyama, K., Keduka, E., Takeshima, H., Imamura, T., Araki, N., Nishino, I. and Hayashi, Y. (2012). The C2A domain in dysferlin is important for association with MG53 (TRIM72). PLoS Curr *4*: e5035add5038caff5034.

Matsumura, K., Burghes, A. H., Mora, M., Tome, F. M., Morandi, L., Cornello, F., Leturcq, F., Jeanpierre, M., Kaplan, J. C., Reinert, P. and et al. (1994). Immunohistochemical analysis

of dystrophin-associated proteins in Becker/Duchenne muscular dystrophy with huge in-frame deletions in the NH2-terminal and rod domains of dystrophin. J Clin Invest *93*(1): 99-105.

McNeil, P. L. and Steinhardt, R. A. (2003). Plasma membrane disruption: repair, prevention, adaptation. Annu Rev Cell Dev Biol *19*: 697-731.

Mingozzi, F. and High, K. A. (2007). Immune responses to AAV in clinical trials. Curr Gene Ther *7*(5): 316-324.

Murakami, T., Nishi, T., Kimura, E., Goto, T., Maeda, Y., Ushio, Y., Uchino, M. and Sunada, Y. (2003). Full-length dystrophin cDNA transfer into skeletal muscle of adult mdx mice by electroporation. Muscle Nerve *27*(2): 237-241.

Musa, H., Orton, C., Morrison, E. E. and Peckham, M. (2003). Microtubule assembly in cultured myoblasts and myotubes following nocodazole induced microtubule depolymerisation. J Muscle Res Cell Motil *24*(4-6): 301-308.

Nagaraju, K., Rawat, R., Veszelovszky, E., Thapliyal, R., Kesari, A., Sparks, S., Raben, N., Plotz, P. and Hoffman, E. P. (2008). Dysferlin deficiency enhances monocyte phagocytosis: a model for the inflammatory onset of limb-girdle muscular dystrophy 2B. Am J Pathol *172*(3): 774-785.

Nguyen, K., Bassez, G., Bernard, R., Krahn, M., Labelle, V., Figarella-Branger, D., Pouget, J., Hammouda el, H., Beroud, C., Urtizberea, A., Eymard, B., Leturcq, F. and Levy, N. (2005). Dysferlin mutations in LGMD2B, Miyoshi myopathy, and atypical dysferlinopathies. Hum Mutat *26*(2): 165.

Nguyen, K., Bassez, G., Krahn, M., Bernard, R., Laforet, P., Labelle, V., Urtizberea, J. A., Figarella-Branger, D., Romero, N., Attarian, S., Leturcq, F., Pouget, J., Levy, N. and Eymard, B. (2007). Phenotypic study in 40 patients with dysferlin gene mutations: high frequency of atypical phenotypes. Arch Neurol *64*(8): 1176-1182.

Obeng, E. A., Carlson, L. M., Gutman, D. M., Harrington, W. J., Jr., Lee, K. P. and Boise, L. H. (2006). Proteasome inhibitors induce a terminal unfolded protein response in multiple myeloma cells. Blood *107*(12): 4907-4916.

Patel, P., Harris, R., Geddes, S. M., Strehle, E. M., Watson, J. D., Bashir, R., Bushby, K., Driscoll, P. C. and Keep, N. H. (2008). Solution structure of the inner DysF domain of myoferlin and implications for limb girdle muscular dystrophy type 2b. J Mol Biol *379*(5): 981-990.

Pedemonte, N., Lukacs, G. L., Du, K., Caci, E., Zegarra-Moran, O., Galietta, L. J. and Verkman, A. S. (2005). Small-molecule correctors of defective DeltaF508-CFTR cellular processing identified by high-throughput screening. J Clin Invest *115*(9): 2564-2571.

Pegoraro, E. and Hoffman, E. P. (1993). Limb-Girdle Muscular Dystrophy Overview. GeneReviews. R. A. Pagon, T. D. Bird, C. R. Dolan, K. Stephens and M. P. Adam. Seattle (WA).

Piccolo, F., Moore, S. A., Ford, G. C. and Campbell, K. P. (2000). Intracellular accumulation and reduced sarcolemmal expression of dysferlin in limb--girdle muscular dystrophies. Ann Neurol *48*(6): 902-912.

Posey, A. D., Jr., Pytel, P., Gardikiotes, K., Demonbreun, A. R., Rainey, M., George, M., Band, H. and McNally, E. M. (2011). Endocytic recycling proteins EHD1 and EHD2 interact with fer-1-like-5 (Fer1L5) and mediate myoblast fusion. J Biol Chem *286*(9): 7379-7388.

Ramakrishnan, N. A., Drescher, M. J. and Drescher, D. G. (2009). Direct interaction of otoferlin with syntaxin 1A, SNAP-25, and the L-type voltage-gated calcium channel Cav1.3. J Biol Chem *284*(3): 1364-1372.

Rawat, R., Cohen, T. V., Ampong, B., Francia, D., Henriques-Pons, A., Hoffman, E. P. and Nagaraju, K. (2010). Inflammasome up-regulation and activation in dysferlin-deficient skeletal muscle. Am J Pathol *176*(6): 2891-2900.

Reed, N. A., Cai, D., Blasius, T. L., Jih, G. T., Meyhofer, E., Gaertig, J. and Verhey, K. J. (2006). Microtubule acetylation promotes kinesin-1 binding and transport. Curr Biol *16*(21): 2166-2172.

Rey, M., Irondelle, M., Waharte, F., Lizarraga, F. and Chavrier, P. (2011). HDAC6 is required for invadopodia activity and invasion by breast tumor cells. Eur J Cell Biol *90*(2-3): 128-135.

Rivieccio, M. A., Brochier, C., Willis, D. E., Walker, B. A., D'Annibale, M. A., McLaughlin, K., Siddiq, A., Kozikowski, A. P., Jaffrey, S. R., Twiss, J. L., Ratan, R. R. and Langley, B. (2009). HDAC6 is a target for protection and regeneration following injury in the nervous system. Proc Natl Acad Sci U S A *106*(46): 19599-19604.

Roostalu, U. and Strahle, U. (2012). In vivo imaging of molecular interactions at damaged sarcolemma. Dev Cell *22*(3): 515-529.

Roux, I., Safieddine, S., Nouvian, R., Grati, M., Simmler, M. C., Bahloul, A., Perfettini, I., Le Gall, M., Rostaing, P., Hamard, G., Triller, A., Avan, P., Moser, T. and Petit, C. (2006). Otoferlin, defective in a human deafness form, is essential for exocytosis at the auditory ribbon synapse. Cell *127*(2): 277-289.

Saitoh, O., Arai, T. and Obinata, T. (1988). Distribution of microtubules and other cytoskeletal filaments during myotube elongation as revealed by fluorescence microscopy. Cell Tissue Res *252*(2): 263-273.

Sakamoto, M., Yuasa, K., Yoshimura, M., Yokota, T., Ikemoto, T., Suzuki, M., Dickson, G., Miyagoe-Suzuki, Y. and Takeda, S. (2002). Micro-dystrophin cDNA ameliorates dystrophic phenotypes when introduced into mdx mice as a transgene. Biochem Biophys Res Commun *293*(4): 1265-1272.

Santos, R., Oliveira, J., Vieira, E., Coelho, T., Carneiro, A. L., Evangelista, T., Dias, C., Fortuna, A., Geraldo, A., Negrao, L., Guimaraes, A. and Bronze-da-Rocha, E. (2010). Private dysferlin exon skipping mutation (c.5492G>A) with a founder effect reveals further alternative splicing involving exons 49-51. J Hum Genet *55*(8): 546-549.

Selcen, D., Stilling, G. and Engel, A. G. (2001). The earliest pathologic alterations in dysferlinopathy. Neurology *56*(11): 1472-1481.

Shao, X., Davletov, B. A., Sutton, R. B., Sudhof, T. C. and Rizo, J. (1996). Bipartite Ca2+-binding motif in C2 domains of synaptotagmin and protein kinase C. Science *273*(5272): 248-251.

Sharma, A., Yu, C., Leung, C., Trane, A., Lau, M., Utokaparch, S., Shaheen, F., Sheibani, N. and Bernatchez, P. (2010). A new role for the muscle repair protein dysferlin in endothelial cell adhesion and angiogenesis. Arterioscler Thromb Vasc Biol *30*(11): 2196-2204.

Singh, L. R., Gupta, S., Honig, N. H., Kraus, J. P. and Kruger, W. D. (2010). Activation of mutant enzyme function in vivo by proteasome inhibitors and treatments that induce Hsp70. PLoS Genet *6*(1): e1000807.

Sinnreich, M., Therrien, C. and Karpati, G. (2006). Lariat branch point mutation in the dysferlin gene with mild limb-girdle muscular dystrophy. Neurology *66*(7): 1114-1116.

Spangenburg, E. E., Bowles, D. K. and Booth, F. W. (2004). Insulin-like growth factor-induced transcriptional activity of the skeletal alpha-actin gene is regulated by signaling mechanisms linked to voltage-gated calcium channels during myoblast differentiation. Endocrinology *145*(4): 2054-2063.

Sterz, J., von Metzler, I., Hahne, J. C., Lamottke, B., Rademacher, J., Heider, U., Terpos, E. and Sezer, O. (2008). The potential of proteasome inhibitors in cancer therapy. Expert Opin Investig Drugs *17*(6): 879-895.

Sudhof, T. C. and Rizo, J. (1996). Synaptotagmins: C2-domain proteins that regulate membrane traffic. Neuron *17*(3): 379-388.

Tan, K., Duquette, M., Liu, J. H., Dong, Y., Zhang, R., Joachimiak, A., Lawler, J. and Wang, J. H. (2002). Crystal structure of the TSP-1 type 1 repeats: a novel layered fold and its biological implication. J Cell Biol *159*(2): 373-382.

Tang, Y., Cummins, J., Huard, J. and Wang, B. (2010). AAV-directed muscular dystrophy gene therapy. Expert Opin. Biol. Ther. *10*(3): 395-408.

Therrien, C., Di Fulvio, S., Pickles, S. and Sinnreich, M. (2009). Characterization of lipid binding specificities of dysferlin C2 domains reveals novel interactions with phosphoinositides. Biochemistry *48*(11): 2377-2384.

Therrien, C., Dodig, D., Karpati, G. and Sinnreich, M. (2006). Mutation impact on dysferlin inferred from database analysis and computer-based structural predictions. J Neurol Sci *250*(1-2): 71-78.

Tran, A. D., Marmo, T. P., Salam, A. A., Che, S., Finkelstein, E., Kabarriti, R., Xenias, H. S., Mazitschek, R., Hubbert, C., Kawaguchi, Y., Sheetz, M. P., Yao, T. P. and Bulinski, J. C. (2007). HDAC6 deacetylation of tubulin modulates dynamics of cellular adhesions. J Cell Sci *120*(Pt 8): 1469-1479.

Urtasun, M., Saenz, A., Roudaut, C., Poza, J. J., Urtizberea, J. A., Cobo, A. M., Richard, I., Garcia Bragado, F., Leturcq, F., Kaplan, J. C., Marti Masso, J. F., Beckmann, J. S. and Lopez de Munain, A. (1998). Limb-girdle muscular dystrophy in Guipuzcoa (Basque Country, Spain). Brain *121 (Pt 9)*: 1735-1747.

van der Kooi, A. J., Barth, P. G., Busch, H. F., de Haan, R., Ginjaar, H. B., van Essen, A. J., van Hooff, L. J., Howeler, C. J., Jennekens, F. G., Jongen, P., Oosterhuis, H. J., Padberg, G. W., Spaans, F., Wintzen, A. R., Wokke, J. H., Bakker, E., van Ommen, G. J., Bolhuis, P. A. and de Visser, M. (1996). The clinical spectrum of limb girdle muscular dystrophy. A survey in The Netherlands. Brain *119 (Pt 5)*: 1471-1480.

van Deutekom, J. C., Janson, A. A., Ginjaar, I. B., Frankhuizen, W. S., Aartsma-Rus, A., Bremmer-Bout, M., den Dunnen, J. T., Koop, K., van der Kooi, A. J., Goemans, N. M., de Kimpe, S. J., Ekhart, P. F., Venneker, E. H., Platenburg, G. J., Verschuuren, J. J. and van Ommen, G. J. (2007). Local dystrophin restoration with antisense oligonucleotide PRO051. N Engl J Med *357*(26): 2677-2686.

Vandre, D. D., Ackerman, W. E. t., Kniss, D. A., Tewari, A. K., Mori, M., Takizawa, T. and Robinson, J. M. (2007). Dysferlin is expressed in human placenta but does not associate with caveolin. Biol Reprod *77*(3): 533-542.

Varga, R., Kelley, P. M., Keats, B. J., Starr, A., Leal, S. M., Cohn, E. and Kimberling, W. J. (2003). Non-syndromic recessive auditory neuropathy is the result of mutations in the otoferlin (OTOF) gene. J Med Genet *40*(1): 45-50.

Waddell, L. B., Lemckert, F. A., Zheng, X. F., Tran, J., Evesson, F. J., Hawkes, J. M., Lek, A., Street, N. E., Lin, P., Clarke, N. F., Landstrom, A. P., Ackerman, M. J., Weisleder, N., Ma, J., North, K. N. and Cooper, S. T. (2011). Dysferlin, annexin A1, and mitsugumin 53 are upregulated in muscular dystrophy and localize to longitudinal tubules of the T-system with stretch. J Neuropathol Exp Neurol *70*(4): 302-313.

Walter, M. C., Reilich, P., Thiele, S., Schessl, J., Schreiber, H., Reiners, K., Kress, W., Muller-Reible, C., Vorgerd, M., Urban, P., Schrank, B., Deschauer, M., Schlotter-Weigel, B., Kohnen, R. and Lochmuller, H. (2013). Treatment of dysferlinopathy with deflazacort: a double-blind, placebo-controlled clinical trial. Orphanet J Rare Dis *8*: 26.

Wang, B., Li, J. and Xiao, X. (2000). Adeno-associated virus vector carrying human minidystrophin genes effectively ameliorates muscular dystrophy in mdx mouse model. Proc Natl Acad Sci U S A *97*(25): 13714-13719.

Wang, B., Yang, Z., Brisson, B. K., Feng, H., Zhang, Z., Welch, E. M., Peltz, S. W., Barton, E. R., Brown, R. H., Jr. and Sweeney, H. L. (2010). Membrane blebbing as an assessment of functional rescue of dysferlin-deficient human myotubes via nonsense suppression. J Appl Physiol *109*(3): 901-905.

Wang, Z., Allen, J. M., Riddell, S. R., Gregorevic, P., Storb, R., Tapscott, S. J., Chamberlain, J. S. and Kuhr, C. S. (2007). Immunity to adeno-associated virus-mediated gene transfer in a random-bred canine model of Duchenne muscular dystrophy. Hum Gene Ther *18*(1): 18-26.

Wang, Z., Kuhr, C. S., Allen, J. M., Blankinship, M., Gregorevic, P., Chamberlain, J. S., Tapscott, S. J. and Storb, R. (2007). Sustained AAV-mediated dystrophin expression in a canine model of Duchenne muscular dystrophy with a brief course of immunosuppression. Mol Ther *15*(6): 1160-1166.

Ward, C. L., Omura, S. and Kopito, R. R. (1995). Degradation of CFTR by the ubiquitin-proteasome pathway. Cell *83*(1): 121-127.

Ward, S., Argon, Y. and Nelson, G. A. (1981). Sperm morphogenesis in wild-type and fertilization-defective mutants of Caenorhabditis elegans. J Cell Biol *91*(1): 26-44.

Washington, N. L. and Ward, S. (2006). FER-1 regulates Ca2+ -mediated membrane fusion during C. elegans spermatogenesis. J Cell Sci *119*(Pt 12): 2552-2562.

Wein, N., Avril, A., Bartoli, M., Beley, C., Chaouch, S., Laforet, P., Behin, A., Butler-Browne, G., Mouly, V., Krahn, M., Garcia, L. and Levy, N. (2010). Efficient bypass of mutations in dysferlin deficient patient cells by antisense-induced exon skipping. Hum Mutat *31*(2): 136-142.

Westermann, S. and Weber, K. (2003). Post-translational modifications regulate microtubule function. Nat Rev Mol Cell Biol *4*(12): 938-947.

Williamson, R. A., Henry, M. D., Daniels, K. J., Hrstka, R. F., Lee, J. C., Sunada, Y., Ibraghimov-Beskrovnaya, O. and Campbell, K. P. (1997). Dystroglycan is essential for early embryonic development: disruption of Reichert's membrane in Dag1-null mice. Hum Mol Genet *6*(6): 831-841.

Wu, Y., Song, S. W., Sun, J., Bruner, J. M., Fuller, G. N. and Zhang, W. (2010). IIp45 inhibits cell migration through inhibition of HDAC6. J Biol Chem *285*(6): 3554-3560.

Wu, Z., Asokan, A. and Samulski, R. J. (2006). Adeno-associated virus serotypes: vector toolkit for human gene therapy. Mol Ther *14*(3): 316-327.

Wu, Z., Yang, H. and Colosi, P. (2010). Effect of genome size on AAV vector packaging. Mol. Ther. *18*(1): 80-86.

Yasunaga, S., Grati, M., Cohen-Salmon, M., El-Amraoui, A., Mustapha, M., Salem, N., El-Zir, E., Loiselet, J. and Petit, C. (1999). A mutation in OTOF, encoding otoferlin, a FER-1-like protein, causes DFNB9, a nonsyndromic form of deafness. Nat Genet *21*(4): 363-369.

Yuasa, K., Sakamoto, M., Miyagoe-Suzuki, Y., Tanouchi, A., Yamamoto, H., Li, J., Chamberlain, J. S., Xiao, X. and Takeda, S. (2002). Adeno-associated virus vector-mediated gene transfer into dystrophin-deficient skeletal muscles evokes enhanced immune response against the transgene product. Gene Ther *9*(23): 1576-1588.

Zhang, X., Yuan, Z., Zhang, Y., Yong, S., Salas-Burgos, A., Koomen, J., Olashaw, N., Parsons, J. T., Yang, X. J., Dent, S. R., Yao, T. P., Lane, W. S. and Seto, E. (2007). HDAC6 modulates cell motility by altering the acetylation level of cortactin. Mol Cell *27*(2): 197-213.

Zhang, Y., Li, N., Caron, C., Matthias, G., Hess, D., Khochbin, S. and Matthias, P. (2003). HDAC-6 interacts with and deacetylates tubulin and microtubules in vivo. EMBO J *22*(5): 1168-1179.

Zilberman, Y., Ballestrem, C., Carramusa, L., Mazitschek, R., Khochbin, S. and Bershadsky, A. (2009). Regulation of microtubule dynamics by inhibition of the tubulin deacetylase HDAC6. J Cell Sci *122*(Pt 19): 3531-3541.